ARLETE RITA PENITENTE

EFEITOS DA RESTRIÇÃO PROTÉICA EXPERIMENTAL SOBRE A MORFOLOGIA DO MIOCÁRDIO E AS PROPRIEDADES MECÂNICAS DOS MIÓCITOS CARDÍACOS ISOLADOS EM RATOS *FISHER* APÓS O DESMAME

Tese apresentada à Universidade Federal de Viçosa, como parte das exigências do Programa de Pós-Graduação em Biologia Celular e Estrutural, para obtenção do título de *Doctor Scientiae*.

VIÇOSA
MINAS GERAIS – BRASIL
2012

Ficha catalográfica preparada pela Seção de Catalogação e Classificação da Biblioteca Central da UFV

T
P411e
2012

Penitente, Arlete Rita, 1973-
Efeitos da restrição protéica experimental sobre a morfologia do miocárdio e as propriedades mecânicas dos miócitos cardíacos isolados em ratos *Fisher* após o desmame / Arlete Rita Penitente. – Viçosa, MG, 2012.
xiii, 78f. : il. (algumas col.) ; 29cm.

Inclui anexos.
Texto em português e inglês.
Orientador: Clóvis Andrade Neves.
Tese (doutorado) - Universidade Federal de Viçosa.
Inclui bibliografia.

1. Coração. 2. Coração - Anatomia. 3. Morfologia. 4. Rato. 5. Miocárdio. 6. *Fischer*. I. Universidade Federal de Viçosa. II. Título.

CDD 22. ed. 571.31

ARLETE RITA PENITENTE

EFEITOS DA RESTRIÇÃO PROTÉICA EXPERIMENTAL SOBRE A MORFOLOGIA DO MIOCÁRDIO E AS PROPRIEDADES MECÂNICAS DOS MIÓCITOS CARDÍACOS ISOLADOS EM RATOS *FISHER* APÓS O DESMAME

Tese apresentada à Universidade Federal de Viçosa, como parte das exigências do Programa de Pós-Graduação em Biologia Celular e Estrutural, para obtenção do título de *Doctor Scientiae.*

APROVADO: 23 de março de 2012.

Maria Lúcia Pedrosa

Marcelo Eustáquio da Silva

Ita de Oliveira e Silva

Izabel Regina S. C. Maldonado

Clóvis Andrade Neves
(Orientador)

"Só por fraqueza nos contentamos com o que os outros e nós mesmos deparamos nessa caça ao saber; os mais aptos não se satisfazem e haverá sempre caminho a percorrer para quem vier depois, e até para nós se agirmos de outro modo."

(Montaigne, Ensaios III, XII)

DEDICATÓRIA

Ao meu ***Esposo Josias,***
pelo amor, dedicação, carinho e
apoio ao longo destes anos.
Ao meu ***Pai Durval***
(sempre presente), mesmo ausente.
A minha ***Mãe Maria*** *pelas orações.*
Às ***Minhas Irmãs*** *pela amizade e apoio.*
Aos ***Meus Sobrinhos****, alegria da minha vida.*

AGRADECIMENTOS

A Deus pelo dom da vida e da saúde. Por me conduzir nos caminhos a seguir, sentindo sempre sua presença ao meu lado.

Ao Meu Esposo Josias Barcelos Jr pelo amor, carinho e cumplicidade. Por estar ao meu lado e me fazer muito feliz! Meu refúgio mais seguro. Amo você!

Ao meu falecido Pai Durval Penitente, pelo orgulho e brilho nos olhos a cada conquista. Exemplo de honestidade, dignidade e respeito que sempre tentei seguir. Obrigada por todas as palavras de incentivo das quais nunca esquecerei.

A minha Mãe Maria Cardoso Penitente, obrigada pelo amor, pela boa educação que me proporcionou e pelas orações que sempre me deram força para ir cada vez mais longe.

As minhas Irmãs Arleide e Rogéria, pelo apoio familiar, incentivo e orações. Obrigada por cuidarem da nossa Mãe enquanto estou ausente! Aos meus cunhados Wilson e Zezinho pela torcida!

Aos meus Sobrinhos Jéssica, Jeisy, Beatriz, Bárbara e Noberto por ser presença constante em todos os momentos da minha vida.

A minha afilhada Jéssica Penitente Passamani, uma das alegrias da minha vida! Obrigada Arleide por me proporcionar este presente de Deus!

A minha prima Ana Cristina pela confiança e amizade em todos os momentos!

Ao meu primo Anderson, Tia Adélia e Tio Eliel pela força, apoio e orações!

Ao meu Orientador Prof. Clóvis Andrade Neves, meus sinceros agradecimentos pelos valiosos ensinamentos, amizade sincera e incentivo. Obrigada por abrir as portas do Laboratório de Biologia Celular e Estrutural e me proporcionar à oportunidade de trilhar novos caminhos. Serei eternamente grata por tudo!

Aos meus Co-Orientadores Prof. Antônio José Natali pelos ensinamentos, pela ótima estrutura do Laboratório de Educação Física que foram fundamentais para a realização deste e de outros trabalhos e Prof. Deoclécio Alves Chianca Jr., pelos ensinamentos, confiança e disposição em ajudar sempre.

Á Amiga de toda vida: Amandinha por estar sempre presente!

As Amigas verdadeiras Fabiana e Lilian, por não medirem forças para me ajudar! Sou grata a Deus pela amizade!

Ao Rômulo, obrigada pela companhia nessa caminhada. Obrigado pela amizade, convivência e ajuda valiosa nos experimentos.

A Marcinha, Amiga e companheira de caminhada! Não tenho dúvida: Deus é mais!!!

A Amiga Ângela pelo apoio e amizade.

A Claudinha pela amizade sincera! Sentirei saudades!

Ao Amigo Kenner pela amizade e importante apoio na realização desse trabalho!

Ao Amigo Alex Bhering por muito nos auxiliar nos procedimentos e técnicas em histologia, pela paciência e disponibilidade em ajudar sem medir esforços.

A Profª. Izabel R. S. C. Maldonado pela sabedoria, simplicidade e grandes ensinamentos!

Aos professores do Programa de Pós-Graduação em Biologia Celular e Estrutural, em especial aos Profs Sérgio, Izabel, Mariana, Juliana e Adilson por todos os ensinamentos e incentivo.

Ao Prof. André Talvani Pedrosa, pelo apoio, disposição sempre em ajudar e incentivo para continuar a caminhada.

Aos Profs. Marcelo Eustáquio da Silva, Maria Lúcia Pedrosa (UFOP), Ita de Oliveira Silva e Izabel Regina S. C. Maldonado pela disposição em participar da Banca Examinadora e aos suplentes Sérgio da Matta, Maria C. G. Pelúzio e Mariana M. Neves pela disponibilidade.

As Professoras Ita e Maria Tereza por todos os valiosos ensinamentos, incentivos e oportunidades!

Ao Professor Vanderson Esperidião Antônio pelo exemplo de profissionalismo e competência!

Aos Colegas do Laboratório de Biologia Celular e Estrutural (UFV), em especial Rômulo, Marli, Daiane, Lilian, Kenner, Alex, Claudinha com as quais sempre

pude contar. Obrigada pela amizade. Daniel, Fernandinho, Jane, Vinícius, Sirlene, Madu, Rafael, Grazi, Tati, Silvinha, Edson, Dani, Maytê, Ana Paula, Michele, Kyvia pelos momentos de descontração e companheirismo.

Ao Pessoal do Biotério de Experimentação Animal: Marcinha, Ângela, Prof. Guto, Judson, Bozzi, Fellipe, Bárbara, Juliana, Nathalia, Lucas, Miguel, Vitor, pelo apoio e pela disponibilidade em ajudar.

Aos Amigos do Laboratório de Fisiologia Cardiovascular UFOP, do presente: Fernanda, Aline Arlindo, Luiz, Nathália, Aline Resende e Alessandra e de outras épocas: Fabiana, Vanessa, Joelma, Leonardo, Graça, Daniela, Eduardo, Antônio pela amizade, incentivo, apoio e companheirismo.

A todos os professores do Programa de Pós-Graduação em Biologia Celular e estrutural, pela disposição em ajudar e por proporcionar um intercâmbio sadio entre os laboratórios da pós-graduação. À Profª. Sílvia Pompolo, por permitir a utilização de seu laboratório para aquisição das imagens utilizadas.

Ao coordenador do Programa de Pós-graduação em Biologia Celular e Estrutural, professor José Eduardo Serrão pelo empenho em melhorar a qualidade do programa e também por sua infinita prestatividade.

Ao Departamento de Biologia Geral, em especial a Beth, Diana e João Bosco por estarem sempre dispostas a ajudar em todos os momentos.

Ao núcleo de Microscopia e Microanálise, em especial Carla, Patrícia e Gilmar e ao Laboratório de Anatomia Vegetal, pelo suporte.

Aos técnicos: Maria Chaves dos Santos (Laboratório de Imunopatologia – UFOP) pelo auxílio na realização desse trabalho, Sr. Miltinho (Laboratório de Fisiologia Cardiovascular - UFOP) e Jair Pastor Mota (Laboratòrio de Nutrição Experimental da Escola de Nutrição), (UFOP) pelo cuidado com os animais, boa vontade e presteza.

À Universidade Federal de Viçosa e ao Programa de Pós-Graduação em Biologia Celular e Estrutural pela valiosa oportunidade na realização do Doutorado e por todo aprendizado.

À FAPEMIG com a concessão da bolsa de estudos, fundamental para a realização desse trabalho.

ÍNDICE

RESUMO

PENITENTE, Arlete Rita, D.Sc., Universidade Federal de Viçosa, março de 2012. **Efeitos da restrição protéica experimental sobre a morfologia do miocárdio e as propriedades mecânicas dos miócitos cardíacos isolados em ratos *Fisher* após o desmame.** Orientador: Clóvis Andrade Neves. Coorientadores: Antônio José Natali e Deoclécio Alves Chianca Jr.

Alterações na nutrição em fases precoces da vida resultam no desenvolvimento de adaptações que podem modificar permanentemente a estrutura de um órgão ou tecido. Embora a função cardíaca esteja alterada em animais com restrição protéica, ainda há informações limitadas sobre a mecânica, morfologia e ultraestrutura dos cardiomiócitos, que levam à alteração da função cardíaca. O presente estudo investigou a relação entre a restrição protéica severa pós-desmame e as alterações morfológicas, moleculares e ultra-estruturais dos cardiomiócitos ventriculares, além de suas propriedades mecânicas, dos *sparks* de cálcio e da atuação do sistema β-adrenérgico, em ratos machos *Fischer,* a partir do desmame. Os animais foram divididos aleatoriamente em grupo controle (GC, n= 36) e grupo com restrição de proteínas (GRP, n= 36). Após o desmame (28 dias após o nascimento), animais do GC e GRP receberam dietas isocalóricas contendo 15% e 6% de proteína, respectivamente, por 35 dias. Em seguida, os animais foram pesados, sacrificados e tiveram os corações removidos para a análise histológica, morfométrica, estereológica e ultraestrutural; ou isolados por dispersão enzimática para análise das propriedades mecânicas. Os resultados encontrados demonstraram que a restrição protéica causou uma drástica redução no peso corporal, do coração e do ventrículo esquerdo dos animais do GRP. Essas alterações foram acompanhadas com uma diminuição no comprimento, largura e área dos cardiomiócitos, além de um aumento da quantidade de colágeno no GRP em relação ao GC de 38%. Porém em relação ao número de células o GRP apresentou o mesmo número de células do GC. As análises ultra-estruturais permitiram a observação de miofibrilas menos desenvolvidas, maior proporção de mitocôndrias e retículo sarcoplasmático menos organizado no GRP. Miócitos ventriculares do GRP também apresentaram alterações nas

propriedades contráteis, tanto em condições basais quanto após estimulação β-adrenérgica. Além disso, o GRP apresentou menor expressão protéica de SERCA2a e menor transiente de cálcio em relação ao GC, provocando prejuízos na mecânica celular. De acordo com esses resultados, foi possível concluir que a restrição protéica severa altera não apenas a morfologia do coração, mas também aspectos bioquímicos e funcionais.

ABSTRACT

PENITENTE, Arlete Rita, D.Sc., Federal Univesity of Viçosa, March, 2012. **Effect of experimental protein restriction on the morphology of myocardial and the mechanical properties of cardiac myocytes isolated from *Fisher* rats after weaning.** Adviser: Clóvis Andrade Neves. Co-advisers: Antônio José Natali and Deoclécio Alves Chianca Jr.

Nutrition deficits early in life result in adaptive changes which can permanently modify the structure of an organ or tissue. Despite the fact that cardiac function seem to be altered in rats fed low protein diet, available information about mechanics, morphology and ultrastructure of cardiomyocytes in this model is still limited. The present study investigated the relation between severe protein restriction post weaning and morphological, molecular and ultrastructural changes in ventricular cardiomyocytes in addition to the mechanics, intracellular calcium sparks and β-adrenergic system action on these cells. Animals were randomly divided in control (CG, n=36) and protein restriction (PRG, n=36) groups. After weaning (28 days), the rats were fed either control (15% casein) or low protein (6% casein) isocaloric diets for 35 days. Following this period, rats were euthanized and hearts were removed for histological, morphometric, estereological and ultrastructural analysis or processed in order to isolated cardiomyocytes by enzymatic dispersion to perform mechanic test. Results showed that protein restriction ended up in body weight, heart weight and left ventricular reduction compared to same aged control rats. These changes were accompanied by individual cardiomyocytes length, diameter and area reduction. It was also noticed 38% increase in collagen deposition in the matrix of PRG compared to CG rats. The number of cardiomyocytes was similar in both groups. Ultrastructural analyses revealed less developed myofibrils and higher proportion of less organized mitochondria and sarcoplasmic reticulum in the cells of PRG. Myocytes of PRG also showed changes in the contractile properties both in baseline and after β-adrenergic stimulation conditions. In addition, cells from PRG exhibited lower expression of SERCA2a protein and smaller calcium transient compared to CG which seems to impair the cell mechanics. Based on these findings, we conclude that severe protein

restriction after weaning may modify not only morphological but also biochemical and functional aspects of the heart.

1. Introdução Geral

1.1. Desnutrição

A desnutrição, definida na literatura como uma deficiência de nutrientes essenciais à sobrevivência e manutenção das funções vitais, pode estar relacionada à ingestão inadequada de nutrientes (proteínas, carboidratos, gorduras, sais minerais e vitaminas); conseqüência, geralmente, de uma dieta restrita, determinando desequilíbrio entre a necessidade corpórea e a ingestão de nutrientes (Sawaya et al, 2003). A desnutrição é considerada uma condição patológica e ainda um sério problema de saúde pública, afetando um número substancial de crianças, em diferentes partes do mundo, o que tem originado expressivo número de estudos na tentativa de elucidar suas consequências no adulto (WHO, 2010).

Dependendo do período de exposição e do grau de desnutrição, severas conseqüências podem ocorrer durante o desenvolvimento do organismo e também na vida adulta, predispondo ao desenvolvimento de doenças crônico-degenerativas como hipertensão, diabetes e doenças cardíacas (Barker et al, 1993; Okoromah et al, 2011). Entretanto, a inter-relação entre os efeitos da desnutrição sobre os diversos órgãos e sistemas, com destaque para o coração, ainda não é totalmente esclarecida.

Todas as células do organismo, em maior ou menor intensidade, sofrem alterações provocadas pela deficiência de qualquer um dos nutrientes indispensáveis à sobrevivência. Assim, esta carência nutricional influencia no grau de comprometimento e no funcionamento dos órgãos, decorrentes do

período de exposição do indivíduo, bem como a severidade desta restrição. Com efeito, na vida fetal os órgãos passam por períodos críticos de desenvolvimento que coincidem com períodos de rápida divisão celular. A carência de nutrientes em períodos críticos de desenvolvimento, mesmo que por pouco tempo, pode reduzir o número de células em alguns órgãos, modificando seu metabolismo e / ou estrutura, afetando seu desenvolvimento e função (Gluckman & Hanson, 2004; Lim et al, 2010). Portanto, devido à suas diversas repercussões ao organismo e alta prevalência, a desnutrição é muito estudada. Em humanos as avaliações epidemiológicas se sobrepõem e o uso de modelos animais tem permitido cada vez mais esclarecimentos para que este problema possa ser desvendado.

A desnutrição experimental pode ser induzida por alteração dos componentes da dieta ou por redução da quantidade da mesma. Ela pode ocorrer em várias fases do desenvolvimento e causar danos variáveis dependendo da fase de desenvolvimento envolvida. A desnutrição intra-uterina, por exemplo, induzida por alteração na dieta das fêmeas grávidas, envolve fases de crescimento rápido e pode causar danos irreversíveis em vários sistemas fetais, incluindo o cardiovascular (Barker et al.; 1993). Várias linhas de pesquisa adotam a hipótese de que a desnutrição intra-uterina leva a uma programação fetal, o que predispõe ao desenvolvimento de doenças crônico-degenerativas. Hipertensão, doenças coronarianas, diabetes tipo II e doenças renais são algumas das desordens relacionadas ao baixo peso ao nascer (Barker e cols., 1993; Phillips e cols., 1994; Hoppe et al., 2007). Durante a amamentação a desnutrição pode ser induzida restringindo a quantidade de proteína dietética das fêmeas (Pedrosa & Moraes-Santos, 1987) ou

aumentando o tamanho da ninhada, provocando competição pelo leite materno (Belmar, 1996). Outros protocolos induzem a desnutrição em animais reduzindo em 50 % todos os componentes da dieta, ou seja, proteínas e calorias (restrição alimentar de 50%) (Cicogna et al., 1999). O modelo de desnutrição proposto neste trabalho foi baseado na redução do conteúdo proteico da dieta oferecida ao grupo desnutrido de 15% para 6%, o que representa uma redução de 68% da proteína dietética (caseína). Esta metodologia assemelha-se aos métodos utilizados em outros trabalhos da literatura (Agarwal e cols., 1981; Benabe e cols., 1998). O rato é o animal mais utilizado nestes estudos por apresentar características como: fácil manuseio, metabolismo acelerado e se adequar às diferentes metodologias de desnutrição. Esta última característica possui relevância especial porque permite investigações experimentais rápidas, principalmente de distúrbios promovidos apenas tardiamente pela desnutrição no indivíduo adulto.

Ratos submetidos a diferentes níveis de desnutrição, inclusive proteica, evidenciaram em seus órgãos, alterações anatômicas e histológicas, compatíveis com a adaptação que o organismo promove para se ajustar às condições nutricionais adversas (Benabe & Martinez-Maldonado, 1998; Christian & Stewart, 2010). Nesse contexto, várias pesquisas apontam que a desnutrição promove alterações de âmbito corpóreo geral, porém, o impacto da mesma não se processa de igual maneira nos vários órgãos e tecidos do organismo. Tal fato acontece devido a uma condição especial que assinala certa seletividade (Freitas et al, 1994), privilegiando órgãos indispensáveis à sobrevivência em relação a outros (Hanson et al., 2002; Gluckman & Hanson, 2004).

Outro fator a ser considerado são as grandes implicações econômicas e sociais que advêm dos efeitos da desnutrição a médio e longo prazo, principalmente porque as maiores taxas de desnutrição ocorrem em países em desenvolvimento, que não podem financiar o tratamento de doenças crônico-degenerativas. Nesse contexto, não há dúvidas da necessidade de estudos relacionados às alterações fisiológicas que a desnutrição pode causar ao organismo.

1.2. Alterações morfológicas do coração associadas à desnutrição proteica

O adequado funcionamento do coração e, portanto, do sistema cardiovascular depende diretamente da forma, da função do músculo e da célula cardíaca. Assim, modificações na estrutura desse órgão podem acarretar falhas, comprometendo outros sistemas e, dessa forma, o organismo (Christian, 2010). O comprometimento muscular afetado pela desnutrição é uma forma de adaptação à redução de nutrientes para suprir a célula, uma vez que os tecidos musculares são fontes imediatas de aminoácidos. Ocorre também enfraquecimento progressivo do miocárdio, diminuição da demanda circulatória, conduzindo a uma situação de risco e sobrevida (Drott & Lundholm, 1992; Gruber, 2012).

Evidências comprovam que restrição proteica materna pode levar à redução no número de cardiomiócitos na prole, um importante fator de risco para desordens cardiovasculares na vida adulta (Lim et al, 2010). Ratos cujas mães foram submetidas à restrição proteica moderada (9% de caseína) apresentaram diminuição no tamanho do coração, devido à redução do número

de cardiomiócitos (Corstius et al., 2005). Esses autores sugerem que tais variações ocasionadas pela desnutrição, podem comprometer a função cardíaca, levando a patologias cardiovasculares como hipertensão e insuficiência cardíaca.

Alterações morfológicas e disfunção sistólica miocárdica foram observadas em animais submetidos à restrição alimentar. Cicogna et al. (1999), utilizando um modelo diferente de desnutrição, reduzindo todos os componentes da dieta (restrição alimentar de 50%), e trabalhando com preparações de músculo papilar isolado, observaram aumento de colágeno intersticial no miocárdio cardíaco, acarretando danos ao sistema circulatório. Cicogna (2000), trabalhando com este mesmo modelo experimental (restrição alimentar de 50%), observou perda de peso corporal desproporcional, com perda de peso maior no grupo experimental. Porém esse autor também observou um aumento do peso relativo (relação peso ventrículo/peso corpo) do ventrículo esquerdo nos animais do grupo experimental. Em outro estudo realizado em ratos jovens desnutridos desde o nascimento (Fioretto et al, 2001), os autores perceberam perda de peso cardíaco, corpóreo e da massa ventricular, indicando que o coração foi afetado pelos efeitos adversos da desnutrição em relação ao peso e massa, verificando também que o ventrículo esquerdo apresentou uma remodelação excêntrica, determinada pela desproporcional redução da massa em relação ao volume. Outro autor (Vandewoude, 2008), verificaram modificações no miocárdio em relação à microvascularização e mecanismo de adaptação dos miócitos desnutridos. Kothari (1992), estudando a massa e função ventricular esquerda de crianças entre 1 e 5 anos de idade, saudáveis e desnutridas, verificou que a massa

ventricular esquerda foi menor nas crianças desnutridas do que nos controles, porém, a relação massa ventricular esquerda / peso corpóreo mostrou-se significativamente aumentada nas crianças desnutridas, sugerindo uma relativa preservação cardíaca nesse grupo, em relação a diminuição do peso corporal.

Em 2002, Cunha, analisando fragmentos do ventrículo esquerdo em humanos adultos desnutridos e nutridos, verificou uma menor espessura dos cardiomiócitos nos desnutridos, com hipotrofia miofibrilar, decorrente da redução da síntese dos componentes das miofibrilas. Outros autores observaram alterações focais em muitas fibras musculares, tais como a desorganização e a perda das miofibrilas causando disfunção miocárdica (Pinotti et al., 2010).

Dessa maneira, existe uma dependência direta entre as condições morfofuncionais das células constituintes dos tecidos cardíacos, seu desempenho e funcionamento normal. Nesse contexto, é de extrema importância, a realização de pesquisa sobre parâmetros morfológicos e funcionais do tecido e da célula cardíaca, podendo contribuir para a elucidação do comportamento morfofuncional desse órgão, fundamental nas funções vitais. Esses estudos seriam uma importante contribuição para a compreensão dos efeitos deletérios causados pela restrição proteica no coração e seu impacto sobre as doenças cardiovasculares.

1.3. Alterações da homeostasia do Ca^{2+} no coração associadas à desnutrição

O íon cálcio (Ca^{2+}) desempenha papel fundamental na regulação e sinalização da função celular para a manutenção da homeostase. É fundamental nos processos de secreção e liberação de neurotransmissores, divisão celular, regulação dos processos de transcrição genética, proliferação celular e apoptose (morte celular programada) (Berridge et al., 2000). No miócito cardíaco, especialmente, o íon Ca^{2+} é fundamental desde a geração e modulação da atividade elétrica do potencial de ação (PA), até a regulação e controle do processo de contração (Bers, 2001; Bers, 2002). É evidente que um dos principais mecanismos reguladores da contratilidade e relaxamento cardíaco é o trânsito de cálcio (Ca^{2+}) intracelular (Opie, 1998; Bers, 2001).

O processo de contração cardíaca inicia-se com a abertura dos canais lentos de Ca^{2+} do sarcolema (canais do tipo L), com conseqüente entrada de Ca^{2+} extracelular. Fabiato (1983) descreveu que a liberação de Ca^{2+} de retículo sarcoplasmático (RS) é induzida pela ligação de Ca^{2+} aos canais de liberação denominados receptores de rianodina (RyRs). É o aumento da concentração de cálcio intracelular $[Ca^{2+}]_i$, no citosol (figura 1) que permite a ligação desse íon à troponina C (TnC), possibilitando a interação actina-miosina. A intensidade da contração depende da quantidade e da sensibilidade dos miofilamentos ao Ca^{2+}. Em condições fisiológicas, a ativação elétrica ou excitação desencadeia a contração; e o aumento de $[Ca^{2+}]_i$ é o fator que acopla os dois fenômenos: excitação/contração. O conjunto desses processos é denominado acoplamento excitação-contração. Quando a concentração intracelular de Ca^{2+} começa a diminuir, principalmente pela recaptura de cálcio pela da bomba de Ca^{2+} do RS (SERCA2a), inicia-se o relaxamento. A atividade

da SERCA2a é o processo mais importante na re-captação do Ca^{2+} nos cardiomiócitos.

Outras proteínas, como o trocador Na^{+}/ Ca^{2+} e a bomba de Ca^{2+} do sarcolema, atuam como reguladores do fluxo de Ca^{2+} no miocárdio. Dessa maneira, o ciclo do trânsito de Ca^{2+} intracelular é modulado pela atividade de diferentes canais. Canais do tipo L, que regulam a contração e a atividade da SERCA2a, regula também o relaxamento miocárdico (Opie, 1998; Bers, 2001; 2002) (figura 1).

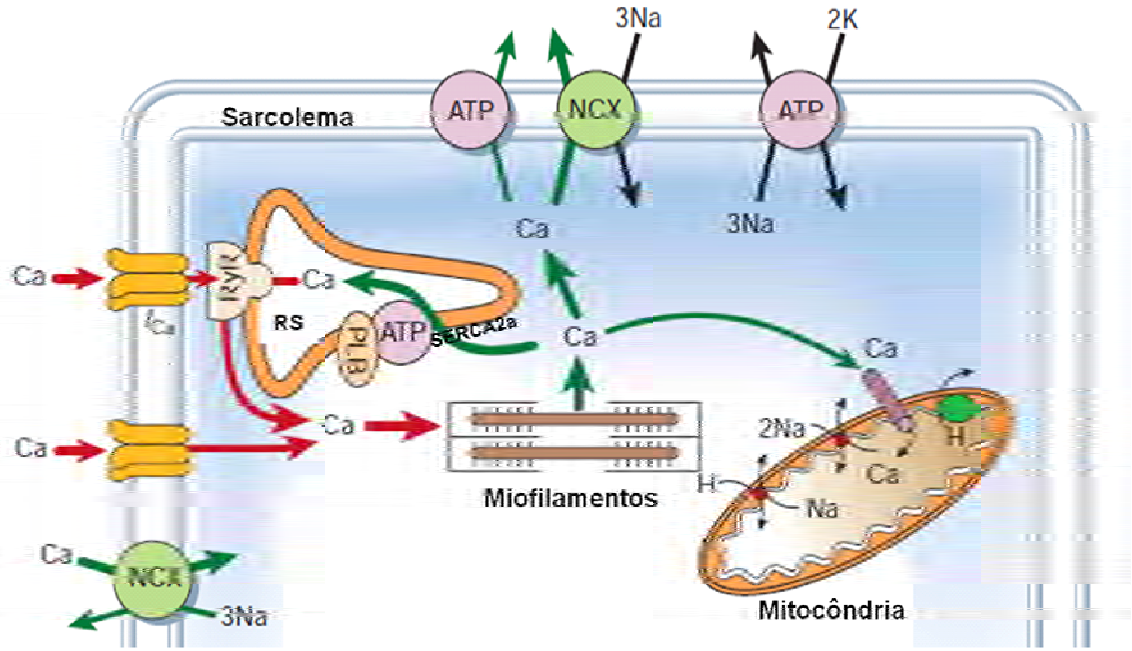

Figura 1: Representação esquemática dos principais mecanismos envolvidos no processo de acoplamento excitação-contração (E-C) no miócito cardíaco de mamíferos. No cardiomiócito normal o potencial de ação (PA), despolariza o sarcolema, iniciando o acoplamento E-C, que resulta na contração e relaxamento do miocárdio. O acoplamento E-C compreende os processos envolvidos na ativação das proteínas contráteis pelos íons cálcio e a sua subseqüente remoção para que o relaxamento muscular aconteça. O PA ativa canais de cálcio voltagem dependentes (canais tipo L) e permitem a passagem de pequenas quantidades de cálcio extracelular para o citosol. Este cálcio, ativa receptores rianodínicos (RyRs) e a liberação rápida de grande quantidade de íons cálcio, presentes no retículo sarcoplasmático (RS), para o citosol. O aumento da concentração de cálcio interage

com a troponina C, o que resulta no encurtamento do sarcômero, e conseqüente, contração muscular. O relaxamento ocorre consecutivo à remoção do cálcio citosólico através da atividade da bomba de cálcio pelo RS, SERCA2a, pela troca Na^{+}/Ca^{2+} e pela bomba de cálcio do sarcolema que retiram, respectivamente, 92%, 7% e 1% do cálcio liberado durante a despolarização celular. RS – retículo sarcoplasmático; NCX - mecanismo de troca sódio-cálcio; ATP - ATPase de Ca; ICa - corrente de Ca por meio de canais tipo L; RyRs – receptores de rianodina; PLB – fosfolambam; ATP – trifosfato de adenosina (modificado de Bers, 2002).

Em relação à estimulação beta-adrenérgica, suas principais conseqüências em nível celular são o aumento da força de contração (efeito inotrópico positivo) e o aumento da taxa de relaxamento (efeito lusitrópico positivo). A via beta-adrenérgica compreende os processos envolvidos na interação das catecolaminas com os receptores (β1 e β2 específicos) presentes na membrana do cardiomiócito (sarcolema). Após a conversão do estímulo extracelular (em resposta intracelular), ocorre uma cascata de eventos, com alterações bioquímicas e moleculares para acontecer a contração e relaxamento dos cardiomiócitos (Opie, 2001).

Este processo ocorre quando um agonista beta-adrenérgico (o isoproterenol, por exemplo), interage com os receptores beta. Esta ligação desencadeia alterações das proteínas G do sarcolema, levando à ativação da adenil-ciclase e formação da adenosina 3'5' monofosfato (AMP-cíclico). O aumento do AMPc ativa a proteinaquinase-A (PKA) do citosol da célula. A PKA estimula o metabolismo dos cardiomiócitos e fosforila as proteínas dos canais tipo L do sarcolema, permitindo uma maior entrada de Ca^{2+} para o citosol, durante a despolarização celular. O aumento do influxo de cálcio induz ainda à liberação de maior quantidade desse íon dos estoques do RS para o citosol, resultando no aumento tanto da atividade ATPásica da miosina, quanto da

velocidade e força de contração (Opie et al., 1998; 2001). A proteína de membrana do RS fosfolambam, inibe a atividade da SERCA2a, dificultando a recaptação do cálcio para o RS. A ativação da PKA tem o papel de fosforilar a proteína de membrana fosfolambam e inibir sua função. Como consequência, ocorre aceleração da contração e do relaxamento miocárdico. Dessa maneira, a estimulação da via beta-adrenérgica aumenta a força de contração e acelera a contração e o relaxamento miocárdico (Strang et al., 1994). Alguns autores relatam que a participação desses transportadores e receptores é dependente da espécie (Bassani et al., 1994), da fase de desenvolvimento pré e pós-natal (Bassani & Bassani, 2002) e pode estar alterada em certas condições fisiopatológicas (Pogwizd et al., 1999). Na literatura, poucos estudos, até o presente momento, avaliaram a relação entre função mecânica cardíaca, morfologia celular, liberação espontânea de cálcio intracelular do RS e restrição proteica após amamentação. Acredita-se que além das alterações morfológicas do miocárdio evidenciadas pela desnutrição proteica também ocorrem modificações nas propriedades mecânicas intrínsecas dos miócitos cardíacos, podendo este ser um fator adicional na disfunção da mecânica do coração. Além disso, ainda é pouco conhecido quais as propriedades mecânicas dos cardiomiócitos são modificadas durante a restrição proteica que podem interferir no funcionamento cardíaco. Elucidar esses mecanismos funcionais e moleculares pode ajudar a compreender de forma mais ampla o impacto da desnutrição sobre o músculo estriado cardíaco, além de definir o quanto as alterações nesses componentes são capazes de contribuir para a disfunção cardíaca.

2.0. Objetivo geral:

Investigar os efeitos da desnutrição proteica sobre os aspectos morfofuncionais, propriedades mecânicas de miócitos ventriculares isolados e perfil molecular das proteínas responsáveis pelo transiente de Ca^{2+} intracelular.

Objetivos Específicos:

- Investigar a influência da restrição proteica experimental sobre a morfologia do miocárdio em ratos *Fisher;*

- Investigar a influência da restrição proteica experimental sobre as propriedades mecânicas de cardiomiócitos isolados do ventrículo esquerdo em ratos *Ficher;*

- Investigar influência da restrição proteica experimental sobre a participação do cálcio e do sistema β-abrenérgico em cardiomiócitos do ventrículo esquerdo em ratos *Fisher.*

- Investigar influência da restrição proteica experimental sobre o transiente e *sparks* de cálcio em cardiomiócitos do ventrículo esquerdo em ratos *Fisher.*

- Investigar a influência da restrição proteica experimental sobre o perfil molecular das proteínas de membrana SERCA2a em cardiomiócitos isolados do ventrículo esquerdo em ratos *Fisher.*

3.0. Referências Bibliográficas

Agarwal KN, Prasad C. & Taneja V. (1981) Protein deprivation and the brain: effect on enzymes and free amino acids related to glutamate metabolism in rats. Ann.Nutr.Metab 25: 228-233.

Barker DJ, Gluckman PD, Godfrey KM, Harding JE, Owens JA, Robinson JS. (1993) Fetal nutrition and cardiovascular disease in adult life. Lancet 341: 938-941.

Bassani RA, Bassani JWM, Bers DM. (1994) Relaxation in rabbit and rat cardiac cells: species dependent differences in cellular mechanisms. J Physiol 476: 279-293.

Bassani RA, Bassani JWM. (2002) Contribution of Ca^{2+} transporters to relaxation in intact ventricular myocytes from developing rats. American Journal of Physiology 282: 2406-2413.

Belmar JCPHA & S-M.R. (1996) Malnutrition early in life impairs alpha-2 adrenoreceptor regulation of noradrenaline release in the rat cerebral cortex. Nutrition Research 16, 1734-1740.

Benabe JE, Martinez-Maldonado M. (1998) The impact of malnutrition on Kidney function. Miner Electrolyte Metab 24: 20-26.

Berridge MJ, Lipp P, Bootman MD. (2000) The versatility and universality of calcium signalling. Nature Reviews 1: 11-21.

Bers DM. (2001) Excitation-Contraction Coupling and Cardiac Contractile Force. The Netherlands: Kluwer Academic Publishers 32: 283-284.

Bers DM. (2002) Cardiac excitation-contraction coupling. Nature 415: 198-205.

Cicogna AC, Padovani CR, Georgette JC, Aragon FF, Okoshi MP. (1999) Effects of Protein-Calorie Restriction on Mechanical Function of Hypertrophied Cardiac Muscle. *Arq. Bras. Cardiol.* 72, 436-440.

Cicogna AC, Padovani CR, Okoshi K, Aragon FF, Okoshi MP. (2000) Myocardial function during chronic food restriction in isolated hypertrophied cardiac muscle. Am J M Sci 320: 244-248.

Cortius HB, Zimanye MA, Maka N, Herath T, Thomas W, Laarse AVD, Wreford NG, Black J. (2005) Effect of intrauterine growth restriction on the number of cardiomyocytes in the rat hearts Pediatric Research 57: 796-800.

Christian P. & Stewart CP. (2010) Maternal micronutrient deficiency, fetal development and the risk of chronic disease. The Journal of Nutrition J Nutr 140: 437-445.

Cunha DF, Cunha SF, Reis MA, Teixeira VP. (2002) Heart weight and heart weight / body weight coefficient in malnourished adults. Arquivos Brasileiros de Cardiologia 78: 382-387.

Drott C, Lundholm K. (1992) Cardiac effects of caloric restriction-mechanisms and potential hazards. Int J Obes Relat Meta Disord 16:481-486.

Fabiato A. (1983) Calcium-induced release of calcium from the cardiac sarcoplasmic reticulum. The American Journal of Physiology 245: 1-14.

Fioretto JR, Querioz SS, Padovani CR, Matsubara LS, Okoshi K, Matsubara BB. (2001) Ventricular remodeling and diastolic myocardial dysfunction in rats submitted to protein-calorie malnutrition. Am J Physiol 282: 1327-1333.

Freitas RA, Souza LB, Pinto LP. (1994) Morphological and morphometric analysis of the parotid glands of rats submitted to different levels of protein deficiency. Rev Odontol Univ São Paulo 8: 43-49.

Gluckman PD, Hanson MA. (2004) The developmental origins of the metabolic syndrome. Trends Endocrinol Metab 15:183-187.

Gruber C, Nink N, Nikam S, Magdowski G, Kripp G, Voswinckel R, Mühlfeld C. (2012) Myocardial remodelling in left ventricular atrophy induced by caloric restriction J Anat 220: 179–185.

Hanson M. (2002) Birth weight and the fetal origins of adult disease. Pediatr Res 52: 473-484.

Hoppe CC, Evans RG, Bertram JF. & Moritz KM. (2007) Effects of dietary protein restriction on nephron number in the rats. Am. J. Physiol. 292: 768-774.

Kothari SS, Patel TM, Shetalwad AN, Patel TK. (1992) Left ventricular mass and function in children with severe protein energy malnutrition. Int J Cardiol 35: 19-25.

Lim K, Zimanyi MA. and Black MJ. (2010) Effect of maternal protein restriction during pregnancy and lactation on the number of cardiomyocytes in the post proliferative weanling rat heart. The Anatomical Record 293: 431-437.

Okoromah CAN, Ekure EN, Lesi FEA, Okunowo WO, Tijani BO, Okeiyi JC. (2011) Prevalence, profile and predictors of malnutrition in children with congenital heart defects: a case–control observational study. Arch Dis Child 96: 354-360.

Opie LH. (1998) Myocardial contraction and relaxation. In: Opie LH, ed. The heart. Physiology, from cell to circulation. Philadelphia: Lippincott-Raven 14: 209-231

Opie LH. (2001) Normal and abnormal cardiac function: mechanism of cardiac contraction and relaxation. In: Braunwald E, Zipes DP, Libby P. Heart disease: a textbook of cardiovascular medicine. 6th ed. Philadelphia: Saunders;. 443-78.

Pedrosa MT.& Moraes-Santos T. (1987) Neuronal protein biosyntesis by neonatally malnourished and nutritional recovered rats. Brazilian Journal of Medical and Biological Research 20: 338-345.

Phillips DIW, Barker DJP, Hales CN, Hirst S. & Osmond C. (1994) Thinness at Birth and Insulin-Resistance in Adult Life. Diabetologia 37: 150-154.

Pinotti MF, Leopoldo AS, Dal-Pai Silva M, Sugizaki MM, Nascimento AF, Lima-Leopoldo AP, Aragon FF, Padovani CR, Cicogna AC. (2010) A comparative study of myocardial function and morphology during fasting/refeeding and food restriction in rats. Cardiovascular Pathology 19: 175-182.

Pogwizd SM, Qi M, Yuan W, Samarel AM, Bers DM. (1999) Upregulation of Na^{+}/Ca^{2+} exchanger expression and function in an arrhythmogenic rabbit model of heart failure. Circulation Research 85: 1009-1019.

Sawaya AL, Martins P, Hoffman D, Roberts SB. (2003) The link between childhood undernutrition and risk of chronic diseases in adulthood: A case study of Brazil. Nutrition Reviews 61: 168-175.

Strang KT, Sweitzer NK, Greaser ML, Moss RL. (1994) Beta-adrenergic receptor stimulation increases unloaded shortening velocity of skinned single ventricular myocytes from rats. Circ Res 74: 542-549.

Vandewoude, MFJ. (2008) Morphometric changes in microvasculature in rat myocardium during malnutrition. J Par Ent Nutrution 19: 376-380.

WHO - World Health Organization. Obesity (2010) Facts related to chronic diseases.
Site: http://www.who.int/dietphysicalactivity/publications/facts/chronic/en

4.1. Paper 1 - Nutrition research submitted

Protein restriction after weaning modifies the calcium transient and induces single left ventricular cardiomyocytes contractile dysfunction in rats

Abstract

Protein restriction (PR) is associated with cardiovascular diseases. The purpose of this study was to investigate the effects of a short-term PR after weaning on single ventricular cardiomyocytes contractile function. Twenty-eight day old male Fischer rats were randomly divided into control group (CG, n = 16) and protein-restricted group (PRG, n = 16). After weaning, CG and PRG animals received isocaloric diets containing 15% and 6% protein, respectively, for 35 days. Then, biometrical parameters were analyzed and single left ventricular (LV) cardiomyocytes were isolated for the measurements of contractile function and calcium transient, both at a pacing frequency of 3Hz at room temperature. PRG animals had lower body weight (BW), LV weight, but increased LV weight to BW ratio than CG animals. PRG animals exhibited reduced cardiomyocyte length, width, volume and sarcomere length compared to CG animals. Cardiomyocytes from PRG animals showed lower amplitude of shortening, slower time to peak of shortening and longer time to half relaxation than those from CG. Cardiomyocytes from PRG animals also presented lower peak of calcium transient and longer calcium transient decay time as compared to CG. Taken together, the results indicated that short-term PR after weaning

induces contractile dysfunctions in single LV cardiomyocytes of rats which is probably associated with pathological changes in the cell calcium transient.

Keywords: Malnutrition, cardiomyocytes, cell contractility, calcium transient, morphology.

1. Introduction

Malnutrition based on reduced protein intake leads to changes in cardiovascular homeostasis [1-3]. Studies from our laboratory have shown that animals submitted to a model of short-term protein restriction (PR) (i.e. reduction of 60% in the dietary protein for 35 days) after weaning are characterized mainly by increased levels of baseline mean blood pressure, sympathetic efferent activity directed to the heart and heart rate [4-6]. Different models of malnutrition such as protein-calorie or food restriction applied to rats have been shown to depress left ventricular (LV) mechanical function [7-11], despite some results in contrast [8,12]. The main mechanical changes observed when using isolated heart or papillary muscle preparations are reduced contractility and prolonged time courses of contraction and relaxation [8,11,13].

Nevertheless, up to date there are no data in the literature showing these deleterious LV mechanical functional changes in response to PR at the cellular level. Thus, the aim of this study was to test the effects of a short-term PR after weaning on single LV cardiomyocyte contractile function. We hypothesized that short-term PR after weaning promotes LV cardiomyocytes dysfunction in rat heart.

2. Methods and materials

2.1. Experimental Protocol

Twenty-eight day old male Fischer rats provided by the animal facilities of the Federal Unversity of Ouro Preto (UFOP), Brazil, were divided according to the diet received: control group (CG = 12) and protein-restricted group (PRG = 12). After weaning, CG animals were fed with standard rodent chow (AIN-93 - 15%

protein) and the PRG animals received a diet containing 6% protein (casein) for 35 days [5]. The diets were isocaloric (422 kcal/100 g of diet) and the salts and vitamins were at similar concentrations in both diets (Table 1). The animals were maintained in a controlled temperature room (22ºC) with 12-hour light/dark cycles and had water *ad libitum*. The experimental protocols were approved by the institutional ethics committee (UFOP protocol 30/2009).

Table 1

Chemical composition of the diets (g/100g of chow)

	CG	**PRG**
Protein (casein)	15	6
Corn starch	68	77
Soybean oil	10	10
Salts mix	5	5
Vitamin mix	1	1
Fiber (cellulose)	1	1
Total caloric values	**422 Kcal**	**422 Kcal**

Control Group (CG) – Protein (Caseín) 15%;

Protein Restriction Group (PRG) - Protein (Caseín) 6%.

2.2. Biometric analysis

Thirty-five days after the protein restriction the animals from each group were weighed and euthanized under anesthesia. The left ventricles were dissected and weighed separately. The relative LV weight was calculated by dividing the left ventricular weight (LVW) by body weight (BW) [5].

2.3. Cardiomyocytes isolation

After euthanasia, the heart was quickly removed and LV cardiomyocytes were isolated as described by Novaes *et al.* [14]. Briefly, the heart was cannulated through the aorta in a Langendorff system and perfused with isolation solution (composition [mM]: 130 Na^+, 5.4 K^+, 1.4 Mg^{2+}, 140 Cl^-, 0.75 Ca^{2+}, 5.0 Hepes, 10 glucose, 20 taurine and 10 creatine, pH= 7.3 at room temperature). Then, the heart was perfused with calcium-free solution containing 0.1 mM ethylene glycol-bis (beta-aminoethyl ether)-*N*, *N*, *N′*, *N′*-tetraacetic acid (EGTA) for 5 min. The heart was then perfused with a solution containing 1.0 $mg.ml^{-1}$ of type 2 collagenase (Worthington, USA) and 100.0 mM $CaCl_2$ for 25 min. The solutions were oxygenated (100% O_2, White Martins, SP, Brazil) and maintained at 35 ºC. After perfusion, the left ventricle was dissected and placed in a glass recipient with an enzyme solution containing collagenase (5.0 ml) and bovine serum albumin (10%). The recipient was shaken moderately for 5 min at 37 ℃, after which the solution was centrifuged. The supernatant was removed and cardiomyocytes were resuspended in isolation solution, stored in a refrigerator (5 ℃) and used in a period up to 4 h after isolation. Only calcium-tolerant, quiescent, rod-shaped cardiomyocytes showing clear cross striations were studied.

2.4. Cell contractile function

Cardiomyocytes contractile function was measured using an edge motion detection system (Ionoptix, Milton, MA, USA) mounted on an inverted microscope (Nikon Eclipse TS100®, Tokyo, Japan), as previously described [14]. Briefly, myocytes were placed in an experimental chamber with the base

glass and bathed in buffer with the following composition (in mM): 136.9 NaCl; 5.4 KCl; 0.37 NaH_2PO_4; 0.57 $MgCl_2$, 5.0 Hepes; 5.6 glucose and 1.8 $CaCl_2$ (pH= 7.4 at room temperature). Cardiomyocytes were field stimulated at a frequency of 3.0 Hz (10 volts, 5 min duration) using a pair of steel electrodes (Myopacer, Ionoptix, MA, USA). Cardiomyocytes were visualized on a personal computer monitor with a NTSC camera (MyoCam, Ionoptix, MA, USA) attached to the microscope using an image detection program (Ionwizard, Ionoptix, MA, USA). This image was used to measure cell shortening (our index of contractility) in response to electrical stimulation using a video motion edge detector (IonWizard; IonOptix, MA, USA). All parameters were evaluated using customized software developed in the MatLab® platform. Cell shortening from stimulation (expressed as a percentage of resting cell length), time to peak of shortening and time to half relaxation were measured and calculated as previously described [14].

2.5. Cell dimensions

Cardiomyocytes were placed in an experimental chamber as mentioned above and were visualized on a personal computer monitor with a NTSC camera (Myocam, Ionoptix, MA, USA) attached to the microscope using an image detection program (Ionwizard, Ionoptix, MA, USA). These resting cell images were used to measure the cell length and width. The cell volume was calculated using the formula: Volume (pL) = length (mm) x width (mm) x (7.59 x 10-3 pL/mm^2) [15]. Using a Fast Fourier Transformation function of the same system of image analysis the cardiomyocytes sarcomere length was also measured.

2.6. Cell calcium transient

Cardiomyocytes were loaded with fluo-4 AM solution 10µmol/L (Molecular Probes, Eugene, OR, USA) for 30 minutes at room temperature. Then, cardiomyocytes were washed with a normal tyrode solution to remove excess dye [16]. Next, cardiomyocytes were stimulated through a pair of platinum electrodes with a voltage pulse of 0.2 ms, at 3 Hz [17]. The confocal scanning system LSM 510® Meta (Zeiss, Jena, Germany) with an immersion objective (x63) was used to obtain fluorescence images. Fluo-4 was excited at 488 nm (argon laser) and emission intensity was measured at 510 nm. Images of cardiomyocytes were scanned with a line of 512 pixels, randomly positioned along a longitudinal axis of the cell, with caution to avoid passing by the nucleus. The cells were scanned every 1.54 ms, and the sequences of scans were transmitted in series to create two-dimensional images on the x-axis with a temporal sequence. Digital images processing was performed using custom routines written in IDL (Research Systems, Boulder, CO, USA). Ca^{2+} levels are presented as $\Delta F/F_0$, where F_0 is the minimum fluorescence intensity measured between contractions at 3 Hz on the diastolic phase of the transient, and ΔF equals $(F-F_0)$.

2.7. Statistics

Data are presented as mean and standard error of mean (mean ± SEM). The normal distribution of data was verified by using the Kolmogorov-Smirnov test. Biometric and cell contractile function data were compared using the unpaired Student's t test. Morphometric data were compared using the Mann-Whitney test. A value of $p < 0.05$ was considered statistically significant.

3. Results

3.1. Biometric parameters

Protein restriction decreased body weight (BW), left ventricular weight (LVW) and increased the LVW to BW ratio (Figure 1).

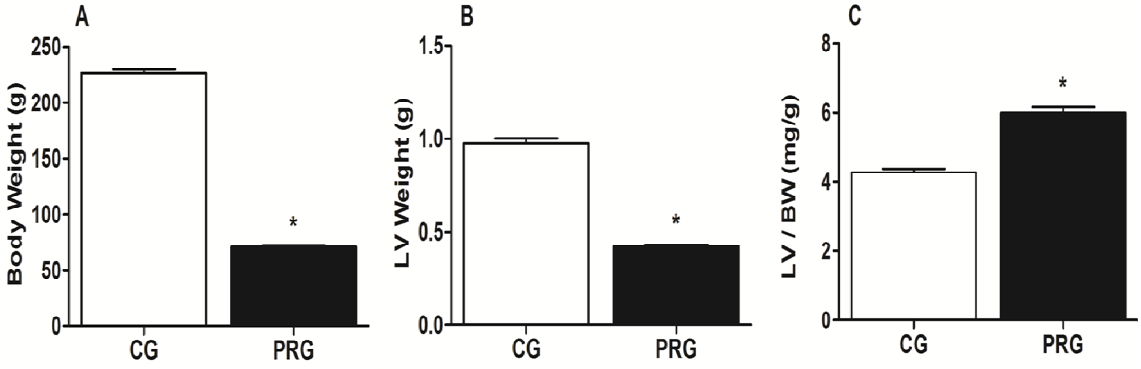

Figure 1. Biometric parameters. CG, control group. PRG, protein-restricted group. LV, left ventricle. LV/BW, left ventricle weight to body weight ratio. Data are means ± SEM of 12 animals in each group. *p <0.05.

3.2. Cell dimensions and contractile function

The protein restriction reduced significantly all cell dimensions analyzed (Table 2). There was significant reduction in shortening amplitude (Figure 2A), prolongation of the time to peak of shortening (Figure 2B) and of the time to half relaxation (Figure 2C) in LV myocytes from PRG animals compared to those from CG.

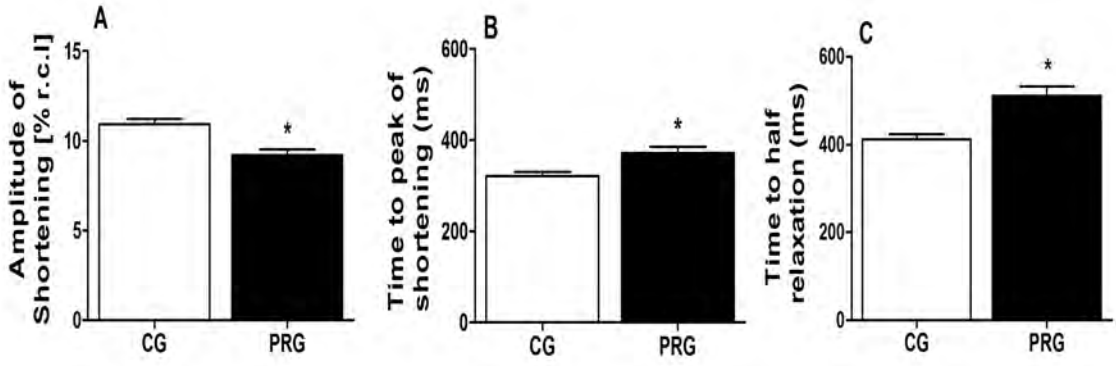

Figure 2. Contractile function of single left ventricular myocytes. CG, control group. PRG, protein-restricted group. Amplitude of shortening is expressed as percentage of resting cell length (% r.c.l.). Data are means ± SEM of 95 cells from PRG and from CG. *p <0.05.

Table 2 Morphological properties of single left ventricular mocytes

	CG	**PRG**	**% PRG / GC**
Length (µm)	130.62 ± 2.35	99.69 ± 1.70*	24%
Width (µm)	24.12 ± 0.35	15.37 ± 0.06*	36%
Sarcomere length (µm)	1.84 ± 0.02	1.6 ± 0.13*	14%
Volume (pl)	23.58 ± 0.98	11.54 ± 0.59*	51%

Data are expressed as mean ± SEM of 80 cardiomyocytes per group. *p<0.05. CG, control group. PRG, protein-restricted group.

3.3. Cell calcium transient

Figure 3 shows typical representative line-scan images recorded from field-stimulated CG (A) and PRG (B) isolated cardiomyocytes loaded with the Ca^{2+} indicator fluo-4 AM. Protein restriction after weaning decreased significantly the peak of the calcium transient in single left ventricular myocytes (Figure 3. C) and increased significantly the calcium transient decay time (Figure 3. D) as compared to CG.

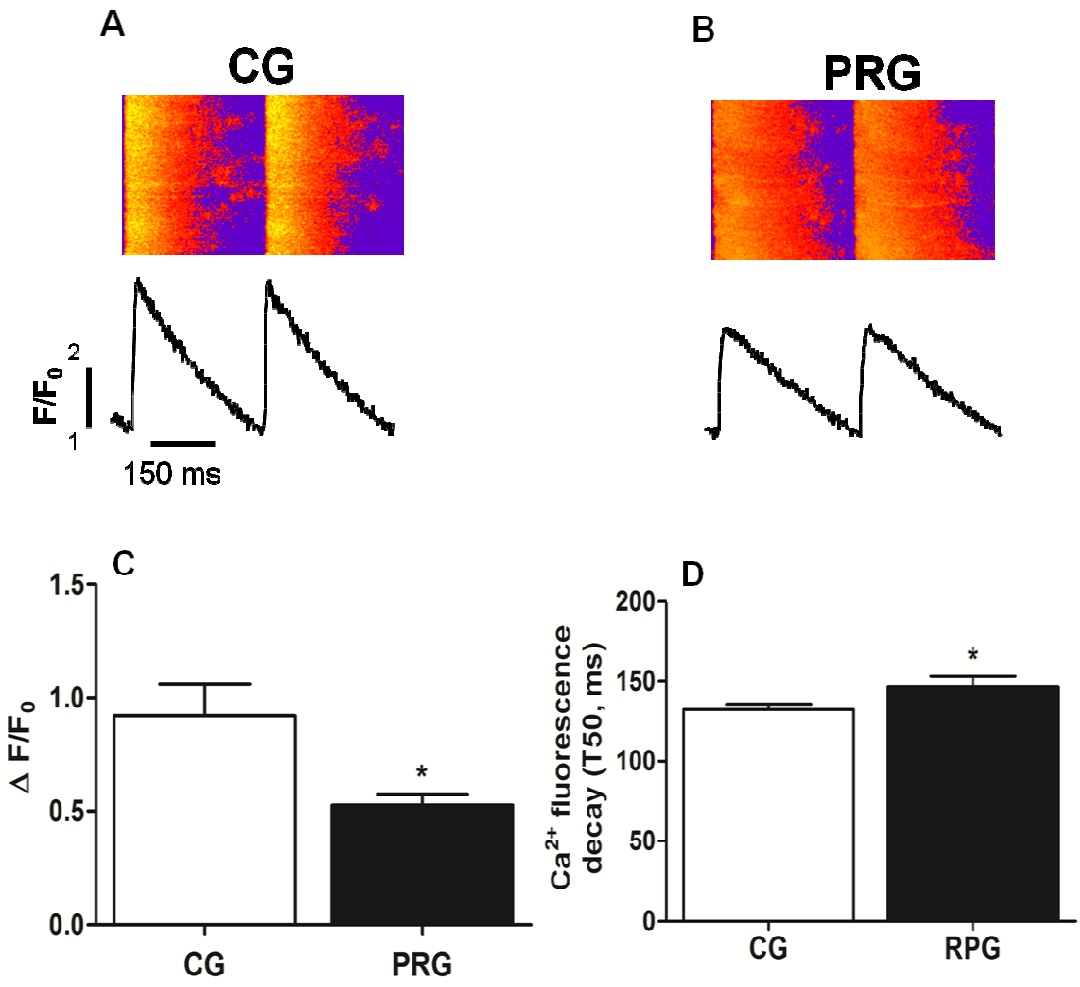

Figure 3. Calcium transients of single left ventricular myocytes. CG, control group. PRG, protein-restricted group. A and B, representative line-scan images recorded from field stimulated CG and PRG cardiomyocytes, respectively, loaded with the Ca^{2+} indicator fluo-4 AM (5μM). Ca^{2+} signal is shown as fluorescence ratio (F/F_0), with the fluorescence intensity (F) normalized to the minimal intensity measured between 3-Hz contractions at diastolic phase (F_0). C, peak of Ca^{2+} transients. D, time to 50% of Ca^{2+} fluorescence decay. CG, control group. PRG, protein-restricted group. Data are means ± SEM of 34 cells from CG and 24 cells from PRG. *p <0.05.

4. Discussion

In this study we demonstrated for the first time that PR induced contractile dysfunctions in single LV cardiomyocytes in rats. Animals submitted to PR after

weaning showed a marked depression in the amplitude of cell shortening and prolongation of cell shortening and relaxation times. In addition, such dysfunctions were accompanied by a reduction in the peak of the calcium transient and by a prolonged calcium transient decay time.

Our model of PR induced inotropic and chronotropic effects on LV cardiomyocytes. Such phenomena is directly affected by intracellular Ca^{2+} handling which is regulated by the sodium-calcium exchanger (NCX), L-type Ca^{2+} channel, sarcoplasmic reticulum (SR), ryanodine receptor channel (RyR2), SR Ca^{2+}-ATPase pump (SERCA2a), phospholamban (PLB), and myofilament Ca^{2+} affinity [18]. Although we did not measure Ca^{2+} regulatory protein content or activity, the reduced cell shortening in PRG might be due to adaptations of such cellular structures. Indeed, food restriction has been shown to diminish the protein content of L-type Ca^{2+} channels [19] and ryanodine receptors (RyR2) [20] and RyR2 activity [21] in the left ventricle of rats. Such adaptations would decrease and slow the intracellular Ca^{2+} availability and thus reduce the cell contraction force and velocity. In fact, the results of the present study demonstrated that our model of short-term PR decreased the peak of LV cardiomyocyte calcium transients.

The time courses of cell contraction and relaxation were prolonged in PRG rats. Such adaptations were accompanied by a slower calcium transient decay time. SERCA2a and PLB are responsible for the higher rate of cytosolic Ca^{2+} reuptake in rats (92%) [18]. Thus, a down-regulation in the expression or function of SERCA2a and PLB can be directly linked to the prolonged relaxation time of cell contraction and calcium transient decay time, as evidenced here in protein restricted rats. Although food restriction did not change the levels of left

ventricle SERCA2a and PLB mRNAs in rats [20], it decreased the SR Ca^{2+} uptake activity in the rat myocardium [22]. In addition, there are evidences that food restriction reduces the rate of dissociation of Ca^{2+} from troponin-C [21-23].

The prolonged cell shortening time courses observed in response to PR may also be due to the changes in the myosin isozyme distribution. In rats, V1 isomyosin shows high ATPase and contractile activity compared with V3 isomyosin [24]. There are evidences that short-term food restriction induces a shift in the myosin isozyme distribution toward the slow V3 isoform [7,25].

In the present study short-term PR reduced the animal BW and LVW, but the LVW to BW ratio increased. These results have been shown previously in this model [4-6] and food restricted rats [8,10,11,20]. At the cellular level, PR reduced the LV myocyte length, width, volume and sarcomere length. These changes reflect the reduced LVW in PRG rats and confirm the remodeling process that occurs in the myocardium in response to PR.

Altogether our data on cellular mechanical dysfunctions in response to PR are consistent with those observed in whole heart and in multicellular preparations which shows reduced contractility and prolonged time courses of contraction and relaxation in undernourished rats. In summary, short-term PR after weaning induces contractile dysfunctions in single LV cardiomyocytes of rats which is probably associated with pathological changes in the cell calcium transient.

Acknowledgements

Research supported by FAPEMIG. Ms. A.R. Penitente was a recipient of a PhD scholarship from FAPEMIG. A.J. Natali is a CNPq fellow.

References

[1] Langley-Evans SC, Phillips GJ, Benediktsson R, Gardner DS, Edwards CR, Jackson AA, Seckl JR. Protein intake in pregnancy, placental glucocorticoid metabolism and the programming of hypertension in the rat. Placenta 1996; 17:169-172.

[2] Barker DJP, Clark PM. Fetal undernutrition and disease in later. Life J Reprod Fertil 1997;2:105-112.

[3] Plagemann A, Harder T, Rake A, Melchior K, Rohde W, Dorner G. Hypothalamic nuclei are malformed in weanling offspring of low protein malnourished rat dams. J Nutr 2000;130:2582-2589.

[4] Oliveira EL, Cardoso LM, Pedrosa ML, Silva ME, Dan NJ, Colombari E, Moraes MF, Chianca DAJr. Alow protein diet causes na increase in the basal levels and variability of mean arterial pressure and heart rate in Fisher rats. Nutr Neurosci 2004;7:201-205.

[5] Penitente AR, Fernandes LG, Cardoso LM, Silva ME, Pedrosa ML, Silva AL, Haibara AS, Moraes MFD, Chianca DAJr. Malnutrition enhances cardiovascular responses to chemoreflex activation in awake rats. Life Sci 2007;81:609-614.

[6] Martins CDD, Chianca DAJr, Fernandes LG. Cardiac autonomic balance in rats submitted to protein restriction after weaning. Clin Exp Pharm Physiol 2011;38:89-93.

[7] Haddad F, Bodel PW, McCue SA, Herrick PE, Baldwin KM. Food restriction-induced transformations in cardiac functional and biochemical properties in rats. J Appl Physiol 1993;74:606-612.

[8] Cicogna AC, Padovani CR, Okoshi K, Matsubara LS, Aragon FF, Okoshi MP. The influence of temporal food restriction on the performance of isolated cardiac muscle. Nutr Res 2001;21:639-648.

[9] Okoshi K, Matsubara LS, Okoshi MP, Cicogna AC, Fioretto JR, Padovani CR. Food restriction-induced myocardial dysfunction demonstrated by the combination of in vivo and in vitro studies. Nutr Res 2002;22:1353-1364.

[10] Gut AL, Okoshi MP, Padovani CR, Aragon FF, Cicogna AC. Myocardial dysfunction induced by food restriction is related to calcium cycling and beta-adrenergic system changes. Nutr Res 2003;23:911-919.

[11] Pinotti MF, Leopoldo AS, Dal-Pai Silva M, Sugizaki MM, Nascimento AF, Lima-Leopoldo AP, Aragon FF, Padovani CR, Cicogna AC. A comparative study of myocardial function and morphology during fasting/refeeding and food restriction in rats. Cardiovasc Pathol 2010;19:175-182.

[12] Nutter DO, Murray TG, Heymsfield SB, Fuller EO. The effect of chronic protein-calorie undernutrition in the rat on myocardial function and cardiac function. Circ Res 1979;45:144-152.

[13] Cicogna AC, Padovani CR, Okoshi K, Aragon FF, Okoshi MP. Myocardial function during chronic food restriction in isolated hypertrophied cardiac muscle. Am J M Sci 2000;320:244-248.

[14] Novaes R.D., Penitente A.R., Gonçalves R.V., Talvani A., Neves C.A., Maldonado I.R.S.C. & Natali A.J. Effects of Trypanosoma cruzi infection on myocardium morphology, single cardiomyocyte contractile function and exercise tolerance in rats. Int J Exp Pathol 2011;92:299-307.

[15] Satoh H, Delbridge LM, Blatter LA, Bers DM. Surface: volume relationship in cardiac myocytes studied with confocal microscopy and membrane capacitance measurements: species-dependence and developmental effects. Biophys J 1996;32:1494-1504.

[16] Lauton-Santos S, Guatimosim S, Castro CH, Oliveira FA, Almeida AP, Dias-Peixoto MF, Gomes MA, Pessoa P, Pesquero JL, Pesquero JB, Bader

M, Cruz JS. Kinin B1 receptor participates in the control of cardiac function in mice. Life Sci 2007;81:814-822.

[17] Guatimosim S, Sobie EA, dos Santos CJ, Martin LA, Lederer WJ. Molecular identification of a TTX-sensitive Ca2+ current. Am J. Physiol-Cell. 2001;280:1327-1339.

[18] Bers DM. Cardiac excitation-contraction coupling. Nature 2002;415:198-205.

[19] De Tomasi LC, Bruno A, Sugizaki MM. Food restriction promotes downregulation of myocardial L-type Ca^{2+} channels. Can J Pharm Sci 2009;87:426-431.

[20] Vizotto VA, Sugizaki MM, Lima AP. Down-regulation of the cardiac sarcoplasmic reticulum ryanodine channel in severely food restricted rats. Braz J Med Biol Res 2007;40:27-31.

[21] O'Brien PJ, Shen H, Bissonette D, Jeejeebhoy KN. Effects of hypocaloric feeding and refeeding on myocardial Ca and ATP cycling in the rat. Mol Cell Biochem 1995;142:151-161.

[22] Rupp H, Maisch B, Brilla CG. Schedule-induced psychological stress and molecular structures of cardiomyocytes. Am J Physiol 1997;272:776-782.

[23] Klebanov S, Herlihy JT. Effect of life-long food restriction on cardiac myosin composition. J Geront 1997;52:184-189.

[24] Pope B, Hoh JF, Weeds A. The ATPase activities of rat cardiac myosin isoenzymes. FEBS Lett 1980;118:205-208.

[25] Morris GS, Surdyka DG, Haddad F. Apparent influence of metabolism on cardiac isomyosin profile of food restricted rats. Am J Physiol 1990;258:346-351.

4.2. Paper 2

Severe protein restriction after weaning reduces the expression of SERCA2a and modifies the basal and β-adrenergic contractility in murine ventricular cardiomyocytes

Abstract

It has been reported that protein restriction (PR) is able to impair cardiac structure and function. However, the mechanisms responsible for the cardiac dysfunction in PR remain poorly understood. The aim of this study was to evaluate the effects of severe protein restriction after weaning on the expression of SERCA2a and basal and β-adrenergic contractility in murine ventricular cardiomyocytes. After breastfeeding (28 days) male *Fisher* rats were randomly divided into two groups: a control group (CG, n = 20) and protein-restricted group (PRG, n = 20). The animals in the PRG and CG received isocaloric diets for 35 days containing 15% and 6% protein, respectively. The animals were then weighed, before being euthanised so that the hearts could be removed for analysis. The myocytes of the left ventricle (LV) were processed for the analysis of contractility, Ca^{2+} *sparks* and the expression of the membrane protein SERCA2a. The animals of the PRG showed a significant reduction in body, heart and left ventricle masses. Cardiomyocytes from the PRG presented with reduced amplitudes of shortening and a maximum velocity of contraction and relaxation at a baseline, as well as after β-adrenergic stimulation compared to the CG. Lower levels of SERCA2a

expression and a higher frequency and lower amplitude of Ca^{2+} *sparks* during cell diastole were observed in the cardiomyocytes from PRG. Severe protein restriction after weaning induces morphological and functional changes to the heart and ventricular cardiomyocytes. The pathological changes of cardiomyocyte mechanics suggest the potential involvement of the β-adrenergic system, which is possibly associated with changes in SERCA2a expression and disturbances in Ca^{2+} intracellular kinetics.

Keywords: isolated cardiac myocytes, left ventricle, cardiac dysfunction, calcium *sparks*, β-adrenergic system.

1. Introduction

There is evidence that malnutrition in early life stages is associated with cardiac dysfunction (De Tomazi et al., 2009). Despite the extensive literature on the impact of malnutrition on the digestive, endocrine, and musculoskeletal systems (Okoromah et al., 2011; Gruber et al, 2012), little is known about the effects of severe protein restriction (PR) on the function of the cardiovascular system (Penitente et al., 2007; Martins et al., 2011). Even more scarce is information regarding the cardiac molecular and cellular adaptations that are induced by protein restriction, which can potentially modify the contractile performance of cardiomyocytes and the whole heart (Cicogna, 2001).

Previous studies indicated that a 50% food restriction is able to induce cardiac dysfunction that manifests as pathological changes in cardiac contraction and relaxation, which are associated with a decreased sensitivity to calcium (Sugizaki et al., 2009; Gut et al., 2003). However, it was not possible to determine how much each of the individual diet components contributed to or was a determinant of cardiac dysfunction. Moreover, the mechanical behaviour of isolated cardiomyocytes under conditions of protein restriction remained an issue that is still not well resolved. To the best of our knowledge, up to the present date no studies have investigated the basic characteristics of cell contractility, autonomic sensitivity, intracellular calcium kinetics and the expression of calcium regulatory proteins in cardiomyocytes in response to severe protein restriction.

Considering that the understanding of the influence of malnutrition on heart dysfunction is essential for the design of rational intervention strategies,

the present study was designed to investigate the Ca^{2+} *sparks*, the expression of SERCA2a and the involvement of the β-adrenergic system in cardiomyocyte mechanical dysfunction induced by severe protein restriction after weaning in rats.

2. Material and Methods

2.1. Animals

Twenty-eight day old male Fischer rats provided by the animal facilities of the Federal Unversity of Ouro Preto (UFOP), Brazil, were divided according to the diet received: control group (CG, n = 20) and protein-restricted group (PRG, n = 20). After weaning, CG animals were fed with standard rodent chow (AIN-93 - 15% protein) and the PRG animals received a diet containing 6% protein (casein) for 35 days (Penitente et al., 2007). The diets were isocaloric (422kcal/100g of diet) and the salts and vitamins were at similar concentrations in both diets (Table 1). The animals were maintained in a room with a controlled temperature (22 ± 2ºC) and humidity (60-70%) with 12-hour light/dark cycles and water *ad libitum*. The experimental protocols were approved by the institutional ethics committee (UFOP protocol 95/2011).

Table 1

Chemical composition of the diets (g/100g of chow)

	CG	**PRG**
Protein (casein)	15	6
Corn starch	68	77
Soybean oil	10	10

Salts mix	5	5
Vitamin mix	1	1
Fiber (cellulose)	1	1
Total caloric values	**422 Kcal**	**422 Kcal**

Control Group (CG) – Protein (Caseín) 15%;
Protein Restriction Group (PRG) - Protein (Caseín) 6%.

2.2. Biometry

Thirty-five days after protein restriction the animals from each group were weighed and euthanised under anaesthesia. The left ventricles (LV) were dissected and weighed separately. The relative heart and LV weight was calculated by dividing the heart mass and LV mass by the tibia length (TL).

2.3. Cardiomyocyte isolation

After euthanasia, the hearts were quickly removed and LV cardiomyocytes were isolated as described by Novaes et al. (2011). Briefly, each heart was cannulated through the aorta in a Langendorff system and perfused with isolation solution (composition [mM]: 130 Na^+, 5.4 K^+, 1.4 Mg^{2+}, 140 Cl^-, 0.75 Ca^{2+}, 5 Hepes, 10 glucose, 20 taurine and 10 creatine, pH = 7.3 at room temperature). Each heart was then perfused with a calcium-free solution containing 0.1mM ethylene glycol-bis (beta-aminoethyl ether)-*N*, *N*, *N′*, *N′*-tetra-acetic acid (EGTA) for 5 min. The hearts were then perfused with a solution containing 1.0mg.ml^{-1} of type 2 collagenase (Worthington, USA) and 100mM $CaCl_2$ for 25 min. The solutions were oxygenated (100% O_2, White Martins, SP, Brazil) and maintained at 35ºC. After perfusion, the left ventricle was dissected and placed in a glass receptacle with an enzyme solution containing collagenase (5ml) and bovine serum albumin (10%). The receptacle was

shaken moderately for 5 min at 37℃, after which the solution was centrifuged. The supernatant was removed and the cardiomyocytes were resuspended in an isolation solution, stored in a refrigerator (5℃) and used up to 4h after isolation. Only calcium-tolerant, quiescent, rod-shaped cardiomyocytes showing clear cross striations were studied.

2.4. Contractile analysis

Cardiomyocyte contractile function was measured using an edge motion detection system (Ionoptix, Milton, MA, USA) mounted on an inverted microscope (Nikon Eclipse TS100®, Tokyo, Japan), as previously described [Novaes et al., 2011]. Briefly, myocytes were placed in an experimental chamber with the base glass and bathed in buffer with the following composition (in mM): 136.9 NaCl; 5.4 KCl; 0.37 NaH_2PO_4; 0.57 $MgCl_2$; 5 Hepes; 5.6 glucose; and 1.8 $CaCl_2$ (pH = 7.4 at room temperature). Cardiomyocytes were field stimulated at a frequency of 3Hz (10 volts, 5 min duration) using a pair of steel electrodes (Myopacer, Ionoptix, MA, USA). Cardiomyocytes were visualised on a personal computer monitor with an NTSC camera (MyoCam, Ionoptix, MA, USA) attached to the microscope using an image detection program (Ionwizard, Ionoptix, MA, USA). This image was used to measure cell shortening (our index of contractility) in response to electrical stimulation using a video motion edge detector (IonWizard; IonOptix, MA, USA). All parameters were evaluated using customised software developed using the MatLab® platform. Cell shortening from stimulation time (expressed as a percentage of resting cell length) to the peak of shortening and time to half relaxation were measured and calculated as previously described.

2.5. β-adrenergic stimulation

The contractile response of cardiomyocytes to β-adrenergic stimulation was assessed using the non-selective agonist isoproterenol (ISO, 1, 2 and 3mM) at a stimulation rate of 1Hz. After recording the baseline cell shortening, ISO was infused in the experimental chamber through an automatic pipette. The cells were electrically stimulated after 5 min of infusion when cell shortening was recorded (Novaes et al. 2011). This procedure was repeated for each ISO concentration in different myocytes.

2.6. Ca^{2+} *sparks* analysis

Cardiomyocytes were incubated with the fluorescent probe fluo-4:00 (10μmol/L, Molecular Probes, Eugene, OR, USA) at room temperature for 20 minutes. The cells were washed with Tyrode's solution to remove the excess probe (Lauton-Santos et al., 2007). Ca^{2+} *sparks* were analysed using a confocal microscope (LSM 510 Meta Zeiss, Jena, Germany) with a 63x oil immersion objective lens and an argon laser at 488nm. The cell images were digitised at 512 pixels and the axis of the cell scan was positioned lengthwise, being careful not to intercept regions of nuclei. Cardiomyocytes were scanned at 1.54ms and the sequence of scans was obtained in a series to create two-dimensional images. Digital image processing was performed using custom routines written in IDL (Research Systems, Boulder, CO, USA). The Ca^{2+} *sparks* amplitudes are represented as ΔF/F0, where ΔF is the variation in fluorescence intensity compared to the minimal fluorescence (F0) measured at each Ca^{2+} *sparks*.

2.7. SERCA2a analysis

After isolation, cardiomyocytes were homogenised in lysis buffer (100mM NaCl, 50mM Tris-base, 5mM EDTA-2Na, 50mM $Na_4P_2O_7.10H_2O$, 1mM $MgCl_2$, 1% Nonidet P40, 0.3% Triton x-100, and 0.5% sodium deoxycholate; pH = 8), containing protease inhibitors (200mM PMSF, 15.7mg/mL benzamidine, and 10µM pepstatin) and phosphatase inhibitors (20mM NaF, and 1mM Na3VO4) and then centrifuged at 8000g (4ºC).

Total proteins were quantified using the Bradford method (Bradford, 1976). 30mg of protein was diluted in buffer (5X-2M Tris, pH = 6.8; 20% Glycerol, 30% SDS, 25% mercaptoethanol, 0.1% Bromophenol Blue) for separation by SDS-PAGE using a standard molecular weight (BIO-RAD). After separation in the gel, proteins were transferred to a PVDF membrane (Millipore, Billerica, MA, USA) with a pore size of 0.45µm. The quality of the transfer was monitored by staining the membrane with solution of Ponceau (0.2%). The membranes were washed with TBS-Tween (0.05% Tween) and placed in blocking solution for 1 hour. They were then incubated at 4℃ with primary specific antibodies: anti-glyceraldehyde 3-phosphate dehydrogenase (GAPDH) [1:6000], (Santa Cruz Biotechnology, Santa Cruz, CA, USA), anti-SERCA2a [1:1000], washed with TBS containing 0.2% Tween20 (TBST) for 5 minutes (three times) and then incubated for 2 hours with secondary antibody conjugated to peroxidase (HRP) (1:5000, anti-goat IgG-HRP and anti-rabbit IgG-HRP (Sigma, St. Louis, MO, USA). The protein bands were detected by a chemiluminescence reaction (kit ECL plus, Amersham Biosciences Limited, Little Chalfont, Buckinghamshire, England, UK). The intensity of bands was evaluated by densitometric analysis using the ImageQuant™ software (Amersham Biosciences Limited). Protein levels were normalised by the GAPDH expression level.

2.8. Statistical analysis

Data are expressed as mean and the standard error of the mean (mean ± SEM). The normal distribution of data was verified using the Kolmogorov-Smirnov test. Biometric and cell contractile function data were compared using the Student's t test. A p value <0.05 was considered statistically significant.

3.0. Results

3.1. Biometry

The biometric parameters of both groups investigated are shown in Table 2. In the PRG, there was a significant decrease in the body, heart and LV masses compared to the CG. In addition, animals in the PRG represented a significant increase in the relationship of heart mass/tibia length and LV mass/tibia length compared to the CG.

Table 2. Biometric parameters of Fisher rats

	CG	**PRG**
Body mass (g)	228.00 ± 3.31	70.00 ±
Heart mass (g)	1.06 ± 0.03	0.45 ± 0.01*
LV Mass (g)	0.98 ± 0.03	0.42 ± 0.01*
Heart mass / TL	0.31 ± 0.05	0.16 ± 0.02*
LV Mass /TL (mg/cm)	0.28 ± 0.06	0.15 ± 0.02*

CG, control group; PRG, protein restriction group; VE, left ventricle; TL, tibia length. Data are expressed as mean ± SEM. *Denotes statistical difference compared to CG (p<0.001).

3.2. Contractile analysis

Figure 1 shows the basal cellular contractile parameters in both of the groups investigated. The animals in the PRG showed a significant reduction in cardiomyocyte contraction amplitudes, and the maximal velocity of contraction and relaxation compared to the CG.

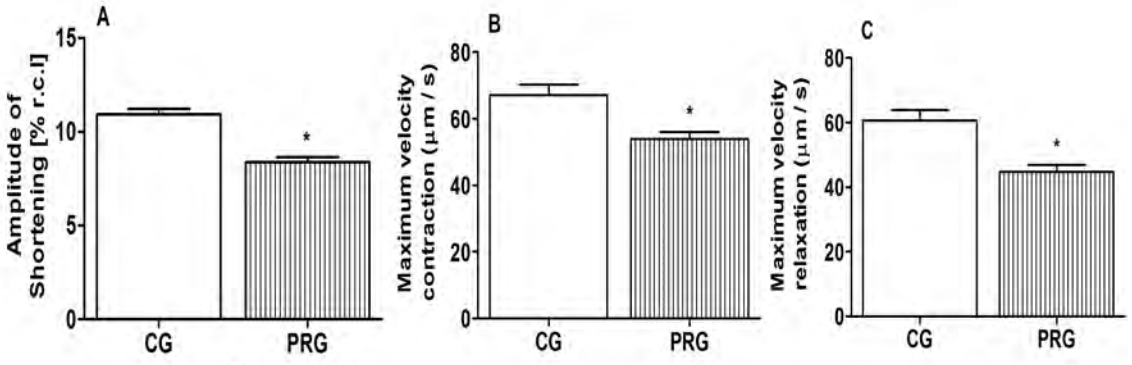

Figure 1. The contractile function of left ventricular cardiomyocytes from Fisher rats. CG, control group; PRG, protein restriction group. The number of cells analysed per group was: CG = 110, PRG = 95. Amplitude of shortening is expressed as a % of resting cell length (% r.c.l.). Data expressed as mean ± SEM. * Statistical difference compared with to CG ($p < 0.001$).

3.3. β-adrenergic stimulation

Figure 2 shows the response of cardiomyocytes to β-adrenergic stimulation. Cardiomyocytes from PRG animals showed an attenuation of contractile response at all concentrations of ISO (1, 2 and 3mM) compared to the CG. In a condition of protein restriction, cardiomyocytes showed a significant reduction in contraction amplitude and a prolongation of relaxation compared to CG animals.

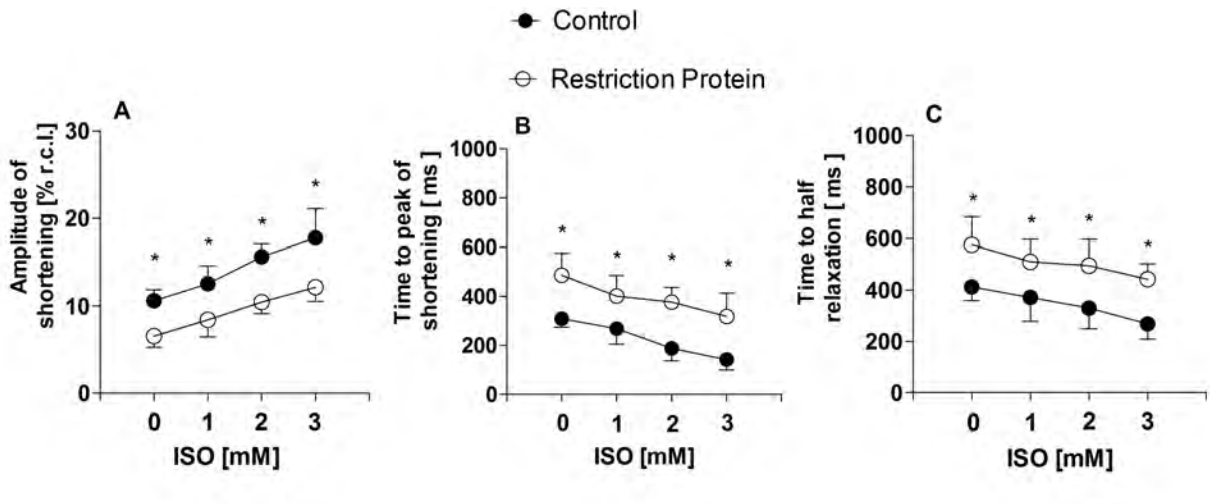

Figure 2. Contractile response to β-adrenergic stimulation in left ventricular cardiomyocytes from Fisher rats. CG, control group; PRG, protein restriction group. The number of cells analysed per group (CG = 60, PRG = 55). Amplitude of shortening is expressed as a % of resting cell length (% r.c.l.). Data expressed as mean ± SEM. * Statistical difference compared to CG ($p < 0.001$).

3.4. Ca^{2+} *Sparks*

The results of spontaneous Ca^{2+} *sparks* in quiescent cardiomyocytes during diastole are shown in Figure 3. The Ca^{2+} *sparks* amplitude was significantly lower in the PRG compared to the CG (0.26 ± 0.001 *vs.* 0.32 ± 0.001ms, respectively). On the contrary, the Ca^{2+} *sparks* frequency was significantly higher in the PRG compared to the CG (9.54 ± 0.25 *vs.* 7.82 ± 0.35 *sparks* x 100 m^{-1} x s^{-1}, respectively).

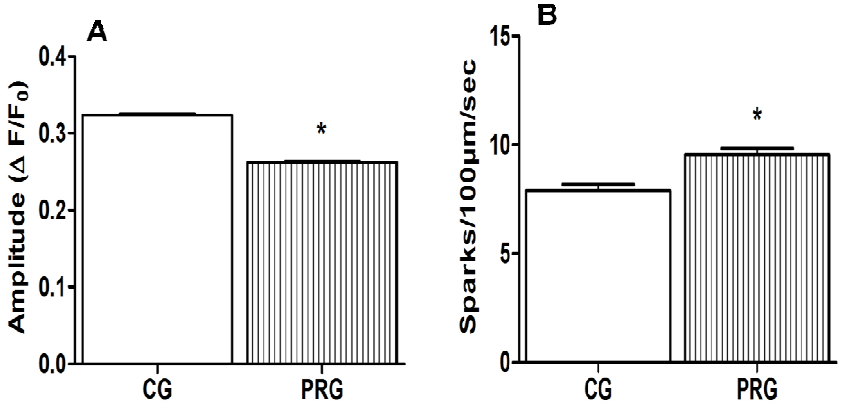

Figure 3. Ca^{2+}*Sparks* in left ventricular cardiomyocytes from Fisher rats. CG, control group; PRG, protein restriction group; ΔF, variation in fluorescence intensity compared to the minimal fluorescence (F_0). The number of cells analysed per group (CG= 91, PRG= 78). Data expressed as mean ± SEM. *Statistical difference compared to CG ($p<0.001$).

3.5. SERCA2a expression

The measurement of SERCA2a expression is illustrated in Figure 4. PRG animals showed a lower SERCA2a expression compared to GC.

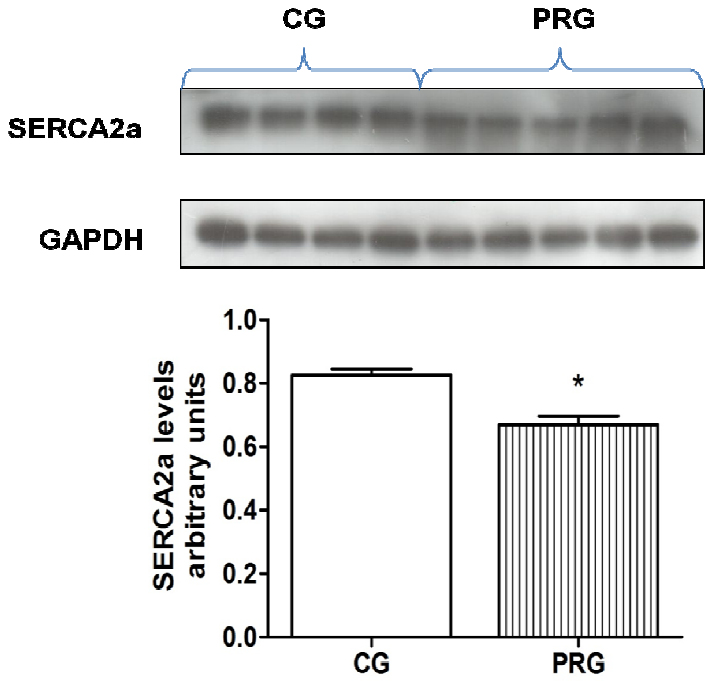

Figure 4. Western blot analysis of SERCA2a protein expression in left ventricular cardiomyocytes from Fisher rats. CG, control group; PRG, protein restriction group. Data expressed as mean ± SEM. * Statistical difference compared to CG ($p <0.001$).

4. Discussion

The results of this study indicated that severe protein restriction after weaning induced morphological and functional changes in the heart. There was

a marked reduction in the absolute and relative biometric variables. It has been shown that nutritional deficiency, even if transitory, could modify the metabolism and structure of various organs, affecting their development and function (Cicogna et al., 2001; Sugizaki et al., 2005, 2009; Lim et al., 2010; Okoromah et al., 2011). It is likely that the anatomical changes observed in the hearts of the PRG are adaptations of the body to adjust to adverse nutritional conditions and survive (Langley-Evans, 2006; Lim et al., 2010).

The animals of the PRG showed marked contractile dysfunction in basal conditions and after β-adrenergic stimulation. Although the response to β-adrenergic stimulation was dose-dependent for both groups, PRG animals presented an attenuation of all contractile parameters that were analysed. In a previous study, a 50% dietary restriction was sufficient to induce pathological changes in response to β-adrenergic stimulation in a preparation of isolated papillary muscle (Carrol et al., 1997). In this study, there was a marked reduction in muscle contractility in response to stimuli of increasing intensity, suggesting a lower reserve function in malnourished rats. It has been suggested that malnutrition may alter the adrenergic response due to attenuation of the phosphorylation of proteins related to the control of intracellular Ca^{2+}, impairing the mechanical cardiac performance in murine models (Li et al., 1997; Sugizaki et al., 2005). Moreover, there is evidence that these changes may be associated with a decreased number of β-adrenergic receptors or alterations of intracellular signal transduction pathways dependent on the adrenergic activation of G protein (Gut et al., 2003).

In addition to contractile dysfunction, a reduced expression of the SERCA2a was observed in cardiomyocytes from the PRG. This finding is

consistent with the potential inhibition of calcium uptake by the sarcoplasmic reticulum during relaxation of cardiomyocytes. The principal component associated with the $[Ca^{2+}]_i$ transient control is the Ca^{2+} ATP-dependent transporter of the sarcoplasmic reticulum (SERCA2a). This transporter is responsible for the higher rate of re-uptake of cytosolic Ca^{2+} (90%) (Bers et al., 2001) and its expression, structure and/or function are often impaired in heart diseases with different aetiologies, such as diabetes mellitus, hypertension, and autoimmune cardiopathies (Bers et al., 2003; Novaes et al., 2011). Pathological changes of SERCA2a resulted in a lower re-uptake of cytosolic Ca^{2+} into the sarcoplasmic reticulum, and an increased cytosolic Ca^{2+} concentration, impairing cell relaxation (Bers et al., 2003; Leopoldo et al., 2011). Thus, it is not unrealistic to assume that the lower activity of SERCA2a induced by protein restriction applied in the experimental model investigated may be related to attenuation of cardiomyocyte relaxation. This explains, in part, the prolongation of relaxation time observed in the PRG ccardiomyocytes, which is possibly related to the elevation of cytosolic Ca^{2+} that is dependent on the lower reuptake of the cytosolic Ca^{2+} to the sarcoplasmic reticulum by SERCA2a.

The frequency and amplitude of basal spontaneous pulses of Ca^{2+} from the sarcoplasmic reticulum (Ca^{2+} *sparks*) are important indicators of the functional state of the ryanodine channels (RyR2) (Bers et al., 2001). A smaller amplitude and higher frequency of Ca^{2+} *sparks* was evidenced in the PRG compared to the CG. These results indicate that protein restriction after weaning can modify the function of RyR2. Other researchers, working with different animal models of cardiac dysfunction, also found similar results to those found in this study (Bers et al., 2003; Vizotto et al., 2007).

The abnormal activity of RyR2 has been shown in different types of heart disease (George, 2008). A common feature in most models of experimental heart failure is the decline of the Ca^{2+} content of the sarcoplasmic reticulum. This change can be caused by changes in the function of SERCA2a, the Na^{+}/Ca^{2+} transporter of the sarcolemma (NCX) and RyR2 (George, 2008). However, detailed analysis of these molecular transporters requires additional studies to define its role in cardiac dysfunction in conditions of protein restriction. Bers et al. (1998) observed that the spontaneous release of Ca^{2+} from the sarcoplasmic reticulum depends mainly on the concentration of cytosolic Ca^{2+} and Ca^{2+}-loading of the sarcoplasmic reticulum. Thus, the reduction of Ca^{2+} mobilisation can act as a trigger point of spontaneous activity, conducing to increase the spontaneous release of Ca^{2+} during diastole. Furthermore, increased Ca^{2+} *sparks* observed in cases of cardiac dysfunction have been related to a change of the control exercised by the protein FKBP12.6 on Ca^{2+} channel release from the sarcoplasmic reticulum (Marks, 2001, Marks et al. 2002). Although the role of FKBP12.6 in the stabilisation of the Ca^{2+} channel from the sarcoplasmic reticulum was recognised, little is known about the role of this regulatory protein in the pathogenesis of heart failure (Marx et al., 2000), which indicates the need for further investigations.

The results indicated that severe protein restriction after weaning is able to induce morphological and functional changes in the heart and ventricular cardiomyocytes. The pathological changes of cardiomyocyte mechanics suggest a potential involvement of the β-adrenergic pathway that participates in the modulation of cellular contractility, which is possibly associated with changes in SERCA2a expression and disturbances in the Ca^{2+} intracellular

kinetics. Although these findings suggest new aspects of the pathophysiology of heart disease associated with malnutrition, the involvement of Ca^{2+} transport proteins and the activation of signalling pathways that regulate the Ca^{2+} intracellular kinetics under conditions of protein restriction remains poorly understood and requires further study.

5. Acknowledgements

We thank the Center for Microscopy and Microanalysis of the Federal University of Viçosa and also FAPEMIG for financial support..

6. References

Bers DM, Li L, Satoh H, Mccall E. (1998) Factors that control sarcoplasmic reticulum release in intact ventricular myocytes. Ann NY Acad Sci 853: 157-177.

Bers DM. (2001) Excitation-contraction coupling and cardiac contractile force. The Netherlands: Kluwer Academic Publishers 32: 283-284.

Bers DM, Eisner DA, Valdivia HH. (2003) Sarcoplasmic reticulum Ca^{2+} and heart failure roles of diastolic leak and Ca^{2+} transport. Circul Res 93: 487-490.

Bradford, M.M. (1976) Rapid and sensitive method for the quantitation of microgram quantities of protein utilizing the principle of protein-dye binding. Anal Biochem 72: 248-254.

Cicogna AC, Padovani CR, Okoshi K, Matsubara LS, Aragon FF, Okoshi MP. (2001) The influence of temporal food restriction on the performance of isolated cardiac muscle. Nut Res 21: 639–648.

George CH. (2008) Sarcoplasmic reticulum Ca^{2+} leak in heart failure: mere observation or functional relevance? Cardiovasc Res 77: 302-314.

Gruber C, Nink N, Nikam S, Magdowski G, Kripp G, Voswinckel R, Mühlfeld C. (2012) Myocardial remodelling in left ventricular atrophy induced by caloric restriction. J Anat 220: 179–185.

Gut AL, Okoshi MP, Padovani CR, Aragon FF, Cicogna AC. (2003) Myocardial dysfunction induced by food restriction is related to calcium cycling and beta-adrenergic system changes. Nutr Res 23: 911-919.

Langley-Evans SC. (2006) Developmental programming of health and disease. Proc Nutr Soc 65: 97-105.

Leopoldo AS, Lima-Leopoldo AP, Sugizaki MM, Nascimento AF, Campos DHS, Luvizotto RAM, Castardeli E, Alves CAB, Brum PC, Cicogna AC. (2011) Involvement of l-type calcium channel and SERCA2a in myocardial dysfunction induced by obesity. Journal of Cellular Physiology 22: 1-29.

Lim K, Zimanyi MA, Black MJ. (2010) Effect of maternal protein restriction during pregnancy and lactation on the number of cardiomyocytes in the post proliferative weanling rat heart. Anatomical Record 293: 431-437.

Li P, Hofmann PA, LI B, Malhotra A, Cheng W, Sonnenblick EH, Meggs LG, Anversa P. (1997) Myocardial infarction alters myofilament calcium sensitivity and mechanical behavior of myocytes. Am J Physiol 272: 360-70.

Marks AR. (2001) Ryanodine receptors/calcium release channels in heart failure and sudden cardiac death. J Mol Cell Cardiol 33: 615-624.

Marks AR, Priori S, Memmi M, Kontula K, Laitinen PJ. (2002a) Involvement of the cardiac ryanodine receptor/calcium release channel in catecholaminergic polymorphic ventricular tachycardia J Cell Physiol 190: 1-6.

Martins CDD, Chianca DAJr, Fernandes LG. (2011) Cardiac autonomic balance in rats submitted to protein restriction after weaning. Clin Exp Pharm Physiol 38: 89-93.

Marx SO, Reiken S, Hisamatsu Y, Jayaraman T, Burkhoff D, Rosemblit N, Marks AR. (2000) PKA Phosphorylation dissociates FKBP12.6 from the calcium release channel (ryanodine receptor): defective regulation in failing hearts. Cell 101: 365-376.

Novaes RD, Penitente AR, Gonçalves RV, Talvani A, Neves CA, Maldonado IRSC, Natali AJ. (2011) Effects of *Trypanosoma cruzi* infection on myocardium morphology, single cardiomyocyte contractile function and exercise tolerance in rats. Int J Exp Pathol 92: 299-307.

Okoromah CAN, Ekure EN, Lesi FEA, Okunowo WO, Tijani BO, Okeiyi JC. (2011) Prevalence, profile and predictors of malnutrition in children with congenital heart defects: a case–control observational study. Arch Dis Child 96: 354-360.

Penitente AR, Fernandes LG, Cardoso LM, Silva ME, Pedrosa ML, Silva AL, Haibara AS, Moraes MFD, Chianca DA Jr. (2007) Malnutrition enhances cardiovascular responses to chemoreflex activation in awake rats. Life Sciences 81: 609-614.

Sugizaki MM, Carvalho RF, Aragon FF, Padovani CR, Okoshi K, Okoshi MP. (2005) Myocardial dysfunction induced by food restriction is related to morphological damage in normotensive middle-aged rats. J Biomed Sci 12: 641-649.

Sugizaki MM, Leopoldo AS, Okoshi MP, Bruno A, Conde SJ, Lima-Leopoldo AP. (2009) Severe food restriction induces myocardial dysfunction related to SERCA2 activity. Can J Physiol Pharmacol 87: 666-673.

Vizotto VA, Carvalho RF, Sugizaki MM, Lima AP, Aragon FF, Padovani CR, Castro AVB, Pai-Silva MDal, Nogueira CR, Cicogna AC. (2007) Down-regulation of the cardiac sarcoplasmic reticulum ryanodine channel in severely food-restricted rats. Braz J Med Biol Res 40: 27-31.

4.3. Paper 3

Protein malnutrition after weaning induces left ventricular morphofunctional remodeling in Fischer rat

Abstract

We investigated the relationship between a low protein diet, morphological, ultrastructural and functional myocardial changes in male *Fischer* rats, after breastfeeding. The animals were divided into control group (CG) and protein-restricted group (PRG). After weaning, animals were weighed PRG and CG and were isocaloric diets containing 15% and 6% protein, respectively, for 35 days. Then the animals were weighed and sacrificed. The hearts were removed and processed for histological, morphometric, stereological and ultrastructural. Cardiomyocytes eight animals from each group were processed for analysis of mechanical properties. The results demonstrated that the restriction protein (PR) caused a reduction in body weight, heart and left ventricular PRG. These changes were accompanied by decreases in length, width and area of cardiomyocytes, in addition to the increased amount of interstitial collagen in PRG. The ultrastructural analysis allowed to observe less-developed myofibrils and an apparent increase in the proportion of mitochondria. In addition, ventricular myocytes PRG also showed changes in contractile responses: increasing the amplitude of contraction, decreasing the time of cardiac contraction and relaxation in the heart of high concentrations of extracellular calcium $[Ca^{2+}]_e$ = 1.8mM to

$[Ca^{2+}]_e$ = 5.0 mM. According to these results, we concluded that protein deficiency affects myocardial performance, and this damage could be attributed to the contractile the contractile, change in morphology and ultrastructure of cardiomyocytes.

Keywords: Ultrastructure, morphology, cardiac dysfunction, cardiomyopathy.

1. introduction

Several studies have associated protein restriction (PR) with an increased incidence of cardiovascular disease (Barker et al., 1989, Lim et al., 2010). Previous studies indicated that intrauterine malnutrition causes a pathological reorganization of the histoarchitecture in vital organs such as lungs, kidneys and heart; aspect directly associated to the permanent reduction of the functional units of these organs (Corstius et al, 2005; Lipsett et al., 2006, Zimanyi et al., 2006, Gruber et al., 2012).

It has been systematically shown that mechanical and hemodynamics dysfunctions observed in cardiac diseases with different etiologies are directly associated with pathological changes in cell structure and function (Leopold et al, 2011). Currently, little is known about the influence of protein restriction (PR) on the cardiac remodeling in the cellular and subcellular level (ultrastructural) (Zucoloto & Rossi, 1982; Pinotti et al., 2010). However, there are strong indications that the pathogenesis of cardiovascular disorders such as poor control of heart rate and blood pressure (Penitent et al., 2007, Martins et al., 2011) and the reduction of the cardiac contraction strength, recognized present in RP, presents a metabolic and cellular basis (Christian & Stewart, 2010; Lima-Leopoldo et al., 2011).

Admittedly, the cardiac development represented by cellular hyperplasia is maintained during the first 2 weeks in the postnatal period in rats (Li et al., 1996). After this period, the cardiomyocytes are no longer proliferate and only the growth becomes viable (Li et al., 1996). It was previously demonstrated that the PR is capable of reducing the number of heart cells only during the cell

hyperplasia (Corstius et al., 2005). However, there is limited information about the potential for malnutrition impairs the cardiac myocytes development after cessation of cell proliferation phase.

Thus, the objective of this study was to investigate the influence of severe protein restriction after weaning on the morphology and ultrastructure of the left ventricle, and the contractile function of isolated cardiac myocytes from Fisher rats.

2. Material and methods

2.1. Animals

Twenty-eight day old male Fischer rats provided by the animal facilities of the Federal Unversity of Ouro Preto (UFOP), Brazil, were divided according to the diet received: control group (CG, n = 16) and protein-restricted group (PRG, n = 16). After weaning, CG animals were fed with standard rodent chow (AIN-93 - 15% protein) and the PRG animals received a diet containing 6% protein (casein) for 35 days (Penitente et al., 2007). The diets were isocaloric (422 kcal/100 g of diet) and the salts and vitamins were at similar concentrations in both diets (Table 1). The animals were maintained in a controlled temperature room (22 ± 2 ºC) and humidity (60-70%) with 12-hour light/dark cycles and had water *ad libitum*. The experimental protocols were approved by the Ethics Committee of the Federal University of Viçosa (UFV protocol 95/2011).

Table 1. Chemical composition of the diets (g/100g of chow)

Nutrients	**CG**	**PRG**

Protein (casein)	15	6
Corn starch	68	77
Soybean oil	10	10
Salts mix	5	5
Vitamin mix	1	1
Fiber (cellulose)	1	1
Total caloric values	422 Kcal	422 Kcal

GC, control group; GRP, protein restriction group.

2.2. Biometric and morphometric analysis

After the experimental protocol, eight animals from each group were weighed and sacrificed. The hearts were removed and weighed. The left ventricles (LV) were dissected, weighed separately and the volume was determined by the method of Scherle (Scherle, 1970). The LV were placed in histological fixative for 48 h (10% formaldehyde in 0.1 M phosphate buffer, pH 7.2). The ventricles were dehydrated in ethanol, clarified in xylene and embedded in paraffin. The blocks were cut into 4 µm thick sections, stained with hematoxylin and eosin (H&E), Masson's trichrome, Sirius red (Sirius Red F3B, Mobay Chemical Co., New Jersey, USA) and mounted on slides. The histological sections stained with H&E were visualized and images captured using a light microscope (Olympus BX-60, Tokyo, Japan) connected to a digital camera (Olympus Q-Color-3, Tokyo, Japan). Through digital images were calculated the length and width of cardiomyocytes in 150 fields for each group. Were investigated fifty cells per animal with a 40x objective lens.

The histological sections stained with Sirius Red were observed under polarized light (Axioscópio, Zeiss, Tokyo, Japan) and used to determine the proportion of collagen present in the extracellular matrix. For this analysis was

used the software Image-Pro Plus 4.5 (Media Cybernetcs, Silver Spring, MD, USA) based on the properties of birefringence of the collagen fibrils under polarized light. Ten fields were investigated by histological animal with 20x objective lens.

2.3. Stereological analysis

Fragments of the LV were obtained by the orientador method to define isotropic and uniform random sections (IUR) required for stereological analysis (Novaes et al., 2012). The stereological analysis was performed on sections stained with Masson's trichrome (figure 1). Were investigated 10 microscopic fields per animal obtained randomly with a 40x objective lens (Olympus BX-60, Tokyo, Japan). The volume of cardiomyocytes (V [imc], mm^3) and blood vessels (V [vessels], mm^3), total length of cardiomyocytes (L [imc], km) and blood vessels (L [vessels], km) in the LV were estimated according to the methodology described by Brüel et al. (2005).

The number of cardiomyocytes (IMC) in a three-dimensional space was estimated using the physical disector method (Novaes et al., 2012). The disector consists of two parallel planes delimited by a test area (AT = 2670 μm^2) and separated by a known distance (h = 3 µm). The numerical density of cardiomyocytes (Nv [imc] imc / mm^3) was determined from 10 disector pairs for each animal, defined as $Nv\,[imc] = Q^-[imc] / h \times AT$, where $Q^-[imc]$ represents the number of cardiomyocyte nuclei counted in the test area on the disector reference plane (look up" plan") (Novaes et al., 2012). The total number of cardiomyocytes in the LV was estimated as the product Nv [imc] / LV volume. According to the protocol described by Eisele et al., (2008) the tissue retraction

of the left ventricle was 19%. Thus, the stereological results were corrected using this index. All stereological analysis was performed in software Image-Pro Plus ® 4.5 software (Media Cybernetics, Silver Spring, MD, USA).

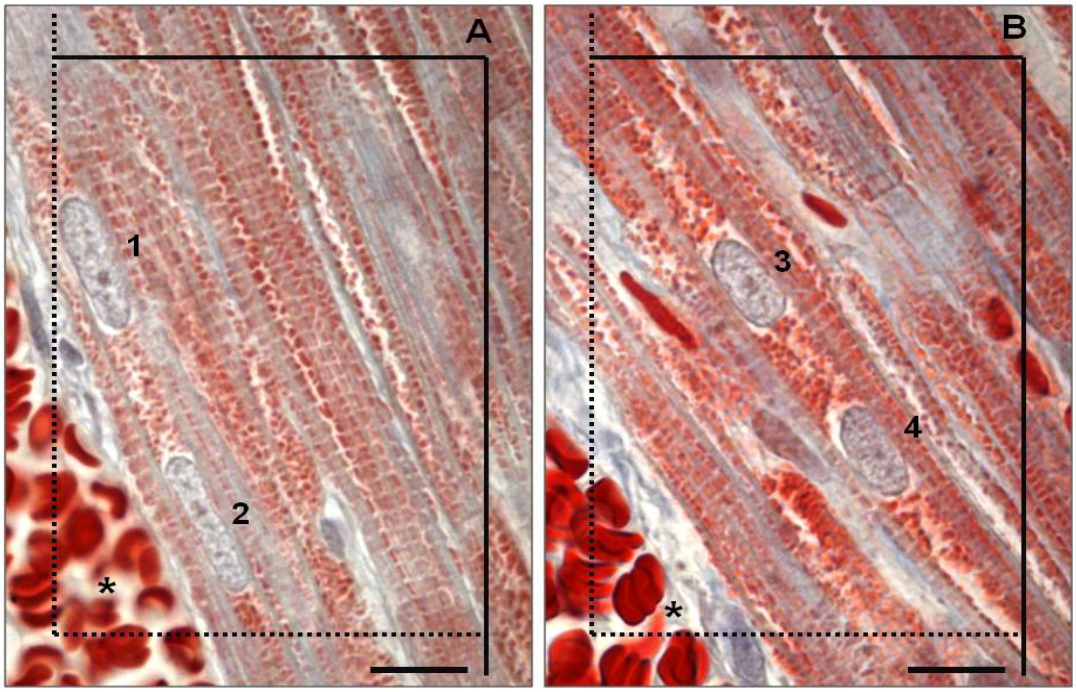

Figure 1 Representative photomicrographs of the physical disector method. The disector is constructed by the union of two reference planes delimited by a two-dimensional test area (TA) separated by 3 µm in distance (h). (bar = 25 micron, Masson's trichrome).

2.4. Cardiomyocytes isolation

After euthanasia, the hearts from 8 animals in each group were quickly removed and LV cardiomyocytes were isolated as described by Novaes et al., (2011). Briefly, the heart was cannulated through the aorta in a Langendorff system and perfused with isolation solution (composition [mM]: 130 Na^+, 5.4 K^+, 1.4 Mg^{2+}, 140 Cl^-, 0.75 Ca^{2+}, 5.0 Hepes, 10 glucose, 20 taurine and 10 creatine, pH= 7.3 at room temperature). Then, the heart was perfused with calcium-free solution containing 0.1 mM ethylene glycol-bis (beta-aminoethyl

ether)-*N*, *N*, *N'*, *N'*-tetraacetic acid (EGTA) for 5 min. The heart was then perfused with a solution containing 1.0 mg.ml-1 of type 2 collagenase (Worthington, USA) and 100.0 mM $CaCl_2$ for 25 min. The solutions were oxygenated (100% O_2, White Martins, SP, Brazil) and maintained at 35 ºC. After perfusion, the left ventricle was dissected and placed in a glass recipient with an enzyme solution containing collagenase (5.0 ml) and bovine serum albumin (10%). The recipient was shaken moderately for 5 min at 37 ℃, after which the solution was centrifuged. The supernatant was removed and cardiomyocytes were resuspended in isolation solution, stored in a refrigerator (5 ℃) and used in a period up to 4h after isolation. Only calcium-tolerant, quiescent, rod-shaped cardiomyocytes showing clear cross striations were studied.

2.5. Cell contractility

Cardiomyocytes contractile function was measured using an edge motion detection system (Ionoptix, Milton, MA, USA) mounted on an inverted microscope (Nikon Eclipse TS100®, Tokyo, Japan), as previously described [Novaes et al., 2011]. Briefly, myocytes were placed in an experimental chamber with the base glass and bathed in buffer with the following composition (in mM): 136.9 NaCl; 5.4 KCl; 0.37 NaH_2PO_4; 0.57 $MgCl_2$, 5.0 Hepes; 5.6 glucose and 1.8 $CaCl_2$ (pH= 7.4 at room temperature). Cardiomyocytes were field stimulated at a frequency of 3.0 Hz (10 volts, 5 min duration) using a pair of steel electrodes (Myopacer, Ionoptix, MA, USA). Cardiomyocytes were visualized on a personal computer monitor with a NTSC camera (MyoCam, Ionoptix, MA, USA) attached to the microscope using an image detection program (Ionwizard, Ionoptix, MA, USA). This image was used to measure cell

shortening (our index of contractility) in response to electrical stimulation using a video motion edge detector (IonWizard; IonOptix, MA, USA). All parameters were evaluated using customized software developed in the MatLab® platform. Cell shortening from stimulation (expressed as a percentage of resting cell length), time to peak of shortening and time to half relaxation were measured and calculated as previously described (Novaes et al., 2011).

2.6. Transmission electron microscopy

Fragments of the left ventricle (1 mm^2) were transferred to fixative solution (2.5% glutaraldehyde in sodium cacodylate buffer 0.1 M [pH 7.2]). After washing with buffer, the samples were post-fixed with 1% osmium tetroxide, in the same buffer for 2 h. Dehydration was performed in a graded series of ethanol, followed by incorporation in LR-White resin (London Resin Company Ltd, England). After inclusion, ultrathin sections were obtained and stained with uranyl acetate 2% lead citrate and 0.2% in 1M sodium hydroxide and observed in transmission electron microscope Zeiss EM 109 (Jena, Germany) in the Nucleus Microscopy and Microanalysis of the Federal University of Viçosa.

2.7. Statistical analysis

Data are expressed as mean and standard error of mean (mean ± SEM). The normal distribution of data was verified by using the Kolmogorov-Smirnov test. Biometric and cell contractile function data were compared using the Student's t test. Morphometric data were compared using the Mann-Whitney U test. A p value <0.05 was considered statistically significant.

3.0. Results

3.1. Effect of protein restriction on weight gain

At the beginning of the experiment (end of lactation), CG animals (n = 8) and PRG animals (n = 8) showed no differences in body weight (70.32 ± 0.15 g and 71.22 ± 0.09 g), respectively. Over the 35 day of standard diet CG animals showed body weight between 185 and 226 g with an average weight gain of 159.4 g. After 35 days, PRG animals presented weight between 67 g and 90, with an average weight gain of 0.7 g. In the second week of diet there was no difference in body weight among the groups, remaining until the end of the experimental protocol (Figure 2).

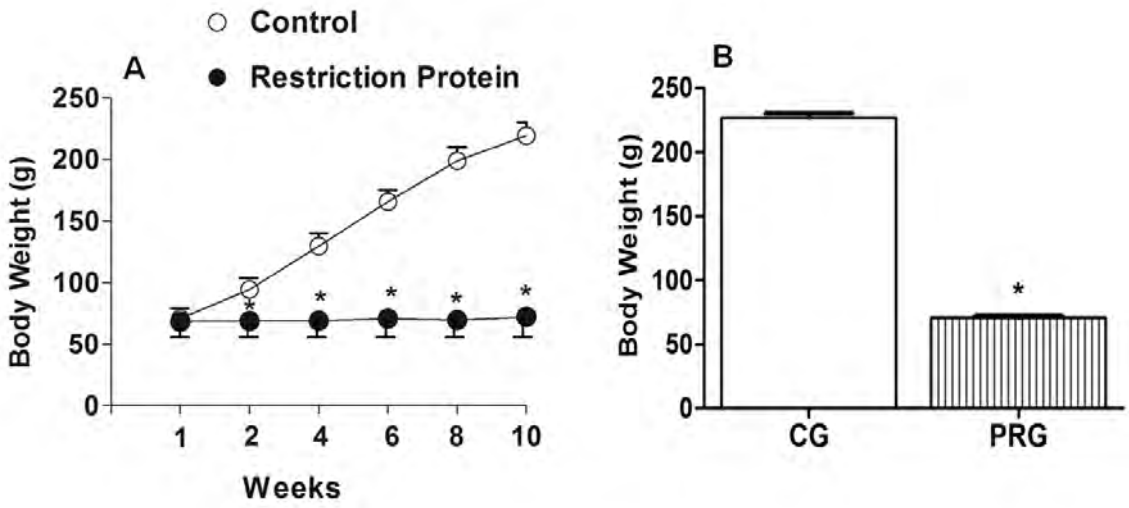

Figure 2. Effect of protein restriction on body weight of Fischer rats. The control group (CG, open circle) received standard diet (15% protein) and the protein restriction group (PRG, closed circle) received a diet with low protein (6% protein). (A) Changes in body weight over 35 days of diet after weaning. (B) Body weight at the end of the experimental protocol. Data are expressed as mean ± SEM. * Statistical difference compared to CG ($p < 0.005$).

3.2. Morphological characteristics of cardiomyocytes

The morphological characteristics of cardiomyocytes are shown in table 2 and Figure 3. Histomorphometric analysis indicated reduction of the length, width and cell area in cardiomyocytes from PRG. Furthermore, the cardiomyocytes of animals in this group also showed increased length / width ratio compared to the CG.

Table 2. Morphological parameters of left ventricular cardiomyocytes in the experimental groups.

	GC	GRP
Length (µm)	99,71 ± 1,70	30,01 ± 2,35*
Width (µm)	24,10 ± 0,35	15,32 ± 0,06*
Length / Width (µm)	5,40 ± 0,03	6,48 ± 0,02*
Area (μm^2)	1157,01 ± 10,15	633,70 ± 15,89*

Data are expressed as mean ± SEM. 80 cells were analyzed for 8 animals per group. The control group (CG) received standard diet (15% protein) and protein restriction group (PRG) received diet with low protein (6%). * Statistically different compared to CG ($p < 0.001$).

Figure 3. Morphological characteristics of cardiomyocytes

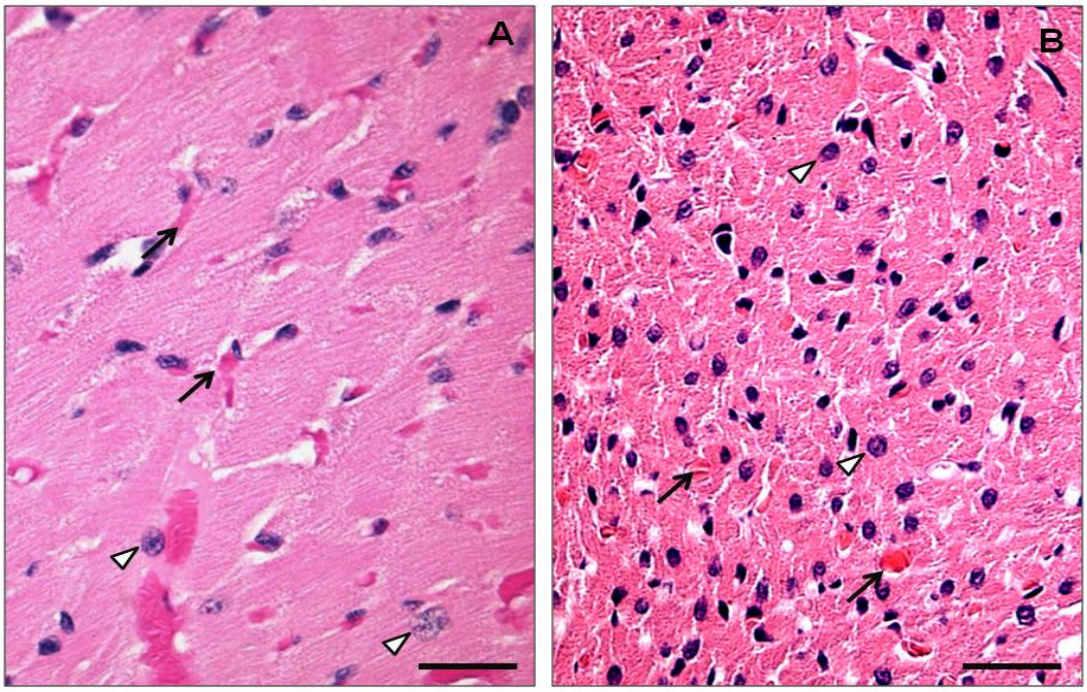

Figure 3. Representative photomicrographs of the left ventricle (LV) of Fisher rats observed under light microscopy. (A) control group (n = 6) received standard diet (15% protein) and (B) protein restriction group (n = 6) received diet with low protein (6% protein). Arrows indicate blood vessels and arrowheads indicate cardiomyocyte nuclei. In B note the higher density histological cardiomyocyte nuclei in the myocardium of the malnourished animals. (stain H &E; bar = 40 µm).

3.3. Stereology parameters

There were no significant differences between groups for all relative and absolute parameters estimated in the stereological analysis (Table 3).

Table 3. Stereological parameters of the left ventricular myocardium in the experimental groups.

Parameter	CG	PRG
V [*VE*] (mm^3)	273,31 ± 18,62	103,84 ± 7,03*
V[*cmy*] (mm^3)	225,10 ± 11,28	66,31 ± 4,26*

V[int] (mm^3)	56,49 ± 1,86	37,54 ± 2,30*
V[*vasos*] (mm^3)	35,05 ± 4,17	14,34 ± 1,57*
L[*cmy*] (km)	6,01 ± 0,32	1,63 ± 0,12*
L[*vasos*] (km)	5,02 ± 0,32	1,62 ± 0,12*
N[*cmy*] x106	76,49 ± 8,22	71,52 ± 3,10

Data are expressed as mean ± SEM. V, volume, LV, left ventricle; cmy, cardiomyocytes. The control group (CG) received standard diet (15% protein) and protein restriction group (PRG) received diet with low protein (6%). * Statistically different compared to CG ($p < 0.001$).

3.4. Colagen content

The distribution of collagen in the left ventricle extracellular matrix it was modified by the low protein diet (Figure 4). The PRG animals showed marked increase in collagen collagen content. For these animals, the percentage area occupied by collagen in relation to other components of the left ventricle was 3.45% while in the control group was only 2.5%.

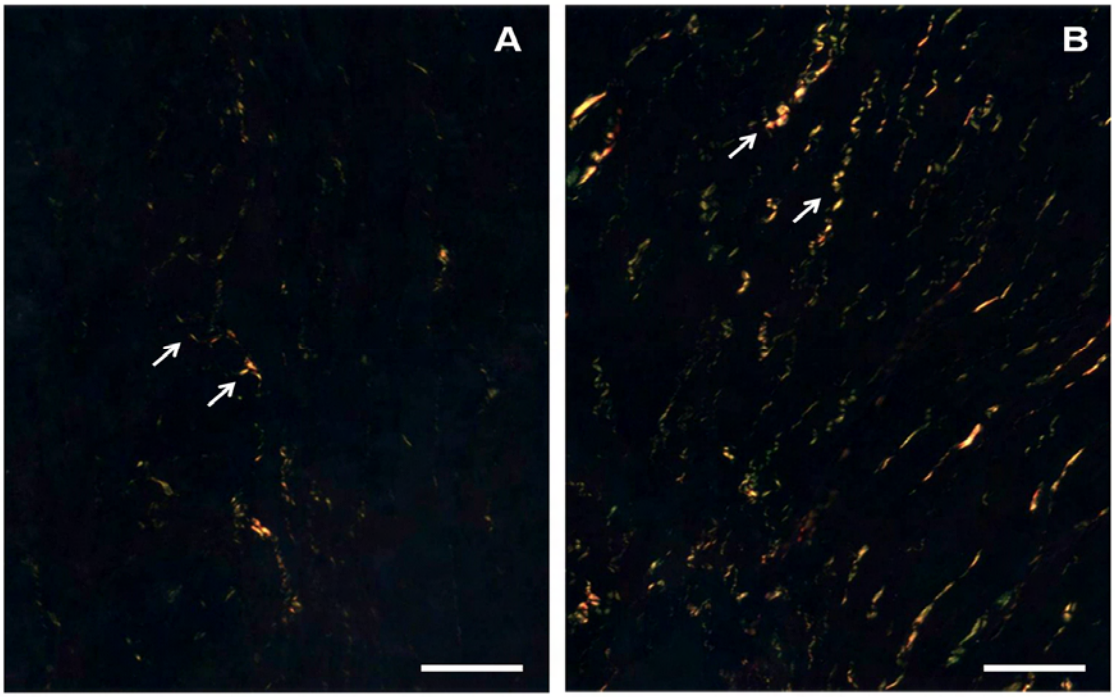

Figure 4. Representative photomicrographs of longitudinal section of the left ventricular myocardium of *Fischer* rats on polarization microscopy. Animals in the control group (CG) received standard diet (15% protein) and the protein restriction group (PRG) received a diet with low protein (6%). Observe a greater distribution of collagen fibers (arrows) in the myocardium of animals subjected to low protein diet (B) compared with controls (A). (Sirius red staining, bar = 60 µm).

3.5. Ultrastructural changes in ventricular cardiomyocytes

Reduction in myofibrils thickness and increased mitochondria density appear to be most obvious ultrastructural changes caused by low protein diet after weaning (Figure 5). Apparently, the membrane system of the sarcoplasmic reticulum and T tubules are less organized in PRG (Fig. 4A and B).

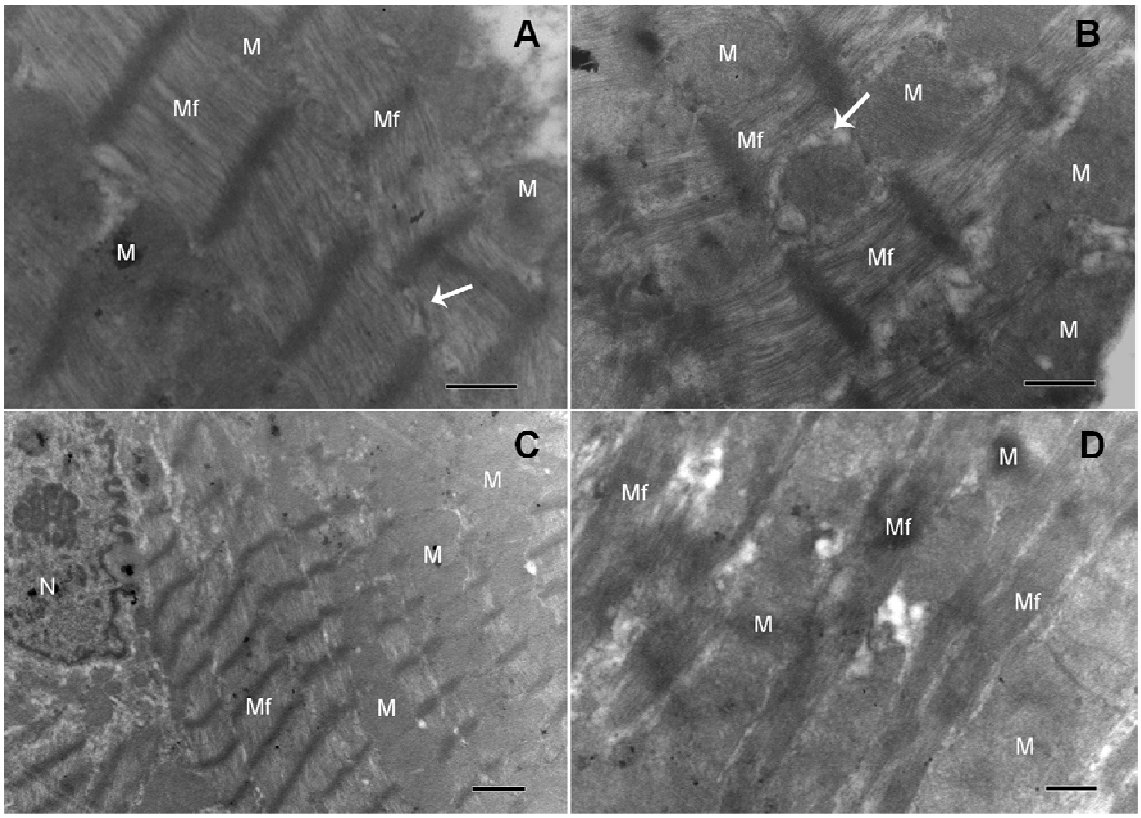

Figure 5. Transmission electron micrographs of left ventricular cardiomyocytes from Fisher rat. (A and C) control group (CG) received standard diet (15% protein) and (B and D) the protein restriction group (PRG) received diet with low protein (6%). The arrows indicate the membrane system of the sarcoplasmic reticulum and T tubule less

organized in PRG. Note the reduced thickness of myofibrils and higher mitochondrial proportion of PRG. Mf = myofibrils mitochondria M = N = core. (A, B and D bar = 0.5 µm and C = 1.0 µm).

3.6. Contractile response in different extracellular calcium concentrations

The effects of elevated extracellular calcium concentrations ($[Ca^{2+}]_e$) on the cardiomyocytes function are summarized and illustrated in Figure 6. The increase in $[Ca^{2+}]_e$ of 1.8 to 5.0 mM caused greater time of cell contraction and relaxation in CG animals than PRG animals. No differences were observed between groups for any of the parameters in $[Ca^{2+}]_e$ = 0.6 mM.

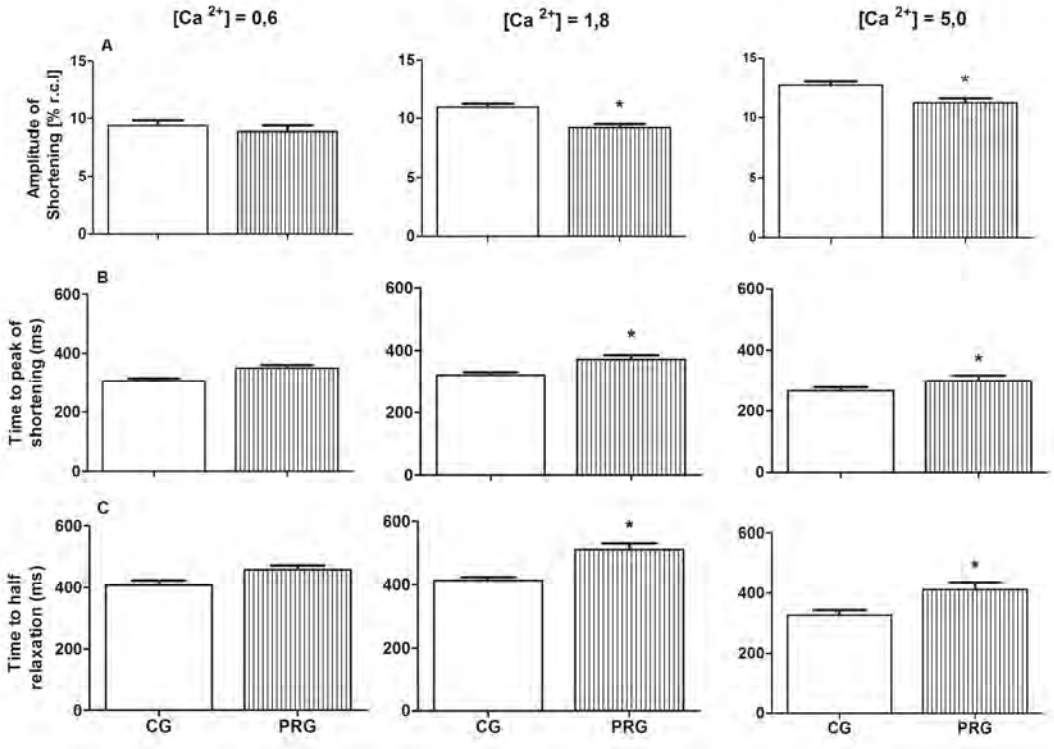

Figure 6. Cardiomyocyte ventricular contractile function in Fischer rats. The control group (CG) received standard diet (15% protein) and the protein restriction group (PRG) received diet with low protein (6%). Graphic (A) corresponds to the amplitude of shortening (% r.c.l); Graphic (B) corresponds to the time to peak of contraction (ms)

and the graph (C) corresponds to the relaxation time (ms). Data expressed as mean ± SEM. * Statistical difference compared with the control group ($p < 0.005$).

4. Discussion

The results of this study showed that severe protein malnutrition (PR) after weaning for 35 days causes a drastic reduction in body weight of approximately 66% compared with the control group (CG). The reduction in body weight, and low birth weight is regarded as a primary indicator of malnutrition (Lucas, 1998). It has been showed that protein restriction in early stages of life can affect both the process of cell proliferation, the size of organs and the weight of rats. There is an impairment in body development through depletion of muscle mass and decreased body weight as an adaptive response of the organism to nutritional insult to adjust and survive to the adverse nutritional conditions (Barker et al., 1993, Christian et al., 2010). The lack of weight gain shows that low dietary protein content probably not provide protein for the formation and growth of the organs. In parallel, low birth weight has been associated with various pathological conditions. Law and Shiell (1996) reported an association between low birth weight and increased blood pressure in childhood and adulthood. Moreover, low birth weight also has been associated with increased prevalence of hypertension (Barker et al., 1990) coronary heart disease (Barker et al., 1993), type II diabetes (Phillips et al., 1994) and renal disease (Hoy et al ., 1999).

The morphometric analyzes showed reduction in the length, width and area of cardiomyocytes of the left ventricle (LV) in PRG compared with CG. However, the length / width ratio was increased in cell from PRG. All the stereological parameters analyzed also showed reduction: low volume occupied

by cardiomyocytes, reduced volume of blood vessels, shorter overall length of cardiomyocytes and blood vessels, the lower number density of cardiomyocytes, but the same number of these cells in the left ventricle of the PRG compared to CG. According Winick and Noble (1965), rat growth bodies is divided into three periods: hyperplasic, hypertrophic and hyperplasic (cell proliferation occurs in a lesser rate, with concomitant increase in cell volume) and hypertrophic. In the present study, protein restriction was imposed during hypertrophy, and was sufficient to prevent the cardiomyocytes growth. Rats whose mothers were submitted to moderate protein restriction (9% casein) showed a reduction in heart size due to cardiomyocyte hypoplasia of the papillary muscle, impairing cardiac function and leading to cardiovascular diseases as hypertension and heart failure in adult life (Corstius et al., 2005). Our results corroborates the Winick and Noble (1965) findings, and in this phase that the low protein diet has been imposed, no formation of new cardiomyocytes in PRG only occurs a variation in their size.

Morphometric analysis further indicated the increased amounts of interstitial collagen in the myocardium of PRG animals. Similarly, Fioretto et al. (2011), using a different model of malnutrition in rats (50% dietary restriction) and working with isolated papillary muscle preparations demonstrated that the animals showed a reduction in cardiomyocytes diameter and volume in addition of increased amounts of interstitial collagen (Cicogna et al., 1999). This new organization of collagen fibers can influence the myocardium mechanical efficiency since part of the force used to pump blood is diverted to correct the abnormal organization of collagen (Diniz et al., 2011). Vandewoude et al. (1995) observed that in cardiac tissue of rats exposed to a diet with protein-calorie

restriction, there is a significant reduction in the diffusion distance of metabolites of the left ventricle, improving the cellular energy supply and offering a metabolic protection to malnourished myocytes. Such tissue changes are the result of quantitative and qualitative changes in the cellular and subcellular composition. This important fact contributes to the idea of preservation of ventricular function, despite the morphological changes (Vandewoude et al., 1995).

The presence of myofibrils less developed, the greater proportion of mitochondria and sarcoplasmic reticulum less organized in ventricular cardiomyocytes of PRG animals, corroborate the results described by Vandewoude (1995). This author found that hypertrophy and myofibrillar disorganization resulting from the reduction in the synthesis of myofibrils components in rats exposed to protein-caloric malnutrition. The greatest proportion of mitochondria in the present study may indicate an attempt to maintain cell homeostasis. Similar observations were made by Sugizaki et al., (2005) using a different model of malnutrition (food restricted to 50%), working with isolated papillary muscle preparations, showed ultrastructural changes in muscle fibers such as absence or disorganization of myofilaments and the Z line, polymorphic mitochondria with disorganized cristae and a large amount of interstitial collagen fibers in malnourished rats. In this context, this study supports the hypothesis that the higher mitochondrial density in ventricular cardiomyocytes of animals subjected to PR could be associated with an increase in energy production to offset or minimize the deficiency in the cell mechanics induced by myofibrillar dysfunction (Lu et al ., 2007, Johnson et al., 2009). Although changes in the production, transfer and use of energy are

considered important markers of abnormalities of the heart muscle function, this relationship is still unclear and requires further studies (Sharov et al., 1994, Klebanov et al., 1997, Ventura-Clapier et al., 2002).

In the present study the elevation of extracellular calcium concentration [Ca^{2+}] stimulated a lower response in the indexes of myocardial function in relation to the time of cardiac contraction and relaxation in PRG. The results of [Ca^{2+}] variation suggested that PR promotes dysfunction of the Ca^{2+} regulatory channels. This event may be related to alterations in Na^{+} / Ca^{2+} (NCX), L-type channels of the sarcolemma, sarcoplasmic reticulum (SR) and myofilament sensitivity to Ca^{2+} (Opie et al, 2004). The elevation of [Ca^{2+}] levels changes the phases of contraction and relaxation due to the increased concentration of Ca^{2+} available in the cytosol, since this directly interferes in the functioning of L-type and NCX channels of the SR (Opie et al, 2004). The lowest response to the increase of [Ca^{2+}]of 1.8 to 5.0 mM in the PRG may be related to a reduction in Ca^{2+} influx through L-type channels and/or changes of the SR function. These results are consistent with previous studies that observed cardiac dysfunction and depressed response to elevation of [Ca^{2+}] in myocytes (Relling et al., 2006) and papillary muscles (Ren et al., 2000) of rats with cardiac dysfunction. Furthermore, the highest relaxation time with an increase in $[Ca^{2+}]_e$ and may be related, in part, to reduced protein expression of SERCA2a in PRG animals, resulting in lower uptake of calcium by the SR during cardiac relaxation, impairing Ca^{2+} homeostasis (Leopold et al., 2011). The hypothesis that the mechanism for contraction / excitation coupling may be involved at the time of cardiac contraction and relaxation is supported by other studies using different

model of malnutrition in rats (50% reduction in feed) in a preparation of isolated papillary muscle (Kaye et al., 2008; Leopold et al., 2011).

In this study it was observed that the PR conduces to a morphofunctional rearrangement of the left ventricle. Although this presents a reorganization characteristic predominantly pathological, it is considered that part of the changes found represents an adaptive mechanism in the quest for survival under conditions of severe protein restriction (Okoshi et al., 2011). Considering the PR as a risk factor related to the pathogenesis of cardiomyopathies, additional studies are needed to identify what biochemical and molecular mechanisms affected by RP can lead to cardiac remodeling.

5. Acknowledgments

We thank the Center for Microscopy and Microanalysis of the Federal University of Viçosa and also FAPEMIG for financial support.

6. References

Bancroft, J.D., Gamble, M. (2008) Theory and Pratices of Histological Techniques. 6ª ed. *Elsevier.*725.

Barker D.J., Osmond C., Golding J., Kuh D., Wadsworth M.E. (1989) Growth in utero, blood pressure in childhood and adult life, and mortality from cardiovascular disease. *B. M. J.* **298**, 564-567.

Barker D.J., Bull A.R., Osmond C., Simmonds S.J. (1990) Fetal and placental size and risk of hypertension in adult life. *BMJ* **301**, 259-262.

Barker D.J., Gluckman P.D., Godfrey K.M., Harding J.E., Owens J.A., Ronbinson J.S. (1993) Fetal nutrition and cardiovascular disease in adult life. *Lancet* **341**, 938-941.

Brüel A., Oxlund H., Nyengaard J.R. (2005) The total length of myocytes and capillaries, and total number of myocyte nuclei in the rat heart are time dependently increased by growth hormone. *Growth Horm. IGF Res*. **15**, 256-264.

Corstius H.B., Zimanyi M.A., Maka N., Herath T., Thomas W., Van der Laarse A., Wreford N.G., Black M.J. (2005) Effect of intrauterine growth restriction on the number of cardiomyocytes in rat hearts. *Pediatr Res* **57**: 796-800.

Christian P. & Stewart C.P. (2010) Maternal Micronutrient Deficiency, Fetal Development, and the Risk of Chronic Disease. *J. Nutr.* **140**, 437-445.

Cicogna A.C., Padovani C.R., Georgette J.C., Aragon F.F., Okoshi M.P. (1999) Effects of Protein-Calorie Restriction on Mechanical Function of Hypertrophied Cardiac Muscle. *Arq. Bras. Cardiol.* **72,** 436-440.

De Tomasi L.C., Bruno A., Sugizaki M.M. (2009) Food restriction promotes downregulation of myocardial L-type Ca^{2+} channels. *Canad. J. Physiol. Pharm.* **87:** 426-431.

Diniz T.G., Benedicto H.G., Agreste F.R., Clebis N. K., Hernandez-Blazquez F.J., Bombonato P.P. (2011) Morphometry of the collagen fibers in healthy and diabetic rats treated with vitamin C. *Pesq. Vet. Bras*. **31**, 1-6.

Eisele J.C., Schaefer I-M., Nyengaard J.R., Post H., Liebetanz D., Brüel A., Mühlfeld C. (2008) Effect of voluntary exercise on number and volume of cardiomyocytes and their mitochondria in the mouse left ventricle. *Basic. Res. Cardiol.* **103**,12-21.

Fioretto J.R. (2011) Ventricular remodeling and diastolic myocardial dysfunction in rats submitted to protein-calorie malnutrition. *Am. J. Physiol*. **282**, 1327-1333.

Haddad F., Bodell P.W., McCue S.A., Herrick R.E., Baldwin K.M. (1993) Food restriction-induced transformations in cardiac functional and biochemical properties in rats. *J. Appl. Physiol*. **74,** 606–612.

Hoy W.E., Rees M., Kile E., Mathews J.D., Wang Z. (1999) A new dimension to the Barker hypothesis: low birthweight and susceptibility to renal disease. *Kidney Int.* **56**, 1072-1077.

Gruber C., Nink N., Nikam S., Magdowski G., Kripp G., Voswinckel R., Mühlfeld C. (2012) Myocardial remodelling in left ventricular atrophy induced by caloric restriction. *J. Anat.* **220**, 179-185.

Johnson W.T. & Johnson L.K. (2009) Copper deficiency inhibits Ca2+-induced swelling in rat cardiac mitochondria. *J. Nutrit. Bioch.* **20**, 248-253.

Kaye D., Hoshijima M., Chien K.R. (2008) Reversing advanced heart failure by targeting Ca2+ cycling. *Ann. Rev. Med.* **59**, 13-28.

Klebanov S., Herlihy J.T., (1997) Efect of life-long food restriction on cardiac myosin composition. *J. Gerontol.* **52**: 184-189.

Law C.M. & Shiell A.W. (1996) Is blood pressure inversely related to birth weight? The strength of evidence from a systematic review of the literature. *J. Hypert.* **14**, 935-941.

Leopoldo A.S., Lima-Leopoldo A.P., Sugizaki M.M., Nascimento A.F., Campos D.H.S., Luvizotto R.A.M., Castardeli E., Alves C.A.B., Brum P.C., Cicogna A.C. (2011) Involvement of l-type calcium channel and SERCA2a in myocardial dysfunction induced by obesity. *J. Cel. Physiol.* **22**, 1-29.

Li F., Wang X., Capasso J.M., Gerdes A.M. (1996) Rapid transition of cardiac myocytes from hyperplasia to hypertrophy during postnatal development. *J. Mol. Cell. Cardiol.* **28**:1737–1746.

Lim K., Zimanyi M.A., Black M.J. (2010) Effect of maternal protein restriction during pregnancy and lactation on the number of cardiomyocytes in the post proliferative weanling rat heart. *The Anat.* **293**, 431-437.

Lima-Leopoldo A.P., Leopoldo A.S., Sugizaki M.M., Bruno A., Nascimento A.F., Luvizotto R.A.M. (2011) Myocardial dysfunction and abnormalities in intracellular calcium handling in obese rats. *Arq. Bras. Cardiol.* **13**, 1-9.

Lipsett J., Tamblyn M., Madigan K., Roberts P., Cool J.C., Runciman S.I., McMillen I.C., Robinson J., Owens J.A. (2006) Restricted fetal growth and lung development: a morphometric analysis of pulmonary structure. *Pediatr. Pulmonol.* **41,** 1138-1145.

Lu MC, Tzang BS, Kuo WW, Wu FL, Chen YS, Tsai CH. (2007) More activated cardiac mitochondrial-dependent apoptotic pathway in obese Zucker rats. Obesit. 15: 2634-2642.

Lucas A., Baker B.A., Desai M., Hales C.N. (1998) Nutrition in pregnant or lactating rats programs lipid metabolism in the offspring. *Br. J. Nutr.* **76**, 605-612.

Martins C.D.D., Chianca D.A.Jr., Fernandes L.G. (2011) Cardiac autonomic balance in rats submitted to protein restriction after weaning. *Clin Exp Pharm Physiol* **38**, 89-93.

Novaes R.D., Penitente A.R., Gonçalves R.V., Talvani A, Neves C.A., Maldonado I.R.S.C., Natali A.J. (2011) Effects of Trypanosoma cruzi infection on myocardium morphology, single cardiomyocyte contractile function and exercise tolerance in rats. *Int. J. Exp. Pathol.* **92**, 299-307.

Novaes R.D., Penitente A.R., Talvani A., Natali AJ., Neves CA., Maldonado I.R. S.C. (2012) Use of fluorescence in a modified disector method to estimate the myocytes number in cardiac tissue. *Arq. Bras. Cardiol.* **98,** 252-258

Okoshi M.P., Okoshi K., Dal-Pai V., Dal-Pai M., Matsubara L.S., Cicogna A.C. (2011) Mechanical, biochemical, and morphological changes in the heart from chronic food-restricted rats. *Can. J. Physiol. Pharm.* **79**, 1-7.

Opie L.H., Bers DM. (2004) Heart physiology: from cell to circulation. In: Opie LH, ditor. Excitation-contraction coupling and calcium. *Philadelphia: Lippincott Williams & Wilkins* **56**, 159-185.

Olfert E.D., Cross B.M., M. A.A. (1993) Canadian Council on Animal Care. Guide to the Care and Use o Experimental Animals. *In Ed Bradda Printing Services.* Ottawa, Ontario.

Penitente A.R., Fernandes L.G., Cardoso L.M., Silva M.E., Pedrosa M.L., Silva A.L., Haibara A.S., Moraes M.F.D., Chianca D.A.Jr. (2007) Malnutrition enhances cardiovascular responses to chemoreflex activation in awake rats. *Lif. Scienc.* **81**, 609-614.

Phillips D.I.W., Barker D.J.P., Hales C.N., Hirst S., Osmond C. (1994) Thinness at Birth and Insulin-Resistance in Adult Life. *Diabet.* **37**, 150-154.

Pinotti M.F., Leopoldo A.S., Dal-Pai S.M., Sugizaki M.M., Nascimento A.F., Lima-Leopoldo A.P., Aragon F.F., Padovani C.R., Cicogna A.C. (2010) A comparative study of myocardial function and morphology during fasting/refeeding and food restriction in rats. *Card. Pathol.* **19**, 175-182.

Relling D.P., Esberg L.B., Fang C.X., Johnson W.T., Murphy E.J., Carlson E.C. (2006) High-fat-diet-induced juvenile obesity leads to cardiomyocyte dysfunction and upregulation of Foxo3a transcription factor independent of lipotoxicity and apoptosis. *J Hypert*. **24**, 549-561.

Ren J., Walsh M.F., Jefferson L., Natavio M., Lig K.J., Sowers J.R. (2000) Basal and ethanol-induced cardiac contractile response in lean and obese Zucker rat hearts. *J Biomed Sci*. **7**, 390-400.

Rossi M.A. & zucoloto S. 1982) Ultrastructural changes in nutritional cardiomyopathy of protein-calorie malnourished rats. *J. exp. Path.* **63**, 242-254.

Sharov V.G., Sabbah H.N., Shimoyama H., Ali A.S., Levine T.B., Lesch M., Goldstein S. (1994) Abnormalities of contractile structures in viable myocytes of the failing heart. *Int. J. Cardiol*. **43:** 287-297.

Scherle W. (1970) A simple method for volumetry of organs in quantitative stereology. *Mikroskopie* **26,** 57-63.

Sugizaki M.M., Carvalho R.F., Aragon F.F. (2005) Myocardial dysfunction induced by food restriction is related to morphological damage in normotensive middle-aged rats. *J. Biomed*. *Sci*. **12**,641–649.

Vandewoude, M.F.J. (1995) Morphometric changes in microvasculature in rat myocardium during malnutrition. *J. Par. Ent. Nutrution*. **19,** 376-380.

Ventura-Clapier R., De Sousa E., Veksler V. (2002) Metabolic Myopathy in Heart Failure. *Physiol. Sci.* **17:** 191-196.

Winick M & Noble A. (1966) This week's citation classic cellular response in rats during malnutrition at various ages. *J. Nutrit.* **89**:300-6.

Zimanyi M.A., Denton K.M., Forbes J.M., Thallas-Bonke V., Thomas M.C., Poon F., Black M.J. (2006) A developmental nephron deficit in rats is associated with increased susceptibility to a secondary renal injury due to advanced glycation end-products. *Diabetol.* **49**, 801-810.

5. Conclusões

Os animais submetidos à dieta hipoproteica (GRP) apresentaram diminuição do peso corporal, peso do coração e do ventrículo esquerdo em relação ao grupo controle, demonstrando que a dieta composta por 6% de proteína, foi eficiente para promover a desnutrição no modelo experimental.

Em nível celular, o GRP apresentou diminuição de todos os parâmetros celulares: morfológicos, estereológicos e alterações na ultra-estrutura do cardiomiócito.

Os resultados confirmam a hipótese de que dieta hipoproteica é capaz de afetar a histoarquitetura dos cardiomiócitos ventriculares, contribuindo para alteração da função contrátil e influenciando de forma negativa na mecânica do miocárdio.

A redução na contratilidade e maior tempo para contração e relaxamento dos cardiomiócitos isolados, tanto em condições basais, quanto após estimulação β-adrenérgica são as principais disfunções mecânicas provocadas pela restrição protéica severa.

As disfunções mecânicas supracitadas estão associadas às alterações no trânsito de cálcio intracelular e menor expressão da SERCA2a.

6. Anexo 1

Artigos publicados com a participação da Autora no período de Doutorado

6.1. Artigo 1: Novaes, Rd; **PENITENTE, AR;** Talvani, A; Natali, AJ; Neves, CA; Maldonado, IRSC. (2012) Use of fluorescence in a modified dissector method to estimate the myocytes number in cardiac tissue. Arquivos Brasileiros de Cardiologia. 62: 199-315

6.2. Artigo 2: Novaes, RD; **PENITENTE, AR**, Gonçalves, RV; Talvani, A; Neves, CA; Maldonado, IRSC; Natali, AJ. (2011) Effects of Trypanosoma cruzi infection on myocardium morphology, single cardiomyocyte contractile function and exercise tolerance in rats. International Journal of Experimental Pathology.

6.3. Artigo 3: Silva MF, Pelúzio MCG, Amorim PRS, Lavorato VN, Santos NP, Bozi LMM, **PENITENTE AR**, Falkoski DL, Berfort FG, Antônio José Natali. Treinamento em Natação Atenua a Disfunção Contrátil de Cardiomiócitos de Ratos Diabéticos. Arquivos Brasileiros de Cardiologia.

Use of Fluorescence in a Modified Disector Method to Estimate the Number of Myocytes in Cardiac Tissue

Rômulo Dias Novaes[1], Arlete Rita Penitente[1], André Talvani[2], Antônio José Natali[1], Clóvis Andrade Neves[1], Izabel Regina Santos Costa Maldonado[1]

Universidade Federal de Viçosa, Viçosa[1]; Universidade Federal de Ouro Perto, Ouro Preto[2], MG, Brazil

Abstract

Background: Conventional disector methods currently require considerable financial, technical and operational costs to estimate the number of cells, including cardyomyocytes, in a 3D area.

Objective: To use fluorescence microscopy in a modified disector method to determine the number of myocytes in cardiac tissue in normal and pathological conditions.

Methods: The study employed four-month-old male Wistar rats with weight of 366.25 ± 88.21g randomized in control (CG, n=8) and infected (IG, n=8) groups. IG animals were inoculated with T. cruzi Y strain (300,000 trypomastigotes/50g wt). After eight weeks, the animals were weighted and euthanized. The left ventricles (LV) were removed for stereological analysis of numerical density of cardiomyocytes (Nv[c]) and total number of these cells in the LV (N[c]). These parameters were estimated using a fluorescent disector (FD) and compared with the conventional optical (OD) and physical (PD) disector methods.

Results: In both disector methods, IG animals presented significant decrease of Nv[c] and N[c] compared to CG animals (P< 0.05). There was no significant difference in these variables despite the disector method applied in CG and IG animals (P> 0.05). A strong correlation, equal or above 96%, was obtained between FD, OD and PD.

Conclusion: The FD method seems to be equally reliable to determine Nv[c] and N[c] in normal and pathological conditions and presents some advantages compared to conventional disector methods: reduction of histological slices and images in the stereological analysis, reduction of time to analyze the images, construction of FD in simple microscopes using the epifluorescence mode, distinction of disector planes in lower magnifications. (Arq Bras Cardiol. 2011; [online].ahead print, PP.0-0)

Keywords: Cell separation; flow cytometry; myocytes, cardiac.

Introduction

Over the past years a great effort was made to develop a reliable and reproducible method to estimate the number of particles in organs and tissues, but until 1984, all these methods had intrinsic biases[1-3]. In 1984, Sterio described several modifications in the approaches used to estimate the quantity of objects in three-dimensional space and introduced the *disector* method[4]. Most authors currently consider the *disector* method unbiased and the well-established theoretical background makes the method largely acceptable[5-7].

The *disector* may be obtained through two different methods based on the same theoretical principles and basic requirements to estimate the number of particles. These methods are the optical and physical disector[4,8-10]. Although both methods have reduced the bias of particle quantity estimation, they still required the acquisition of a large number of histological images and a great deal of time to perform the counts. Particularly, the optical *disector* also requires a light microscope of high cost adapted with axis-Z mobile stage[11]. Moreover, the physical *disector* is extremely laborious because it requires serial histological sections and images with a perfect alignment in the different parallel sections[3,10].

Considering that the aim of the sampling design for stereology is to obtain the maximal amount of quantitative structural information at a given total cost, time or effort, the purpose of this study was to use fluorescence microscopy in a modified *disector* method to determine the number of myocytes in cardiac tissue in normal and pathological conditions. Thus, a murine model of *T. cruzi* infection that recognizably conduces to disruption of cardiac myocytes and modifies the number of these cells in the myocardium was used.[12] We hypothesized that the proposed method would reduce the operational cost observed in conventional methods, while maintaining the accuracy of cell quantity measurements.

Mailing Address: Rômulo Dias Novaes •
Av. PH Rolfs, S/N - Campus Universitário - Centro - 36570-000 – Viçosa, MG, Brasil
E-mail: romuonovaes@yahoo.com.br
Manuscript received July 08, 2011, revised manuscript received August 18, 2011; accept August 26, 2011.

Methods

Animals and experimental groups

Four-month-old male Wistar rats with initial weight of 366.25 ± 88.21 g were provided with rodent chow and water *ad libitum* and maintained in animal facilities in a controlled environment (temperature at 22 ± 3 ºC, humidity at 60 - 70 % and 12 hour light/dark inverted cycles). Sample sizes were determined considering the probability $p = 1/2$ to occur increase or decrease of the variables of interest. Thus, considering the significance level $\alpha = 0.05$, the minimal significant number of animals used in the statistical analysis was: $p = (1/2)^{events}$; therefore, if $n = 5$, $p = (1/2)^5$ or $p = 0.03$; then, $p < 0.05$.[10] Due to the intrinsic variability of the parasitism in target organs and the mortality associated with *T. cruzi* infection, a correction factor of 50% was incorporated into the initial calculation, determining samples of 8 animals, randomly allocated into control (CG, n = 8) and infected (IG, n = 8) groups.

Infection

IG animals were inoculated intraperitoneally with *T. cruzi* Y strain (300,000 trypomastigotes/50g body weight in 1 mL of infected mice blood[13]. Infection was confirmed four days post-inoculation by the presence of trypomastigotes in peripheral blood collected from the rat's tail as described by Brener[14]. All experimental procedures were conducted in accordance with the Brazilian College of Animal Experimentation and approved by the Animal Research Ethics Commission of the Veterinary Department of the Universidade Federal de Viçosa, Brazil (protocol number 30/2009).

Biometrical analysis

Eight weeks after inoculation, the animals were euthanized under anesthesia and the hearts were removed. The left ventricles (LV) were dissected and weighed separately. LV volume was obtained by the submersion method, where the liquid displacement from the organ volume is weighed. As the specific gravity (σ) of isotonic saline is 1.0048, the volume is obtained by: volume= weight/σ, or simply volume (10^3 mm^3) ≈ weight (g)[15]. LV weight and volume was determined including the interventricular septum.

Tissue processing and determination of histological areas

The atria and ventricles were put into histological fixative for 48 hours (freshly prepared 10% w/v formaldehyde in 0.1 M phosphate buffer pH 7.2)[16,17]. LV fragments were obtained through the *orientator* method to define isotropic and uniform random sections (IUR) required in the stereological study[3]. These fragments were dehydrated in ethanol, cleared in xylol and waxed. Blocks were cut into 3 μm sections and stained by hematoxylin-eosin (H&E) or 4',6-diamidino-2-phenylindole at 0.2% (DAPI)[18].

The representative number of *disectors* used in the stereological analysis for each animal was determined considering the stabilization of the coefficient of variation (CV) of number of myocytes nuclei in ascending random samples of *disectors* (5, 10, 15, 20 and 25). Then, the arithmetical mean and the respective CV for each sample size were calculated. When the increase of *disector* numbers resulted in no significant difference of CV between 3 consecutive samples, the smallest sample size was considered as the minimal representative size[19]. Using this method, the variation of number of myocytes nuclei was stabilized from the sample of 10 *disectors*.

Optical and physical disector methods

Sections stained with H&E were mounted on histology slides using Entelan® mounting medium (Merk, Darmstadt, Germany) and the images were captured using a light microscope (Olympus BX-60®, Tokyo, Japan) connected to a digital camera (Olympus QColor-3®, Tokyo, Japan). Observation was made with a 100× planachromatic oil immersion objective (NA= 1.25) to clearly identify cardiomyocyte (*cmy*) nuclei boundaries[16,17].

The number of cardiomyocyte nuclei (*cmyn*) in a 3-dimensional probe was estimated using the optical (OD) and physical (PD) *disector* methods[3]. The *disector* consists of 2 parallel planes aimed at sampling ''top points'' of particles in between. Sampling volume was created with 2 parallel sections separated by 3 μm (h) and 2 reference planes both containing a test frame (A_T). In both *disector* methods, a pair of photomicrographs separated by h distance is used to form the two reference planes. In the OD, the parallel photomicrographs are obtained in the same histological area adjusting the focal plane ($h = 3\ \mu$m) using the micrometrical screw. In the PD, two serial sections are obtained in the microtome ($h = 3\ \mu$m) and the same histological area is photographed in both sections, supplying two photomicrographs physically separated.

Fluorescent disector method

In the fluorescent *disector* method (FD), sections stained with DAPI were mounted on histology slides using 50% sucrose solution in distillated water (w/v). Images were captured in an epifluorescence mode of the same microscope using a HBO 100 mercury lamp and a filter for dye excitation at 365 nm and a light emission at 460 nm. Observation was made with the same 100× planachromatic lens previously described. In this method, using the 3 μm (h) sections, the two reference planes required to delimitate the *disector* are obtained in a unique image and pairs of photomicrographs are not required as in the conventional methods. Furthermore, the *cmyn* present over the thickness of the section may be observed inside or outside the focal plane. To avoid repeat cells count, sections were obtained in semi-series, using 1 in every 20 sections. The FD was additionally obtained with a 40× objective lens only to demonstrate the possibility of applying the method using smaller magnifications.

Estimation of numerical density and total number of cardiomyocytes

The numerical density of *cmyn* (Nv[c], *cmyn* per mm^3) was determined from 10 random *disector* pairs for each animal, defined as $Nv[c] = Q^-[cmyn] / h \times A_T$; where Q^- represents the number of profiles of *cmyn* counted in the test area on the

disector reference section (''look-up'' plane).[3,17] In the FD, the *Q*- value in the Nv[c] formula was multiplied by a correction factor of 0.5 to avoid overestimation of measures. The total number of *cmyn* in the LV (N[c]) was estimated as the product of Nv[c] / LV volume. The counts were performed in an $A_t = 2670\ \mu m^2$. All stereological analyses were performed using the software Image Pro-Plus 4.5® (Media Cybernetics, Silver Spring, USA).

Statistical analysis

All analyses were performed using the statistical platform GraphPad Prism (version 5.01, GraphPad Software, San Diego, CA). Data are expressed as mean and standard deviation (mean ± S.D.). The normality of data distribution was verified using the Kolmogorov-Smirnov test. Based on this test, weight and volume data were compared using the t-test. The Mann-Whitney U test was used to compare the stereological data between the groups. The disector methods were compared using the Kruskal-Wallis test and correlated using the Spearman's method. Statistical significance was established at $\alpha = 0.05$.

Results

There was no statistical difference in body mass (CG, 502.17 ± 57.76 g vs. IG, 494.69 ± 87.90 g; $p > 0.05$) and left ventricle volume (CG, 456.47 ± 26.18 mm^3 vs. IG, 487.69 ± 34.89 mm^3; $p > 0.05$) between the groups.

The histopathological analysis of the LV showed a marked diffuse inflammatory infiltrate in IG. Moreover, this group had a disorganization of histological structure with an increased interstitial area and a larger distance between the ventricular myocytes. These cells also showed an increased cross-sectional area and some these presented a narrowing of cytoplasm region induced by a large amount of *T. cruzi* amastigote forms (Fig. 1).

The conventional OD is represented in fig. 2. In this method, the disector was obtained in the same microscopic image adjusting the Z axis of the microscope to create an optical separation of 3 μm between the images. In the physical method (image not shown), the *disector* was obtained using the microscopic images of two different serial histological sections physically separated at the same distance as in the OD (3 μm).

The proposed *disector* method, named fluorescent *disector* (FD), is represented in fig. 3. In this method, the *disector* was obtained in the same microscopic image through the differential fluorescence emission by the *cmyn*. While in the OD and PD 160 photomicrographs (80 *disector* pairs) were required in the stereological analysis, in FD, half of the microscopic images (80 individual *disectors*) was used.

In the FD, a correction factor of 50% was incorporated into the formula used to determine Nv[c] in OD and PD.

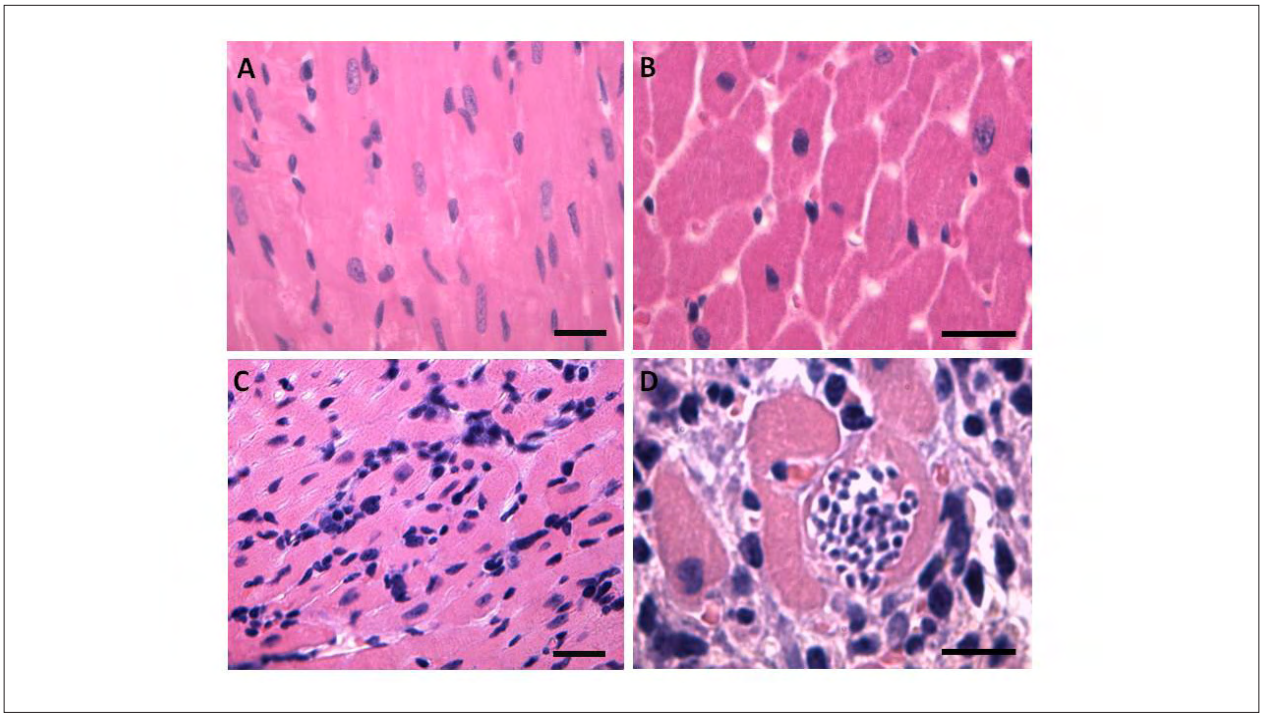

Figure 1 - *Representative photomicrographs of left ventricle of control (A and B) and infected (C and D) groups. The infected animals were inoculated intraperitoneally with T. cruzi Y strain (300,000 trypomastigotes/50 g body weight). (A) Myocardial longitudinal section showing a well-organized structure (magnification 400×, bar = 15µm, H&E stain). In B, we see a myocardial cross-section showing reduced interstitial space and a close relation between the myocytes (magnification 1000×, bar = 15µm, H&E stain). (C) Longitudinal section showing a diffuse inflammatory infiltrate and a disorganization of myocardium structure (magnification 400×, bar = 15µm, H&E stain). D panel shows diffuse inflammatory infiltrate with evident increase of interstitial space and myocyte diameter. This panel shows a large number of amastigote forms of T. cruzi in the myocyte cytoplasm (magnification 1000×, bar = 15µm, H&E stain).*

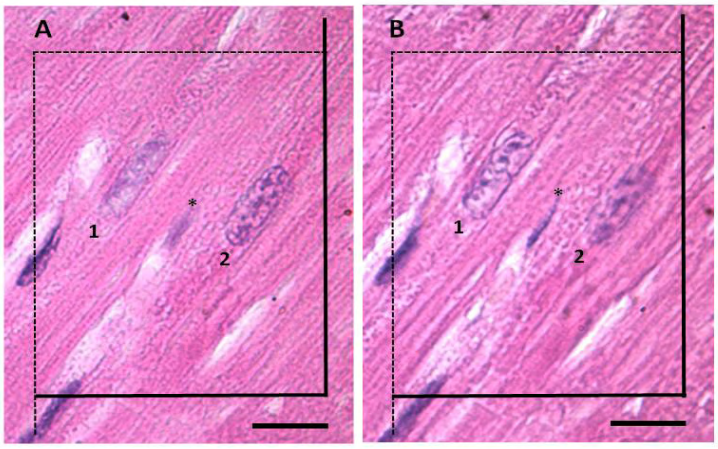

Figure 2 - *Representative photomicrographs of the two disector focal planes separated by 3 µm of distance (h). Disector is the union of a reference plane with an unbiased counting frame of area (AT) and a look-up plane at distance h apart. Cardiomyocyte nuclei (cmyn) are counted or sampled because 1) they are hit by the reference plane, 2) their transects are captured by the counting frame in there, and 3) they are not hit by the "look-down" plane and in the forbidden edge of AT (thick edge). (A) There are two cmyn in the frame of the "look-up" plane (numbered) and only the cmyn 2 should be counted. In this plane, we also observe the shadow of the other cmyn (1) and a fusiform fibroblast nuclei (*) that are not counted because they violate at least 1 of the 3 preceding requirements. (B) The cmyn 1 is in the focus of the "look-down" plane and the cmyn 2 is a shadow outside the focus. If h and AT are known, the disector volume is determined. Dividing the number of nuclei by this volume, a direct estimate of Nv[c] is obtained (magnification 1000×, bar= 15µm, H&E stain).*

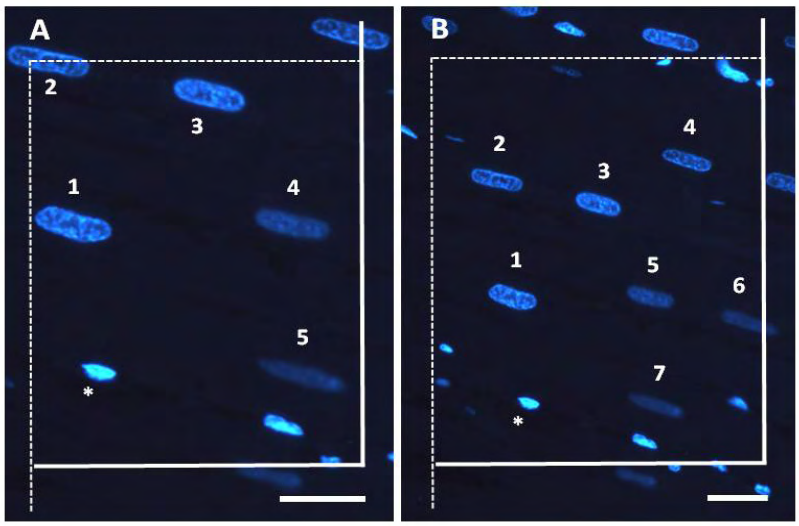

Figure 3 - *Representative photomicrograph of the fluorescent disector method obtained using 100× (A) and 40× (B) objective lens. In this method, two different focal planes are formed in the same microscopic image through the differential fluorescence emission by the cardiomyocyte nuclei (cmyn). Superficial cmyn (look-up plane) appears in the focal plane with more brightness, and cmyn in deep planes (look-down plane) is observed outside the focal plane with low brightness. The unions of these reference planes at distance h apart with an unbiased counting frame of area (A_T) constitute a Fluorescent disector (FD). (A) The cmyn 1, 2 and 3 in the "look-up" plane may be counted and the nuclei 4 and 5 are in the look-down plane and should not be counted. Fibroblast nuclei are indicated by asterisk (magnification 1000×, bar= 15µm, 6-diamidino-2-phenylindole stain). (B) There are four cmyn into the frame in the "look-up" plane (1, 2, 3 and 4) that may be counted. The cmyn 5, 6 are observed in the look-down plane and the nucleus 7 hit on forbidden edge of A_T. Therefore, these should not be counted because they violate the counting requirements (magnification 400×, bar= 15µm, 6-diamidino-2-phenylindole stain). The same principles for cmyn count described for the conventional disector are used in this method.*

Table 1 - Numerical density and absolute number of cardiomyocytes in the left ventricular myocardium of control and infected rats

	OD	PD	FD
Nv[c] / mm^3			
Control	17,5424.64 ± 6,135.36	18,3977.32 ± 9,162.78	17,2429.44 ± 8,123.37
Infected	90,771.41 ± 3,314.30*	95,352.20 ± 3,144.13*	91,141.127 ± 3,741.09*
N[c] x 10^4			
Control	7,948.51 ± 471.45	8,302.75 ± 519.98	8,017.90 ± 474.789
Infected	4,665.58 ± 318.99*	5,042.18 ± 371.44*	4,969.99 ± 354.77*

Data are expressed as mean ± S.D; OD - Optical disector; PD - Physical disector; FD - Fluorescent disector; Nv[c] - numerical density of cardiomyocytes; N[c] - absolute number of cardiomyocytes. All values were obtained using a 100× objective lens (magnification 1000×), denoting a statistical difference compared to CG ($p < 0.01$), Mann-Whitney U test. There are no statistical differences between the disector methods, Kruskal-Wallis test.*

Table 2 - Correlations between the results of numerical density and absolute number of left ventricular myocytes obtained using different *disector* methods in control and infected rats

	Nv[c] / mm^3		N[c]	
	Correlation (r)	p value	Correlation (r)	p value
Control				
OD x PD	0.98	<0.0001	0.98	<0.0001
OD x FD	0.96	<0.0001	0.97	<0.0001
PD x FD	0.96	<0.0001	0.96	<0.0001
Infected				
OD x PD	0.99	<0.0001	0.99	<0.0001
OD x FD	0.97	<0.0001	0.98	<0.0001
PD x FD	0.97	<0.0001	0.97	<0.0001

OD - Optical disector; PD - Physical disector; FD - Fluorescent disector; Nv[c] - numerical density of cardiomyocytes; N[c] - absolute number of cardiomyocytes. The results relate to the data obtained using a 100× objective lens (magnification 1000×). Correlations were tested using the Spearman's method.*

Thus, the formula used to estimate Nv[c] in the FD was $Nv[c] = Q^{-}[cmyn] \times 0.5 / h \times A_f$; where the constant 0.5 was established to avoid overestimation of *cmyn* count in FD.

The results of Nv[c] and N[c] obtained using the different *disector* methods are showed in table 1. In both *disector* methods, the infected animals presented significant decrease of both variables compared to control animals. There was no significant difference in the values of these variables despite the *disector* methods used.

Table 2 shows the result of correlation analysis of Nv[c] and N[c] obtained using the different *disector* methods. A strong, direct and significant correlation was obtained in all correlations between both methods.

Discussion

For many years, the morphological studies of biological tissues were based on ambiguous histopathological descriptions. The symbols used to indicate the increase or decrease of a variable is the best way to express the data in a semi-quantitative context[20]. As these morphological approaches were further refined, a two-dimension (2D) quantitative system was incorporated into the histological and pathological analysis to describe the morphometrical characteristics of organs and tissues[1,21,22]. These refinements introduced significant advances in histo-quantitative studies. However, the estimation of microscopic parameters in a three-dimension (3D) space remained as an issue still not well resolved, and the conventional morphometric methods presented intrinsic biases that reduced the reliability of morphological measurements[2,3,23].

Considering the intrinsic bias of several morphometrical measurements, calculations of probability statistics and geometry applied in geology and other soil sciences were adapted to the study of biological materials[1,24], forming the basis of current stereology[3]. The development of stereology is an important evolution in histo-quantitative methods, allowing the development of more accurate and reliable morphological data[9,10,25,26].

Estimation of quantity of objects in biological tissue has been a crucial issue in morphological studies and diagnostic pathology, constituting the more refined measures in stereology[3,7]. The development of *disector* methods by Sterio in 1984 led to a creative and relatively simple way

to estimate the number of particles in an organ or tissue[4]. However, the *disector* method still requires a series of technical requirements that increase the time and cost of data acquisition[5,8,10]. The need to obtain and analyze a large number of microscopic images is a common limitation of both OD and PD methods, especially when several groups and tissue samples are studied at once. Moreover, the costs for acquiring or adapting a microscope with controlled Z axis contribute to limit the application of OD[11]. On other hand, obtaining a PD is extremely laborious because it involves the quality of the microtomy, appropriate processing of serial sections and technical ability to determine a perfect alignment of these sections[4]. Furthermore, minimal alignment error can lead to a bias in the cell count characterized by an overestimation or underestimation of stereological outcomes. Thus, these conventional *disector* methods still require considerable financial, technical and operational costs to estimate the quantity of particles in a 3D area[11].

This study proposes an alternative method to estimate the quantity of myocytes in the cardiac tissue using fluorescence microscopy in a modified *disector* method. The construction of a FD was based on similar requirements as used for particle counts described in the conventional disector methods. However, an adaptation of the formula to determine N[c] was required in FD. The introduction of a correction factor was necessary to reduce overestimation of measurements. In conventional methods, particle count results exclude those which hit the forbidden plane (generally look-down plane), contributing to reduce the measurement bias[27,28]. As in the FD, the presence or absence of the same particle cannot be observed in both *disector* planes, as it occurs in OD and PD. The calculation of probability determines a 0.5 correction factor to the N[c] formula, considering 50% of chances of a particle be observed or not in both planes.

The application of the FD using the proposed method provided similar results of Nv[c] and N[c] compared to the other *disector* methods, without any significant differences between the methods. Both methods presented sufficient sensibility to determine the reduction of left ventricle myocyte number in the murine model of *T. cruzi*-induced cardiac infection. This model was selected for this study due to the well-established tropism to cardiac tissue presented by this parasite and its ability to reduce the number of myocytes due to parasite replication, differentiation and cell evasion, which propagates in an ongoing destructive process[12,13]. In addition, the correlations between the FD with conventional methods were strong, indicating that the FD method may be equally reliable to estimate the number of myocytes in the cardiac tissue. The reliability of these measures seems to be maintained in both health and pathological conditions.

Although the FD is also an optical method, this study demonstrated that the FD may also be obtained using objective lens with lower magnifications (40×) compared with conventional lens (100×) required in OD. In OD, lower magnifications are not often used because they determine a large depth-of-field, which hinders the acquisition of different *disector* focal planes (look-up and look-down) because it maintains all section structures inside the focus, in despite of the Z axis adjustment[3].

Conclusion

The FD described in this study offered an alternative method to estimate the number of myocytes in the cardiac tissue. This method seems to be equally reliable in normal and pathological conditions to determine the same parameters of Nv[c] and N[c] obtained using conventional *disector* methods. Although the results has been similar between the three methods, the FD showed some advantages compared to OD and PD such as: 1) reduction (by half) of the number of histological slices and images required in the stereological analysis, 2) reduction of time to analyze the required images, 3) construction of FD in simple microscopes using the epifluorescence mode, 4) distinction of *disector* look-up and look-down planes using lower magnifications, 5) reliability of stereological results demanding reduced technical and operational cost compared to the OD and PD methods.

References

1. Weibel ER, Kistler GS, Scherle WF. Practical stereological methods for morphometric cytology. J Cell Biol. 1966;30(1):23-38.
2. Aherne WA. Methods of counting discrete tissue components in microscopical sections. J R Micr Soc. 1967;87(3):493-508.
3. Mandarim-de-Lacerda CA. Stereological tools in biomedical research. An Acad Bras Cienc. 2003;75(4):469-86.
4. Sterio DC. The unbiased estimation of number and sizes of arbitrary particles using the disector. J Microsc. 1984;134(Pt2):127-36.
5. Dorph-Petersen KA, Nyengaard JR, Gundersen HJ. Tissue shrinkage and unbiased stereological estimation of particle number and size. J Microsc. 2001;204(Pt3):232-46.
6. Charleston LB, Thyer AC, Klein NA, Soules MR, Charleston JS. An improved method for the production of slides from oversized samples of glycol methacrylate-embedded tissues: Application for optical disector based stereology. J Histotechnol. 2003;26(1):49-52.
7. Eisele JC, Schaefer I-M, Nyengaard JR, Post H, Liebetanz D, Brüel A, et al. Effect of voluntary exercise on number and volume of cardiomyocytes and their mitochondria in the mouse left ventricle. Basic Res Cardiol. 2008;103(1):12-21.
8. Gundersen HJ, Bagger P, Bendtsen TF, Evans SM, Korbo L, Marcussen N, et al. The new stereological tools: disector, fractionator, nucleator and point sampled intercepts and their use in pathological research and diagnosis. APMIS. 1988;96(10):857-81.

9. Weibel ER. Measuring through the microscope: development and evolution of stereological methods. J Microsc. 1989;155(Pt3):393-403.

10. Cruz-Orive LM, Weibel ER. Recent stereological methods for cell biology: a brief survey. Am J Physiol. 1990;258(4 Pt1):148-56.

11. Xavier-Vidal R. Disector Z-axis mechanical method for stereology. An Acad Bras Cienc. 2010;82(2):539-44.

12. Marin-Neto JA, Cunha-Neto E, Maciel BC, Simões MV. Pathogenesis of chronic Chagas' heart disease. Circulation. 2007;115(9):1109-23.

13. Martinelli PM, Camargos ER, Azevedo AA, Chiari E, Morel G, Machado CRS. Cardiac NGF and GDNF expression during Trypanosoma cruzi infection in rats. Auton Neurosci. 2006;130(1-2):32-40.

14. Brener Z. Therapeutic activity and criterion of cure on mice experimentally infected with *Trypanosoma cruzi*. Rev Inst Med Trop São Paulo. 1962;4:389-96.

15. Scherle W. A simple method for volumetry of organs in quantitative stereology. Mikroskopie. 1970;26(1):57-60.

16. Xavier-Vidal R, Neves MC, Villar VC, Viana WN, Mandarim-de-Lacerda CA. Estereologia do miocárdio em fetos humanos: estudo quantitativo das modificações estruturais nos dois últimos trimestres de gestação. Arq Bras Cardiol. 1993;60(4):221-4.

17. Xavier-Vidal R, Madi K. Comparação entre os miocárdios ventriculares direito e esquerdo durante período fetal humano: uma avaliação estereológica. Arq Bras Cardiol. 1999;72(5):581-6.

18. Masotti L, Cavatorta P, Avitabile M, Barcellona ML, von Berger J, Ragusa N. Characterization of 4'-6 diamidino-2 phenylindole (DAPI) as a fluorescent probe of DNA structure. Ital J Biochem. 1982;31(2):90-9.

19. Moro L, Vasconcelos AC, Santos FGA, Alves CM, Nunes JES, Sampaio IBM. Determination of the minimal representative number of microscopical fields to quantify apoptosis in canine lymph nodes. Arq Bras Med Vet Zootec. 2004;56(3):408-10.

20. Bucher O. [Contribution on the method of morphometry]. Anat Anz. 1967;120(1):39-40.

21. Rohr H. Principles, possibilities of use and limits of morphometry. Acta Histochem Suppl. 1976;16:83-9.

22. Rohr H, Oberholzer M, Barstsch G, Keller M. Morphometry in experimental pathology: methods, baseline data and applications. Int Rev Exp Pathol. 1976;15:233-325.

23. Elias H, Hyde DM. A guide to practical stereology. NewYork: Karger; 1983.

24. Chalkley HW. Methods for quantitative morphological analysis of tissues. J Natl Cancer Inst. 1943;4:47-53.

25. Collan Y. Stereology in diagnostic pathology. Pathologica. 1997;89(4):462-6.

26. von Bartheld C. Counting particles in tissue sections: choices of methods and importance of calibrationto minimize biases. Histol Histopathol. 2002;17(2):639-48.

27. Weibel ER. Stereological methods: practical methods for biological morphometry. London: Academic Press; 1979.

28. Mouton PR. Principles and practices of unbiased stereology: an introduction for bioscientist. Baltimore: John Hopkins University Press; 2002.

INTERNATIONAL JOURNAL OF Experimental Pathology

Int. J. Exp. Path. (2011), 92, 299–307

ORIGINAL ARTICLE

Effects of *Trypanosoma cruzi* infection on myocardial morphology, single cardiomyocyte contractile function and exercise tolerance in rats

Rômulo D. Novaes*, Arlete R. Penitente*, Reggiani V. Gonçalves*, André Talvani†, Clóvis A. Neves*, Izabel R. S. C. Maldonado* and Antônio J. Natali‡

*Department of General Biology, Federal University of Viçosa, Viçosa, Minas Gerais, Brazil, †Department of Biological Sciences and NUPEB, Federal University of Ouro Preto, Ouro Preto, Minas Gerais, Brazil and ‡Department of Physical Education, Federal University of Viçosa, Viçosa, Minas Gerais, Brazil

INTERNATIONAL JOURNAL OF EXPERIMENTAL PATHOLOGY

doi: 10.1111/j.1365-2613.2011.00781.x

Received for publication: 21 February 2011
Accepted for publication: 27 May 2011

Correspondence:
Antônio José Natali
Department of Physical Education
Federal University of Viçosa
Av. Peter Henry Rolfs, s/nº
Zip code: 35.570-000
Viçosa-MG
Brazil
Tel.: +55 (031) 3899 4390
Fax: +55 31 3899 2249
E-mail: anatali@ufv.br

Summary

The aim of this study was to investigate the effects of *Trypanosoma cruzi* (*T. cruzi*) infection on myocardial morphology, single cardiomyocyte contractile function and exercise tolerance in rats. Adult Wistar rats were randomized into control (n = 14) and infected (n = 14) groups. Infected animals were inoculated with *T. cruzi* Y strain (300,000 trypomastigotes/50 g body weight). After 9 weeks, the animals were subjected to a treadmill running protocol. Then, the right atrium (RA) and left ventricle (LV) were removed for morphological and cell contractile evaluation. The infected animals exhibited a significant reduction in distance travelled, total time to fatigue and workload. In addition, these animals had hypertrophy, increased myocardial cellularity, and an increase in the proportion of collagen and blood vessels. RA and LV myocytes from infected animals showed marked contractile dysfunction under basal conditions and a reduced contractile response to β-adrenergic stimulation. The workload of infected animals was correlated closely with the amplitude of cell shortening of RA and LV myocytes. *T. cruzi* infection influenced the myocardial morphology and the mechanical properties of RA and LV single myocytes negatively and reduced exercise tolerance. Single cardiomyocyte contractile dysfunction could constitute an additional mechanism of cardiac impairment and reduced exercise tolerance in this infection.

Keywords
cellular contractility, Chagas' cardiomyopathy, myocytes, physical capacity

Chagas' disease is an underappreciated illness caused by the intracellular protozoan parasite *Trypanosoma cruzi* (*T. cruzi*) that is an important health problem in 18 developing countries in South and Central America (Biolo *et al.* 2010; Rassi *et al.* 2010). Its main clinical manifestations are cardiac and/or digestive disturbances, with a prevalence of about 12–14 million cases worldwide, and it has been considered a major cause of cardiac infectious disease in endemic countries (WHO 2005). Chronic Chagasic cardiomyopathy is the main cause of death and occurs in approximately 30% of infected subjects (Marin-Neto *et al.* 2007; Rassi *et al.* 2010). The clinical course of Chagas' disease shows great variability, and the mechanisms responsible for the development of this potentially lethal cardiomyopathy are not understood (Biolo *et al.* 2010; Rassi *et al.* 2010).

Cardiac denervation, interstitial mononuclear infiltrate, myocyte and vascular degenerative changes, fibrosis and hypertrophy characterize the main pathologic features of chronic Chagasic cardiomyopathy (Marin-Neto *et al.* 2007; Biolo *et al.* 2010; Rassi *et al.* 2010). These morphological changes coexist and are associated with abnormalities of the electrical and contractile cardiac activities characterized mainly by conduction defects, frequent and complex ventricular arrhythmias and systolic ventricular dysfunction (Marin-Neto *et al.* 2007; Biolo *et al.* 2010). In addition, the chronotropic incompetence caused by changes in the sympa-

© 2011 The Authors. International Journal of Experimental Pathology © 2011 International Journal of Experimental Pathology

thetic and parasympathetic tonus induced by an immune-mediated process has been recognized as one of the mechanisms capable of interfering with the capacity of the heart to increase heart rate in response to different stimuli, including physical exercise (Colucci *et al.* 1989; Talvani *et al.* 2006; Sousa *et al.* 2009).

Few studies have evaluated exercise performance and the factors affecting functional capacity and exercise tolerance in patients with Chagas' disease. Moreover, it is not known whether *T. cruzi* infection can also lead to changes in exercise tolerance in experimental animal models. The reduction of exercise tolerance in individuals with Chagas' disease is multifactorial and is involved with pathological changes in several organs and tissues, such as peripheral nervous system, skeletal and cardiac muscles (Meiler *et al.* 1987; Montes de Oca *et al.* 2004). Moreover, previous studies indicated that atrial and ventricular mechanical and electrical abnormalities may have an important role in exercise intolerance in Chagas' disease (Gallo *et al.* 1975; Mady *et al.* 2000; Lima *et al.* 2010). However, several aspects of the cellular and molecular basis of these changes remain to be clarified.

Recently, our group showed for the first time changes in the cellular mechanics of cardiac myocytes isolated from the atrium and ventricle of C57BL/6 mice infected with *T. cruzi* (Roman-Campos *et al.* 2009). We observed decreased myocyte contraction amplitude and a prolonged contraction and relaxation time course in the very beginning of the parasitism that remained until the chronic phase of the disease. Data from our laboratory also showed that in normal rats, exercise performance is significantly influenced by the electromechanical characteristics of cardiomyocytes (Prímola-Gomes *et al.* 2009). In this study, cardiomyocytes isolated from rats with high running capacity had greater calcium (Ca^{2+}) transients, amplitude of cell contraction, maximum velocity of contraction and relaxation compared with rats of the same progeny with standard running capacity.

The aim of this study was to investigate the effects of *T. cruzi* infection on myocardial morphology, single cardiomyocyte contractile function and exercise tolerance in rats. We hypothesized that *T. cruzi* infection can lead to changes in cardiac morphology, and to single cardiomyocyte contractile dysfunction and can also influence exercise tolerance in rats.

Materials and methods

Animals and infection

Four-month-old male Wistar rats with an initial weight of 366.25 ± 31.17 g were given rodent chow and water *ad libitum* and maintained in animal facilities with a controlled temperature of 22 °C and 12-h light/dark inverted cycles. Animals were randomly divided into control (CG = 14) and infected (IG = 14) groups. Animals from the IG were inoculated intraperitoneally with *T. cruzi* Y strain (300,000 trypomastigotes/50 g body weight, about 21,00000 trypomastigotes) (Martinelli *et al.* 2006) contained in 700 μl of infected blood from mouse diluted in saline solution 0.9% (Brener 1962). Infection was confirmed 4 days postinoculation by the presence of trypomastigotes in peripheral blood collected from the rat's tail, and the level of parasitaemia was recorded daily after inoculation as described by Brener (1962). Mortality was investigated during the experiment. All experimental procedures were conducted in accordance with the Brazilian College of Animal Experimentation and approved by the Animal Research Ethics Commission of the Veterinary Department at the Federal University of Viçosa, Brazil (protocol 30/2009).

Measurement of exercise tolerance

Nine weeks after inoculation, all animals were evaluated for exercise tolerance using a treadmill incremental running protocol adapted from Koch and Britton (2001). Briefly, the rats were familiarized with the motor-driven treadmill (Insight Instruments®, Ribeirão Preto, Brazil) by running at a speed of 10 m/min at 5% inclination for 5 min/day for seven consecutive days. Two days after familiarization, the exercise trial was performed on three consecutive days at a constant slope of 5% with the starting speed at 10 m/min. Treadmill velocity was increased by 1 m/min every 2 min, and each rat ran until fatigue. Fatigue was defined as the point at which the animals were no longer able to keep pace with the treadmill. Travelled distance (m), time until fatigue and workload were used as indexes of exercise tolerance (Lacerda *et al.* 2006). Workload (W; kg) was calculated using the equation $W = \text{body mass (kg)} \times \text{TTF (total time to fatigue) (min)} \times \text{treadmill speed (m/min)} \times \sin\theta$ (treadmill inclination), where TTF is time until fatigue (Brooks *et al.* 1984). Because of variability in the performance data, the mean of the indices of running performance was calculated for the three trials for each rat and analysed.

Heart biometry and myocardial stereology

Forty-eight hours after the exercise test, five animals from each group were sacrificed, and the hearts were removed and weighed. The atria and ventricles were dissected, weighed separately and the right atrium (RA) and left ventricle (LV) isolated. Hypertrophy was determined by measuring RA and LV volume using the submersion method described by Scherle (1970).

The atria and ventricles were fixed for 48 h (in freshly prepared 10% w/v formaldehyde in 0.1 M phosphate buffer, pH 7.2). The fragments of the RA and LV were obtained through the Orthrip method for stereological study (Mandarim-de-Lacerda 2003). These fragments were dehydrated in ethanol, cleared in xylol and embedded in paraffin. Blocks were cut into 4-μm sections and stained by Masson's trichrome or haematoxylin–eosin (H&E) and mounted on histology slides. The slides were visualized and the images captured using a light microscope (Olympus BX-60®; Olympus, Tóquio, Japan) connected to a digital camera (Olympus QColor-3®; Olympus, Tóquio, Japan). Sixty fields from each

Masson's trichromic (objective ×20) and H&E (objective ×40) stain were randomly chosen, and a total of 4.37×10^6 μm^2 and 1.41×10^6 μm^2 of myocardium area, respectively, were analysed. Sections stained with Masson's trichromic were used for myocardial stereological analysis. For this analysis, a test system of 72 points was used in a standard test area of 73×10^3 μm^2 (Mandarim-de-Lacerda 2003). All the stereological analyses were performed according to Bezerra *et al.* (2008).

The stereological parameter of volume density (Vv) was estimated by point counting for cardiomyocytes [cmy], collagen [col] and intramyocardial blood vessels [ibvs] according to the formula Vv [structure] = P_P [structure]/P_T, where P_P is the number of points that hit the structure and P_T is the total number of test points. The amount of intramyocardial vascularization was defined as the ratio of Vv [ibvs]/Vv [cmy]. The mean cross-sectional area of cardiomyocytes was estimated according to the following relationship: A [cmy] = Vv [cmy]/2.Q_A [cmyn]; Q_A [cmyn] = N [cmy]/A_T, where Q_A [cmyn] is the number of cardiomyocyte nuclei profiles in the analysed area (A_T). Overestimation of the measurements was avoided by the exclusion of nuclei profiles incident on two edges of the A_T.

Myocardial histopathology

For each group, 25 sections of 8 μm thickness stained with Sirius red and Fast green were used to quantify collagen and total protein in cardiac tissue using a spectrophotometric method previously described (López-De León & Rojkind 1985).

The inflammatory process was evaluated by the correlation index between the number of cells observed in the myocardium from CG and IG animals (Caldas *et al.* 2008). All morphological analyses were performed using the software IMAGE PRO-PLUS 4.5® (Media Cybernetics, Silver Spring, MD, USA).

Cardiomyocytes isolation

Nine animals from each group were used in this set of experiments. At the time of sacrifice, the heart was removed rapidly and extraneous tissue dissected away. The heart was flushed immediately with modified HEPES (4-2-hydroxyethyl-1-piperazineethanesulfonic acid)-Tyrode's solution of the following composition (mM): 130 NaCl, 5.4 KCl, 1.4 $MgCl_2$, 0.4 NaH_2PO_4, 0.75 $CaCl_2$, 5 HEPES, 10 glucose, 20 taurine and 10 creatine (pH 7.4) and then blotted and weighed before being mounted onto a Langendorff perfusion apparatus for the isolation of myocytes using a collagenase–protease dispersion technique as described previously (Natali *et al.* 2002). Briefly, the heart was perfused for 10–15 min with a solution containing 1 mg/ml collagenase type II (Worthington Biochemical Co.; Worthington, OH, USA). The digested heart was removed from the cannula, and the RA and LV were separated and cut into small pieces. Ventricular and atrial cardiomyocyte cells were isolated mechanically (5 min at 37 °C), and single cells were separated from the non-dispersed tissue by filtration. The resulting cell suspension was centrifuged at 30 ***g*** for 45 s, resuspended in HEPES-Tyrode's and stored at 4 °C until analysis. Only calcium-tolerant, quiescent, rod-shaped cardiomyocytes showing clear cross-striations were studied. The isolated cardiac myocytes were used within 4 h after isolation.

Measurements of cell contractility

Cellular contractile function was evaluated as described by Natali *et al.* (2002). Isolated cells were placed in a chamber with a glass coverslip base mounted on the stage of an inverted phase-contrast video microscope (Eclipse-TS100®; Nikon, Tóquio, Japan). The chamber was perfused with Tyrode's solution (in mM): 140 NaCl, 5.4 KCl, 1 $MgCl_2$, 1.8 $CaCl_2$, 10 HEPES and 10 glucose (pH 7.4) at room temperature (approximately 28 °C). Myocytes were stimulated via platinum bath electrodes with voltage pulses of a duration of 5 ms and an intensity of 20 V at the stimulation frequency of 3 Hz. Cells were visualized on a PC monitor with a NTSC camera (Myo-Cam CCD100V®; Ionoptix, Milton, MA, USA) in partial scanning mode. This image was used to measure cell shortening (index of contractile function) in response to electrical stimulation using a video motion edge detection system (Ionoptix). The cell image was sampled at 240 Hz, and cell shortening was calculated from the output of the edge detector using an IonWizard A/D converter (Ionoptix). Eight to 16 consecutive contractions were averaged, and cell shortening (expressed as a percentage of resting cell length), time to peak shortening and time to half relaxation were calculated (Roman-Campos *et al.* 2009).

β-Adrenergic stimulation

The contractile response of isolated cardiomyocytes to β-adrenergic stimulation was assessed using the non-selective agonist isoproterenol (ISO, 1, 2 and 3 mM) at a stimulation rate of 1 Hz. After recording the baseline cell shortening, ISO was infused in the experimental chamber through an automatic pipette. The cells were electrically stimulated after 5 min of infusion when cell shortening was recorded (Prahash *et al.* 2000). This procedure was repeated for each ISO concentration in different myocytes. Cell contractile function was analysed, and the variation (Δ) from the baseline to the larger stimulus (ISO, 3 mM) was used as an index of β-adrenergic sensitivity.

Statistics

Data are presented as mean and standard error of the mean (mean ± SEM). The normal distribution of the data was verified using the Kolmogorov–Smirnov test. Parameters of exercise tolerance, biometric and cell contractile function data were compared using the Student's *t*-test. Stereological data and karyometric parameters were compared using the Mann–Whitney *U* test. The relationship between cell con-

tractile function and exercise workload was assessed by linear regression. A probability of $P < 0.05$ was considered statistically significant.

Results

Parasitaemia and mortality

The presence of parasites in the bloodstream of IG animals began on the fourth day, disappearing completely on the eighth day. The peak parasitaemia occurred on the sixth day after inoculation. The same analysis was performed to CG animals and demonstrates the absence of circulating parasites (Figure 1). No animals died during the experiment in both groups.

Exercise tolerance

Infection with *T. cruzi* impaired the exercise tolerance of IG animals resulting in significantly reduced distance travelled, total time to fatigue and workload compared to CG animals (Figure 2).

Heart biometry and myocardial stereology

There was no significant difference in body weight between the CG and the IG (Table 1). Infected group animals presented a higher heart and ventricular weight compared to CG animals, whereas the AT weight did not differ between the groups. Left ventricle volume was significantly higher in IG animals as compared to CG animals.

Table 1 Biometric parameters of control and infected rats

	Control	Infected
Body mass (g)	509.76 ± 16.48	497.90 ± 17.31
Heart mass (g)	2.01 ± 0.06	2.17 ± 0.41*
AT mass (g)	0.59 ± 0.05	0.59 ± 0.08
VE mass (g)	1.42 ± 0.05	1.58 ± 0.04*
RA volume (mm^3)	140.83 ± 3.79	143.91 ± 4.52
LV volume (mm^3)	447.15 ± 9.21	496.08 ± 7.95*

AT, atrium; VE, ventricle; RA, right atrium; LV, left ventricle.
Data of five animals from each group were collected 9 weeks after inoculation and are expressed as mean ± SEM. Animals of the infected group were inoculated intraperitoneally with *Trypanosoma cruzi* Y strain (300,000 trypomastigotes/50 g body weight).
*Denotes statistical difference from Control ($P < 0.001$).

Infected group animals exhibited a higher LV cardiomyocyte cross-sectional area and volumetric density of blood vessels (Vv [ibvs]) and collagen (Vv [col]) compared to CG animals. According to the spectrophotometric analysis, the amount of collagen in the LV of the IG animals was also significantly higher compared to CG animals. In addition, IG animals showed a higher index of myocardial vascularization in both RA and LV as compared to CG, demonstrated by the increased Vv [ibvs]-to-Vv [cmy] ratio (Table 2).

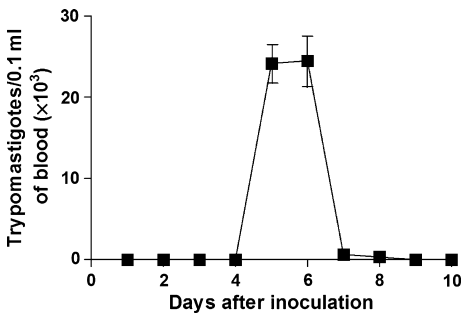

Figure 1 Parasitemia curve in Wistar rats inoculated with *Trypanosoma cruzi* Y strain (300,000 trypomastigotes/50 g body weight). Data of 14 animals are expressed as mean ± SEM.

Myocardial histopathology

The intensities of the fibrosis and the interstitial inflammatory infiltrate in the LV of IG and CG animals were significantly different (Figure 3). The histopathology of the myocardium showed an occurrence of inflammatory infiltrate with a predominance of mononuclear cells and the presence of mast cells in IG animals, which characterizes the chronic inflammatory processes (Figure 3c). Intracellular amastigote forms of *T. cruzi* were identified after the infection persisted for 9 weeks (Figure 3f). The LV of IG animals presented a higher collagen content (Figure 3h), and the myocardial cellularity was significantly more intense in IG animals (3422 ± 732.60 cells in 1.4×10^6 μm^2) compared to CG animals (2217 ± 520.19 cells in 1.4×10^6 μm^2). The RA

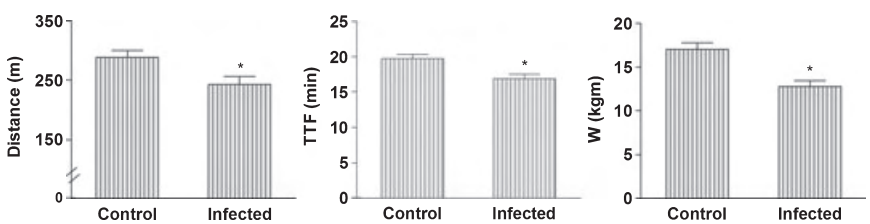

Figure 2 Exercise tolerance of control and infected rats. Infected animals were inoculated intraperitoneally with *Trypanosoma cruzi* Y strain (300,000 trypomastigotes/50 g body weight). TTF, total time to fatigue; W, workload. Data of 14 animals from each group were collected 9 weeks after inoculation and are expressed as mean ± SEM. *Denotes statistical difference from the Control ($P < 0.001$).

Table 2 Quantitative parameters of the myocardium from control and infected rats

	Right atrium		Left ventricle	
	Control	Infected	Control	Infected
A [cmy] (μm^2)	101.94 ± 14.09	105.24 ± 16.69	376.11 ± 39.98	414.85 ± 42.74*
Vv [cmy] (%)	72.04 ± 1.87	72.18 ± 2.64	72.82 ± 3.02	67.11 ± 2.96*
Vv [ibvs] (%)	11.11 ± 0.92	13.29 ± 1.43*	15.83 ± 1.15	18.91 ± 1.58*
Vv [ibvs]/Vv [cmy]	15.66 ± 2.17	18.85 ± 2.68†	22.31 ± 3.52	29.82 ± 4.59*
Vv [col] (%)	16.81 ± 2.09	14.68 ± 2.96	11.25 ± 1.40	14.03 ± 1.56*
Collagen (μg/mg protein)	19.02 ± 3.85	18.52 ± 3.27	20.33 ± 2.83	27.51 ± 3.39*

A, cross-sectional area of cardiomyocytes; Vv, volumetric density; cmy, cardiomyocytes; ibvs, intramyocardial blood vessels; col, collagen. Data of five animals from each group were collected 9 weeks after inoculation and are expressed as mean ± SEM. Infected animals were inoculated intraperitoneally with *Trypanosoma cruzi* Y strain (300,000 trypomastigotes/50 g body weight).
*Denotes statistical difference from Control ($P < 0.001$) for the same segment.
†Denotes statistical difference from Control ($P < 0.01$) for the same segment.

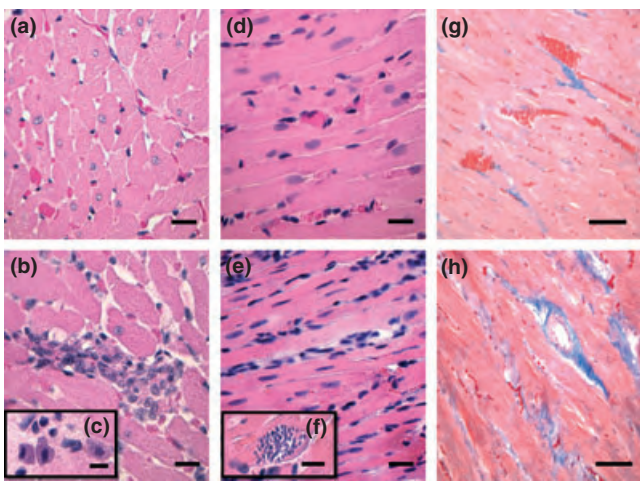

Figure 3 Representative photomicrographs of the left ventricle from control (a, d and g) and infected (b, c, e, f and h) rats. The infected animals were inoculated intraperitoneally with *Trypanosoma cruzi* Y strain (300,000 trypomastigotes/50 g body weight). Nine weeks after inoculation, five animals from each group were euthanized and heart fragments were collected for morphological analysis. (a) A myocardial cross-section showing a well-organized structure (H&E staining, bar = 30 μm). In panel b cardiac myocytes with increased diameters and focal inflammatory infiltrate are observed (H&E staining, bar = 30 μm). Mast cells were also observed in the infected myocardium (c, bar = 12 μm). Differences in myocardial cellularity between the control (d) and infected (e) groups are also shown (H&E staining, bar = 30 μm). Intracellular amastigotes of *T. cruzi* can be seen in panel f (H&E staining, bar = 10 μm). (g) A longitudinal section of myocardium showing blood vessels and thin collagen bundles between muscle fibers (Masson trichrome staining, bar = 20 μm). In panel h thick bundles of collagen with pericellular and perivascular distribution are shown (Masson trichrome staining, bar = 20 μm).

of IG animals showed no significant differences either in collagen content or in myocardial cellularity compared to CG animals (data not shown).

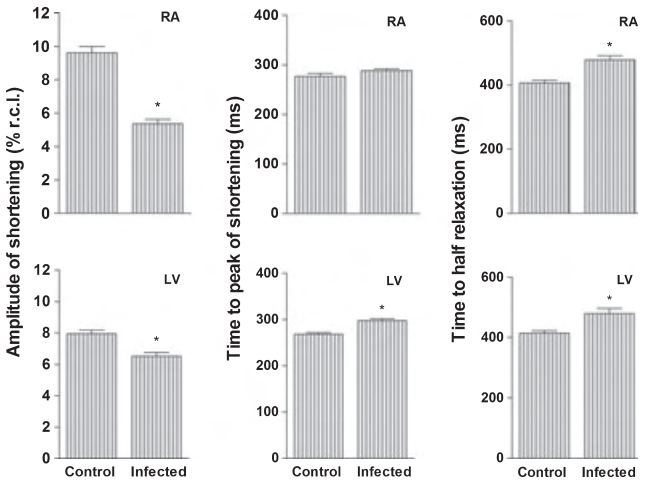

Figure 4 Cell shortening in myocytes isolated from the right atrium and left ventricle from control and infected rats. For each cardiac segment were analyzed 81 ± 18 cardiomyocytes. Infected animals were inoculated intraperitoneally with *Trypanosoma cruzi* Y strain (300,000 trypomastigotes/50 g body weigh). Data of nine animals from each group were collected 9 weeks after inoculation and are expressed as mean ± SEM. Amplitude of shortening is expressed as a % of resting cell length (% r.c.l.). *Denotes statistical difference from the Control in the same segment ($P < 0.001$).

Cell contractility and β-adrenergic stimulation

Right atrium myocytes from the IG had a significant reduction in the amplitude of shortening and an increase in time to half relaxation compared to the CG (Figure 4, upper panel). The time to peak shortening did not differ between the groups. Left ventricular myocytes from IG animals exhibited a significant reduction in amplitude of shortening and an increase in the time to peak shortening and the time to half relaxation as compared to CG animals (Figure 4, lower panel).

The RA and LV myocytes response to ISO is shown in Figure 5. Myocytes from IG animals exhibited an impaired

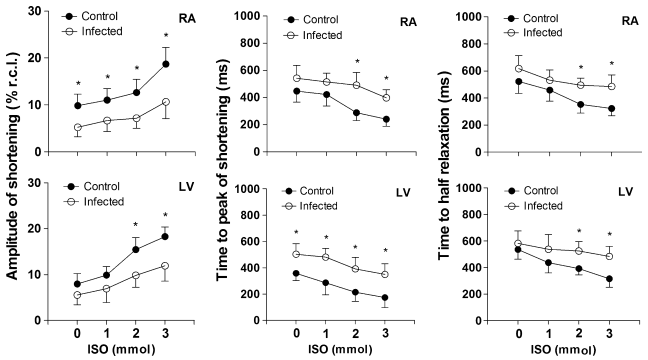

Figure 5 Cardiomyocyte response to β-adrenergic stimulation. Cell shortening, time to peak and time to half relaxation of shortening in myocytes from the right atrium (upper panel) and left ventricle (lower panel) of control (closed circles) and infected (open circles) rats plotted *vs.* concentration (0–3 mmol) of isoproterenol. For each cardiac segment were analyzed 74 ± 8 cardiomyocytes. The infected animals were inoculated intraperitoneally with *Trypanosoma cruzi* Y strain (300,000 trypomastigotes/50 g body weight). Data of nine animals from each group were collected 9 weeks after inoculation and are expressed as mean ± SEM for the numbers of myocytes indicated from nine animals per group. Shortening is expressed as a % of resting cell length (% r.c.l.). *Denotes statistical difference from the Control in the same segment ($P < 0.001$).

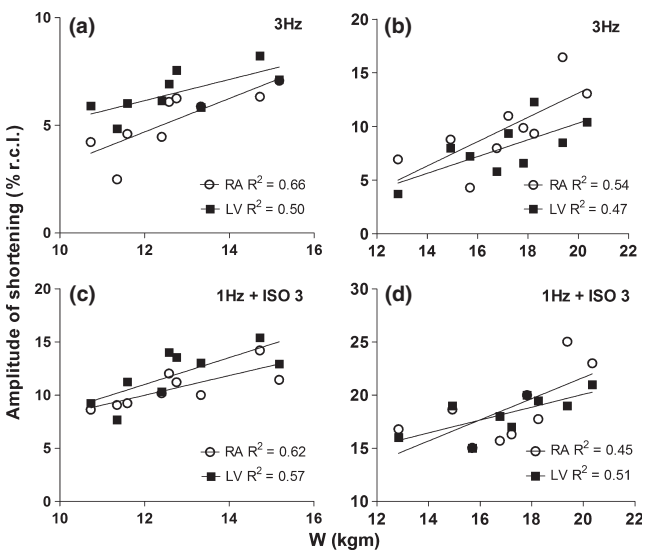

Figure 6 Correlation between cell shortening and workload. Myocytes from right atrium (open circle) and left ventricle (LV, closed square) stimulated at 3 Hz without isoproterenol in infected (a) and control rats (b). Right atrium and LV myocytes stimulated at 1 Hz in the presence of 3 mmol of isoproterenol in infected (c) and control group (d). The mean of cell shortening per animal was plotted against the workload of each animal per group. Data used in the correlation were collected from nine animals in each group 9 weeks after inoculation. Shortening expressed as % of resting cell length (% r.c.l.). W, workload. The infected animals were inoculated intraperitoneally with *Trypanosoma cruzi* Y strain (300,000 trypomastigotes/50 g body weight). All correlations presented statistical significance ($P < 0.05$).

cell contractile response to β-adrenergic stimulation compared to CG animals, with significant differences observed mainly with 2 and 3 mmol concentrations of ISO. Myocytes from the IG presented significantly less variation of shortening than those from the CG in both cardiac segments for amplitude (RA, 5.44 ± 2.13 *vs.* 8.87 ± 2.05% respectively; LV, 6.36 ± 1.72 *vs.* 10.32 ± 2.17% respectively), time to peak shortening (RA, −144.65 ± 18.26 *vs.* −206.56 ± 23.19 ms respectively; LV, −153.93 ± 11,53 *vs.* −183.46 ± 14.07 ms respectively) and time to half relaxation (RA, −132.51 ± 23.89 *vs.* −200.05 ± 19.37 ms respectively; LV, −98.45 ± 29.15 *vs.* −220.65 ± 24.71 ms respectively).

The linear regression analysis showed a moderate and significant correlation between the amplitude of cell shortening in basal and ISO-stimulated conditions and the workload of IG and CG animals in the exercise tolerance protocol (Figure 6).

Discussion

Our results confirmed our hypothesis that *T. cruzi* infection is able to impair myocardium morphology and single cardiomyocyte contractile function and influence negatively the exercise tolerance in the murine model investigated.

Infected animals had LV hypertrophy that was evidenced by the presence of cellular hypertrophy and an increased amount of collagen in the myocardium. The abnormal pattern of accumulation and organization of collagen during the progression of the disease has been previously described in Chagas' disease-induced pathological cardiac hypertrophy (Higuchi *et al.* 1999; Marin-Neto *et al.* 2007; Rassi *et al.* 2010). This new organization of collagen fibres may decrease the myocardial mechanical efficiency to the extent that part of the force used for pumping blood is diverted to correct the geometric distortion determined by the abnormal organization of collagen and muscle bundles (Mady *et al.* 1999). Moreover, there is evidence that the progressive accumulation of collagen reduces the myocardium compliance and the efficiency of the regulatory mechanism of cellular and muscular contraction force based on the length–tension relationship (Kitzman *et al.* 1991; Higuchi *et al.* 1999).

The volumetric density of the blood vessels and the blood vessel-to-cardiomyocyte volumetric density ratio did not indicate a reduction in the myocardial vascularization of infected animals. However, these findings do not exclude the possibility of vascular dysfunction of vasomotor origin and an inadequate balance in the blood flow distribution. For example, our stereological data indicated the occurrence of microvascular dilatation that may have resulted from altered blood flow induced by diffuse fibrosis and vascular derangement. The presence of inflammatory infiltrate and mast cells 9 weeks after infection with *T. cruzi* favour this hypothesis because the continuous production of cytokines and oxidant components by these cells in a chronic inflammatory process may be conducive to vascular dysfunction. Indeed, mechanisms such as endothelial dysfunction, persistence of *T. cruzi* antigens and release of nitric oxide associated with the

chronic inflammatory process have been implicated in vascular dilatation and dysfunction of Chagas' disease (Higuchi *et al.* 1999; Marin-Neto *et al.* 2007). The presence of vascular damage is not unusual in *T. cruzi* infection, and the reduction in myocardial vascularization has been considered as an important component involved in the deterioration of cardiac function (Higuchi *et al.* 1999; Marin-Neto *et al.* 2007) and exercise tolerance (Meiler *et al.* 1987). Previous studies have shown that myocardial hypoperfusion significantly limits the exercise tolerance because of the occurrence of abnormal heart rhythm with the onset of arrhythmias and cardiac pump dysfunction (Verani *et al.* 1981; Meiler *et al.* 1987).

Our data showed contractile dysfunction of RA and LV myocytes (i.e. reduced cell shortening amplitude and increased time to peak shortening and time to half relaxation) in *T. cruzi* -infected rats. Mechanisms such as downregulation of ion channels that modulate Ca^{2+} flux and cell contraction and relaxation have been implicated in the pathogenesis of cardiomyocyte mechanical dysfunction observed in heart disease of different aetiologies (Wisloff *et al.* 2002; Kemi & Wisloff 2010). In myocardial infarction, diabetic cardiomyopathy and autoimmune myocarditis, the reduced expression and/or inhibition of the sodium and calcium exchanger of the sarcolemma (NCX), the ryanodine channel (RyR2), phospholamban (PLB) and the calcium ATPase of the sarcoplasmic reticulum (SERCA-2) have been reported to be important in chronotropic, inotropic and lusitropic cardiomyocyte dysfunction (Wisloff *et al.* 2002; Afanasyeva *et al.* 2004; Kemi & Wisloff 2010). However, whether these molecular changes are promoted by *T. cruzi* infection warrants further investigation.

Previous studies have demonstrated a positive relationship between improved cardiomyocyte mechanical properties and parameters of exercise performance, such as higher maximal oxygen consumption (Wisloff *et al.* 2002; Kemi & Wisloff 2010) and intrinsic aerobic exercise capacity in healthy rats (Prímola-Gomes *et al.* 2009). There is evidence that in animals without disease (Kemi *et al.* 2004; Kemi & Wisloff 2010) and in animal models of cardiovascular disease, the improvement in mechanical properties of cardiomyocytes because of chronic physical exercise programmes occurs in association with an increased density and sensitivity of Ca^{2+} ion channels of the sarcolemma and sarcoplasmic reticulum. An important finding is that these contractile and molecular adaptations of cardiomyocytes in response to physical exercise are accompanied by simultaneous improvement in physical performance (Wisloff *et al.* 2002; Kemi & Wisloff 2010). It is believed that the results of high physical fitness are because of better provision and use of oxygen in exercised tissues and that part of this adaptation is because of the high capacity of cells and the myocardium to produce greater cardiac output (Kemi & Wisloff 2010). In this context, it is not unrealistic to assume that conditions that impair cellular contractility and, consequently, myocardial function have the potential to reduce physical capacity and exercise tolerance. The reduction in physical capacity in individuals with Chagas' disease has been linked to disturbances in cardiac mechanics and haemodynamics (Gallo *et al.* 1975; Lima *et al.* 2010). Indeed, in the present study, the amplitude of cell shortening in RA and LV myocytes correlated closely with workload in control and infected animals. This correlation was observed in the absence and in the presence of β-adrenergic stimulation. Thus, this finding indicates that the level of cell shortening was an important component impaired by *T. cruzi* infection that contributed to the reduction in exercise tolerance. However, it is well recognized that the determination of exercise tolerance is multifactorial. Thus, as *T. cruzi* is able to parasitize and damage structures such as peripheral nerves and skeletal muscles, equally important elements in determining the exercise tolerance (Meiler *et al.* 1987; Montes de Oca *et al.* 2004), we cannot attribute the results exclusively to cardiac and cellular changes. In this context, the weak correlation between single cardiomyocyte contractile parameters and workload indicates that other organs and tissues should be investigated to improve the knowledge about the pathophysiological mechanism related to exercise intolerance in Chagas' disease.

We also observed that in association with reduced basal myocyte contractility, *T. cruzi* -infected animals shared reduced sensitivity to β-adrenergic stimulation. The inotropic and lusitropic responses to ISO were dose dependent in both IG and CG animals; however, all of the contractile parameters examined showed lower amplitude of variation in animals from the IG. In clinical and experimental studies on Chagas' disease, physical and pharmacological cardiac tests have shown reduced ability of the myocardium to respond to stimuli of progressive intensity, suggesting a lower cellular functional reserve (Gallo *et al.* 1975; Talvani *et al.* 2006; Sousa *et al.* 2009; Lima *et al.* 2010). In this disease, changes in electrical and mechanical cardiac function have been more pronounced in conditions of cardiac stress, as occurs during exercise, and the reduction in cardiac responsiveness to β-adrenergic stimulation has been considered to be an important factor involved in reducing exercise tolerance (Gallo *et al.* 1975; Colucci *et al.* 1989). Data exist to support the role of the immune system in pathological remodelling of cardiomyocyte contractility (Sterin-Borda *et al.* 1999; Chakraborti *et al.* 2000; Afanasyeva *et al.* 2004), including Chagas' disease (Roman-Campos *et al.* 2009). It has been demonstrated that in humans and experimental animals with Chagas' disease, anti-β-adrenoreceptor antibodies produced during infection by *T. cruzi* can inhibit the signalling pathway triggered by these receptors (Sterin-Borda *et al.* 1999; Chakraborti *et al.* 2000). Under normal conditions, β-adrenergic pathways lead to the phosphorylation and inhibition of PLB, which reduces its activity on SERCA-2 and improves inotropic, lusitropic and chronotropic activity of cardiomyocytes (Afanasyeva *et al.* 2004). However, direct allosteric inhibition of β-adrenoreceptors by autoantibodies or desensitization mediated by upregulation of β-adrenergic receptor kinase may impair cardiomyocyte contractile function because this receptor is the main signalling pathway that

regulates cellular mechanics through adjustments in Ca^{2+} kinetics. Furthermore, inhibition of β signalling reduces the phosphorylation and activation of RyR2 and Ca^{2+} entry into the cell via the L-type current mediated by the Ca^{2+}-induced Ca^{2+}-release mechanism (Afanasyeva *et al*. 2004).

In summary, we showed that experimental *T. cruzi* infection negatively influenced myocardial morphology, the mechanical properties of single RA and LV myocytes and exercise tolerance in rats. The results of the cell mechanics associated with β-adrenergic stimulation support the hypothesis that single cardiomyocyte contractile dysfunction could constitute an additional mechanism of cardiac impairment and reduced exercise tolerance in animals infected with *T. cruzi*. The experimental model presented here can be useful for future studies investigating, in addition to the cardiac muscle, the participation of other tissues in exercise intolerance. However, little is known about the influence of the parasite in the signalling pathways through which it acts to modulate the single cardiomyocyte mechanics: thus, further studies are needed in this area.

Acknowledgements

Research supported by FAPEMIG (PRONEX). Rômulo D. Novaes was a recipient of the MS scholarship from FAPEMIG. Antonio J. Natali is a CNPq fellow.

Contributions

All listed authors meet ICMJE authorship criteria and nobody who qualifies for authorship has been excluded. Authors contributed to research design, acquisition, analysis and interpretation of data; drafting the paper or revising it critically; and approval of the submitted and final versions.

References

Afanasyeva M., Georgakopoulos D., Rose N.R. (2004) Autoimmune myocarditis: cellular mediators of cardiac dysfunction. *Autoimmun. Rev*. **3**, 476–486.

Bezerra D.G.A., Andrade L.M.L., Cruz F.O.P., Mandarim-de-lacerda C.A. (2008) Atorvastatin attenuates cardiomyocyte loss in adult rats from protein-restricted dams. *J. Card. Fail*. **14**, 151–160.

Biolo A., Ribeiro A.L., Clausell N. (2010) Chagas cardiomyopathy-where do we stand after a hundred years? *Prog. Cardiovasc. Dis*. **52**, 300–316.

Brener Z. (1962) Therapeutic activity and criterion of cure on mice experimentally infected with *Trypanosoma cruzi*. *Rev. Inst. Med. Trop. São Paulo* **4**, 389–396.

Brooks G.A., Donovan C.M., White T.P. (1984) Estimation of anaerobic energy production and efficiency in rats during exercise. *J. Appl. Physiol*. **56**, 520–525.

Caldas I.S., Talvani A., Caldas S. *et al*. (2008) Benznidazole therapy during acute phase of Chagas disease reduces parasite load but does not prevent chronic cardiac lesions. *Parasitol. Res*. **103**, 413–421.

Chakraborti S., Chakraborti T., Shaw G. (2000) Beta-adrenergic mechanisms in cardiac diseases: a perspective. *Cell. Signal*. **12**, 499–513.

Colucci W.S., Ribeiro J.P., Rocco M.B. *et al*. (1989) Impaired chronotropic response to exercise in patients with congestive heart failure: role of postsynaptic beta-adrenergic desensitization. *Circulation* **80**, 314–323.

Gallo L. Jr, Neto J.A., Manco J.C., Rassi A., Amorim D.S. (1975) Abnormal heart rate responses during exercise in patients with Chagas' disease. *Cardiology* **60**, 147–162.

Higuchi M.L., Fukasawa S., Brito T., Parzianello L.C., Bellotti G., Ramires J.A.F. (1999) Different microcirculatory and interstitial matrix patterns in idiopathic dilated cardiomyopathy and Chagas' disease: a three dimensional confocal microscopy study. *Heart* **82**, 279–285.

Kemi O.J. & Wisloff U. (2010) Mechanisms of exercise-induced improvements in the contractile apparatus of the mammalian myocardium. *Acta Physiol*. **199**, 425–439.

Kemi O.J., Haram P.M., Wisloff U., Ellingsen O. (2004) Aerobic fitness is associated with cardiomyocyte contractile capacity and endothelial function in exercise training and detraining. *Circulation* **109**, 2897–2904.

Kitzman D.W., Higginbotham M.B., Cobb F.R., Sheikh K.H., Sullivan M.J. (1991) Exercise intolerance in patients with heart failure and preserved left ventricular systolic function: failure of the Frank-Starling mechanism. *J. Am. Coll. Cardiol*. **17**, 1065–1072.

Koch L.G. & Britton S.L. (2001) Artificial selection for intrinsic aerobic endurance running capacity in rats. *Physiol. Genomics* **5**, 45–52.

Lacerda A.R., Marubayashi U., Balthazar C.H., Coimbra C.C. (2006) Evidence that brain nitric oxide inhibition increases metabolic cost of exercise, reducing running performance in rats. *Neurosci. Lett*. **393**, 260–263.

Lima M.M.O., Pereira M.C., Rocha M.O.C., Beloti F.R., Alencar M.C.N., Ribeiro A.L.P. (2010) Left ventricular diastolic function and exercise capacity in patients with Chagas cardiomyopathy. *Echocardiography* **27**, 519–524.

López-De León A., Rojkind M. (1985) A simple micromethod for collagen and total protein determination in formalin-fixed paraffin-embedded sections. *Histochem. Cytochem*. **33**, 737–743.

Mady C., Ianni B.M., Arteaga E. *et al*. (1999) Relation between interstitial myocardial collagen and the degree of clinical impairment in Chagas' disease. *Am. J. Cardiol*. **84**, 354–356.

Mady C., Ianni B.M., Arteaga E., Salemi V.M.C., Frimm C.C. (2000) Maximal functional capacity in patients with chagas' cardiomyopathy without congestive heart failure. *J. Card. Fail*. **3**, 220–224.

Mandarim-de-Lacerda C.A. (2003) Stereological tools in biomedical research. *An. Acad. Bras. Ciênc*. **75**, 469–486.

Marin-Neto J.A., Cunha-Neto E., Maciel B.C., Simões M.V. (2007) Pathogenesis of chronic Chagas' heart disease. *Circulation* **115**, 1109–1123.

Martinelli P.M., Camargos E.R.S., Azevedo A.A., Chiari E., Morel G., Machado C.R.S. (2006) Cardiac NGF and GDNF expression during *Trypanosoma cruzi* infection in rats. *Auton. Neurosci*. **130**, 32–40.

Meiler S.E.L., Ashton J.J., Moeschberger M.L., Unverferth D.V., Leier C.V. (1987) An analysis of the determinants of exercise performance in congestive heart failure. *Am. Heart J*. **113**, 1207–1217.

Montes de Oca M., Torres S.H., Loyo J.G. *et al.* (2004) Exercise performance and skeletal muscles in patients with advanced Chagas disease. *Chest* **125**, 1306–1314.

Natali A.J., Wilson L.A., Peckham M., Turner D.L., Harrison S.M., White E. (2002) Different regional effects of voluntary exercise on the mechanical and electrical properties of rat ventricular myocytes. *J. Physiol.* **541**, 863–875.

Prahash A.J.C., Gupta S., Anand I.S. (2000) Myocyte response to β-adrenergic stimulation is preserved in the noninfarcted myocardium of globally dysfunctional rat hearts after myocardial infarction. *Circulation* **102**, 1840–1846.

Prímola-Gomes T.N., Campos L.A., Lauton-Santos S. *et al.* (2009) Exercise capacity is related to calcium transients in ventricular cardiomyocytes. *J. Appl. Physiol.* **107**, 593–598.

Rassi A. Jr, Rassi A., Marin-Neto J.A. (2010) Chagas disease. *Lancet* **375**, 1388–1402.

Roman-Campos D., Duarte H.L.L., Sales P.A. Jr *et al.* (2009) Changes in cellular contractility and cytokines profile during *Trypanosoma cruzi* infection in mice. *Basic Res. Cardiol.* **104**, 238–246.

Scherle W. (1970) A simple method for volumetry of organs in quantitative stereology. *Mikroskopie* **26**, 57–63.

Sousa L.A.P., Rocha M.O.C., Britto R.R., Lombardi F., Ribeiro A.L. (2009) Chagas disease alters the relationship between heart rate variability and daily physical activity. *Int. J. Cardiol.* **135**, 257–259.

Sterin-Borda L., Gorelik G., Postan M., Gonzalez Cappa S., Borda E. (1999) Alterations in cardiac beta-adrenergic receptors in chagasic mice and their association circulating beta-adrenoceptor-related autoantibodies. *Cardiovasc. Res.* **41**, 116–125.

Talvani A., Rocha M.O.C., Ribeiro A.L., Borda E., Sterin-Borda L., Teixeira M.M. (2006) Levels of anti-M2 and anti-β1 autoantibodies do not correlate with the degree of heart dysfunction in Chagas' heart disease. *Microbes Infect.* **8**, 2459–2464.

Verani M.S., Hartung G.H., Hoepfel-Harris J., Welton D.E., Pratt C.M., Miller R.R. (1981) Effects of exercise training on left ventricular performance and myocardial perfusion in patients with coronary artery disease. *Am. J. Cardiol.* **47**, 797–803.

WHO, World Health Organization (2005) Tropical Disease Research: Progress 2003–2004 seventeenth programme report of the UNICEF/UNDP/World Bank/WHO. Special Programme for Research & Training in Tropical Diseases (TRD). Programme report, n. 17. Geneva pp. 31–33.

Wisloff U., Loennechen J.P., Currie S., Smith G.L., Ellingsen O. (2002) Aerobic exercise reduces cardiomyocyte hypertrophy and increases contractility, Ca^{2+} sensitivity and SERCA-2 in rat after myocardial infarction. *Cardiovasc. Res.* **54**, 162–174.

Treinamento em Natação Atenua a Disfunção Contrátil de Cardiomiócitos de Ratos Diabéticos

Swimming Training Attenuates Contractile Dysfunction in Diabetic Rat Cardiomyocytes

Márcia Ferreira da Silva, Maria do Carmo Gouveia Pelúzio, Paulo Roberto dos Santos Amorim, Vitor Neiva Lavorato, Natália Pereira do Santos, Luiz Henrique Marchesi Bozi, Arlete Rita Penitente, Daniel Luciano Falkoski, Felipe Gomes Berfort, Antonio Jose Natali

Universidade Federal de Viçosa, Viçosa, MG - Brasil

Resumo

Fundamento: O diabete experimental promove disfunção contrátil em cardiomiócitos, mas os efeitos do treinamento em natação nesta disfunção não são conhecidos.

Objetivo: Testar os efeitos de um programa de treino em natação (PTN) sobre a disfunção contrátil de cardiomiócitos de ratos com diabete experimental.

Métodos: Ratos Wistar (idade: 30 dias; peso corporal médio: 84,19 g) com diabete induzida por estreptozotocina (60 mg/kg de peso corporal; glicemia > 300 mg/dl) foram alocados em diabéticos sedentários (DS, n = 10) e diabéticos exercitados (DE, n = 13). Animais da mesma idade e peso serviram de controles sedentários (CS, n = 10) e controles exercitados (CE, n = 06). Os animais DE e CE foram submetidos a um PTN (05 dias/semana, 90 min/dia), por 08 semanas. Os miócitos do ventrículo esquerdo (VE) foram isolados e estimulados eletricamente a 3,0 Hz em temperatura ambiente (~ 25º C).

Resultados: O diabete reduziu a função contrátil nos cardiomiócitos dos animais em relação aos controles (i.e., menor amplitude de contração, maior tempo de contração e relaxamento). O PTN atenuou a redução na amplitude de contração (CS, 11 ± 0,2% *vs* DE, 11,6 ± 0,2%), o tempo para o pico de contração (CS, 319 ± 5,8 ms *vs* DE, 333 ± 4,8 ms) e o tempo para 50% de relaxamento (CS, 619 ± 22,2 ms *vs* DE, 698 ± 18,6 ms) dos cardiomiócitos dos animais diabéticos. O diabete reduziu as dimensões dos cardiomiócitos, porém, o PTN minimizou a redução da largura e volume celular, sem alterar o comprimento.

Conclusão: O programa de treino em natação atenuou a disfunção contrátil dos miócitos do VE de ratos com diabete experimental. (Arq Bras Cardiol. 2011; [online].ahead print, PP.0-0)

Palavras-chave: Natação, esforço físico, miócitos cardíacos, ratos, diabete melito.

Abstract

Background: *Experimental diabetes promotes contractile dysfunction in cardiomyocytes, but the effects of swimming in this disorder are not known.*

Objective: *To test the effects of a swimming training program (STP) on cardiomyocyte contractile dysfunction in rats with experimental diabetes.*

Methods: *Wistar rats (age: 30 days; mean body weight: 84.19 g) with diabetes induced by streptozotocin (60 mg/kg body weight; glucose > 300 mg/dl) were divided into sedentary diabetic rats (SD, n = 10) and exercised diabetic rats (ED, n = 13). Animals of same age and weight served as sedentary controls (SC, n = 10) and exercised controls (EC, n = 06). Animals and ED and EC underwent a STP (05 days/week, 90 min/day) for 08 weeks. Left ventricular (LV) myocytes were isolated and electrically stimulated at 3.0 Hz at room temperature (~ 25° C).*

Results: *Diabetes reduced contractile function in cardiomyocytes of animals compared to controls (i.e., lower amplitude of contraction, longer duration of contraction and relaxation). The STP attenuated the reduced amplitude of contraction (SC, 11 ± 0.2% vs ED, 11.6 ± 0.2%), time to peak contraction (SC, 319 ± 5.8 ms vs ED, 333 ± 4.8 ms) and time to 50.0% of relaxation (SC, 619 ± 22.2 ms vs ED 698 ± 18.6 ms) of cardiomyocytes of diabetic rats. Diabetes reduced the size of cardiomyocytes, however, the STP minimized the reduction of cell volume and width, without changing length.*

Conclusion: *The swimming training program attenuated the contractile dysfunction of the LV myocytes of rats with experimental diabetes. (Arq Bras Cardiol. 2011; [online].ahead print, PP.0-0)*

Keywords: *Swimming; physical exertion; myocytes, cardiac; rats; diabetes mellitus.*

Full texts in English - http://www.arquivosonline.com.br

Correspondência: Antonio Jose Natali •
Av. PH Rolfs, s/n - Departamento de Educação Física - Campus Universitário da Universidade Federal de Viçosa - 36570-000 - Viçosa, MG - Brasil
E-mail: anatali@ufv.br
Artigo recebido em 06/08/10; revisado recebido em 29/10/10; aceito em 21/12/10.

Introdução

O diabete melito do tipo 1 é um fator de risco para eventos cardiovasculares, incluindo o desenvolvimento da cardiomiopatia diabética. A incapacidade em manter a homeostase da glicose no miocárdio compromete a estrutura e a função cardíaca em humanos e em animais com diabete experimental[1-4]. Em nível celular, foi demonstrado que o diabete prejudica a função contrátil dos cardiomiócitos, principalmente por provocar alterações estruturais e funcionais na regulação do cálcio (Ca^{2+}) intracelular[5-7].

O exercício físico regular tem sido usado como um agente efetivo de proteção cardíaca para diabéticos, uma vez que as anormalidades estruturais e funcionais do coração diabético respondem favoravelmente ao exercício[8-10]. Por exemplo, em animais diabéticos, o exercício crônico atenuou alterações na função ventricular esquerda, tais como redução nos volumes sistólico, diastólico final e de ejeção, no débito cardíaco e na fração de encurtamento[7,11,12].

Em nível celular, entretanto, poucos estudos sobre os efeitos do exercício crônico na função contrátil de cardiomiócitos de animais diabéticos foram realizados e, além de usarem exclusivamente a corrida em esteira, apresentaram resultados controversos. Por exemplo, programas de corrida contínua em esteira com intensidade leve (09 m/min, 0% de inclinação, 30 min/dia) ou moderada (18 m/min, 0% de inclinação) não afetaram a contração dos cardiomiócitos de ratos[13]. Outro programa de corrida contínua com intensidade alta (18 m/min, 5% de inclinação, 60 min/dia) provocou adaptações negativas, pois prolongou o tempo de contração celular e não alterou a amplitude de contração dos cardiomiócitos de ratos[14]. Entretanto, programas de corrida em esteira com intensidade mais alta (20-25 m/min, 5% de inclinação, 60 min/dia) foram capazes de restaurar a função contrátil dos cardiomiócitos de ratos e camundongos[7,15]. Portanto, até o momento, os efeitos do exercício contínuo com duração superior a 60 minutos diários, especificamente a natação, sobre a função contrátil de cardiomiócitos de ratos diabéticos não são conhecidos.

Assim, este estudo tem como objetivo testar se um programa de natação, com duração diária de 90 minutos, altera a função contrátil de cardiomiócitos isolados do ventrículo esquerdo de ratos com diabete experimental.

Métodos

Animais de experimentação e tratamentos

Ratos Wistar (idade 30 dias; peso corporal médio de 84,19 g) foram divididos em 04 grupos: Controle sedentário (CS, n = 10); Controle exercitado (CE, n = 10); Diabético sedentário (DS, n = 20); e Diabético exercitado (DE, n = 20) e foram mantidos em ambiente com temperatura média de 22° C e regime de luminosidade invertido de 12/12 horas claro/escuro com água e ração comercial *ad libitum*.

Foram seguidas as normas estabelecidas no *Guide for the Care and Use of Laboratory Animals* (*Institute of Laboratory Animal Resources, National Academy of Sciences*, Washington, D.C., 1996) e respeitados os Princípios Éticos na Experimentação Animal do Colégio Brasileiro de Experimentação Animal (COBEA). O estudo foi aprovado pela Comissão de Ética da Universidade Federal de Viçosa (processo nº 03/2009).

Indução do diabete

Após jejum de 12 horas, os animais dos grupos DE e DS receberam uma injeção intraperitoneal (60 mg/kg de peso corporal) de estreptozotocina (STZ, Sigma, St. Louis, EUA), diluída em 1,0 ml de tampão citrato de sódio (0,1 M, pH 4,5). Os animais dos grupos CS e CE receberam a mesma dose de tampão citrato de sódio (0,1 M, pH 4,5) sem STZ. Sete dias após a aplicação de STZ e jejum de 12 horas, a glicose sanguínea de repouso foi aferida (One touch ultra - Johnson & Johnson, México). Animais com níveis de glicose sanguínea de jejum superior a 300 mg/dl foram considerados diabéticos (DS, n = 10; DE, n = 13). A glicose sanguínea de jejum e o peso corporal foram monitorados semanalmente durante o período experimental.

Programa de treino em natação

Após 45 dias de hiperglicemia, os animais do grupo DE e CE foram submetidos a um programa de treinamento em natação (adaptado de Medeiros e cols.[16]), por 8 semanas. Na primeira semana, os animais exercitaram-se na água, sem sobrecarga, durante 10-50 min, sendo a duração aumentada em 10 min/dia. Na segunda semana, os animais exercitaram com uma carga de 1% de seu peso corporal e a duração do exercício foi aumentada em 10 min/dia até atingir 90 min de natação ininterruptos. A partir da terceira semana, a carga foi aumentada semanalmente (0,5% do peso corporal) até atingir 4% do peso corporal na 8ª semana. Durante as sessões de natação, os animais dos grupos DS e CN eram colocados em uma caixa de polipropileno com água aquecida (28-30° C) e profundidade de 10 cm.

Quatro animais do grupo CE morreram por afogamento.

Isolamento dos cardiomiócitos

Após eutanásia, o coração foi removido e os miócitos do ventrículo esquerdo foram isolados conforme descrito por Natali e cols.[17]. Resumidamente, o coração foi canulado via artéria aorta em um sistema Langendorff e perfundido com solução de isolamento [composição (mM): 130 Na^+; 5,4 K^+; 1,4 Mg^+; 140 Cl^-; 0,75 Ca^{2+}; 5,0 Hepes; 10 glicose; 20 taurina; e 10 creatina; pH = 7,3 em temperatura ambiente]. Em seguida, o coração foi perfundido com solução livre de cálcio contendo 0,1 mM de *ethylene glycol-bis (ß-aminoethyl ether)-N, N, N′, N′-tetraacetic acid (EGTA)*, por um período de 4-6 min. Na sequência, o coração foi perfundido com solução contendo 1,0 $mg.ml^{-1}$ de colagenase tipo 2 (*Worthington*, EUA) e 100,0 mM de $CaCl_2$ por 20 a 25 min. As soluções utilizadas foram oxigenadas (O_2 100% - *White Martins*, Brasil) e mantidas em temperatura de 35° C. Após perfusões, os ventrículos foram separados dos átrios e pesados. Em seguida, o ventrículo esquerdo foi colocado em frasco contendo 5,0 ml da solução enzimática (colagenase) e albumina sérica bovina (10%). O frasco foi agitado moderadamente durante 05 min, em banho-maria a 37° C, após o qual o tecido foi retirado do frasco e o restante foi centrifugado (3.000 rpm)

por 30 s. O sobrenadante foi removido e os cardiomiócitos foram suspendidos na solução de isolamento e armazenados em refrigerador (5º C) até serem utilizados.

Função contrátil dos cardiomiócitos

As contrações celulares foram medidas através da técnica de alteração do comprimento dos cardiomiócitos usando-se o sistema de detecção de bordas (Ionoptix, Milton, MA-EUA) montado num microscópio invertido (Nikon Eclipse - TS100, Japão), conforme descrito previamente[18]. Resumidamente, os miócitos foram acomodados em uma câmara experimental com a base de vidro e banhados por solução tampão com a seguinte composição (em mM): 136,9 NaCl; 5,4 KCl; 0,37 NaH_2PO_4; 0,57 $MgCl_2$; 5,0 Hepes = 5; 5,6 Glicose e 1,0 $CaCl_2$ (pH = 7,4 em temperatura ambiente). Os miócitos foram visualizados em um monitor através de uma câmera (Myocam, Ionoptix, frequência de 240 Hz) acoplada ao microscópio utilizando-se um programa de detecção de imagens (Ionwizard, Ionoptix). Os cardiomiócitos foram estimulados externamente na frequência de 3,0 Hz (10 Volts, duração de 5 min) utilizando-se um par de eletrodos de aço e um estimulador elétrico de campo (Myopacer, Ionoptix). Os movimentos das bordas longitudinais dos miócitos foram capturados pelo sistema de detecção de bordas (Ionwizard, Ionoptix) e armazenados para análise posterior. Foram utilizados para as medidas de contração somente os cardiomiócitos que estavam em boas condições, com as bordas e as estriações sarcoméricas bem definidas, relaxados em repouso, sem apresentar contrações voluntárias. As contrações foram analisadas conforme descrito previamente[19].

Dimensões dos cardiomiócitos

O comprimento e a largura dos miócitos foram medidos usando-se um sistema de captação de imagens, a partir das imagens dos cardiomiócitos visualizados horizontalmente no monitor de um microcomputador, conforme descrito[17]. O comprimento celular foi determinado medindo-se a imagem da célula gerada no monitor, desde a borda direita até a borda esquerda, no ponto médio da largura do cardiomiócito. A largura celular foi determinada medindo-se a imagem gerada no monitor, desde a borda superior até a borda inferior, no ponto médio do comprimento dos cardiomiócitos. O volume celular foi calculado usando-se a fórmula: [Volume (pL) = comprimento (mm) x largura (mm) x (7,59 x 10^{-3} pL/mm^2)], conforme Satoh e cols.[20].

Análise estatística

Para a comparação das médias das variáveis analisadas entre os 04 grupos (fatores exercício e diabete, dois grupos cada), utilizou-se a análise de variância de duas entradas (ANOVA *two-way*) e *post hoc* de Tukey para as comparações múltiplas. Essa análise foi feita através do *software* Sigma Stat, versão 3,0. Adotou-se o nível de significância de até 5% ($p \leq 0,05$).

Resultados

Antes da aplicação de STZ, não houve diferença estatística da glicose sanguínea entre os grupos experimentais (Tabela 1). Quarenta e cinco dias após a aplicação de STZ (início do exercício) e ao final do experimento, os animais diabéticos apresentaram glicose sanguínea superior a dos animais controle. Os níveis de glicose sanguínea não foram alterados pelo exercício, tanto nos animais diabéticos (DE *vs* DS) quanto nos controle (CE *vs* CS). Não houve interação entre os fatores exercício e diabete (ANOVA *two-way*, $p > 0,05$) para esta ou para as demais variáveis analisadas.

Os pesos corporais iniciais não foram diferentes entre os quatro grupos (Tabela 1). Quarenta e cinco dias após a aplicação de STZ, os animais dos grupos DS e DE apresentaram pesos corporais inferiores aos controles CS e CE. O mesmo ocorreu ao final do experimento. Da mesma forma, o programa de natação não alterou esses parâmetros nos animais tanto do grupo DE, quando comparados a DS, quanto nos CE comparados a CS.

Os animais DS apresentaram menores pesos ventriculares ($p < 0,05$) que os CS (Tabela 1). O programa de natação não alterou o peso ventricular dos animais diabéticos (DS *vs* DE). Entretanto, nos animais controles, o peso ventricular foi maior nos animais CE que nos CS. O peso dos ventrículos relativo ao peso corporal, índice de hipertrofia ventricular, foi maior no grupo DS que no CS. Entre os animais diabéticos, os DE apresentaram peso relativo dos ventrículos maior que os DS. Entre os controles, os animais CE exibiram maior peso relativo dos ventrículos que os CS.

Tabela 1 - Pesos corporais e dos ventrículos e níveis de glicose sanguínea dos ratos controles e diabéticos

	CS (n = 10)	CE (n = 06)	DS (n = 10)	DE (n = 13)
PC inicial (g)	83,51 ± 1,9	82,72 ± 1,8	87,80 ± 2,0	82,71 ± 1,8
PC após 45 dias (g)	353,93 ± 11,3*	352,12 ± 11,3*	193,72 ± 11,9	186,91 ± 10,7
PC final (g)	443,50 ± 18,1*	410,81 ± 25,7*	198,82 ± 18,1	204,25 ± 18,1
GS inicial (mg/dl)	82,4 ± 4,2	84,0 ± 4,2	89,0 ± 4,5	93,0 ± 4,0
GS após 45 dias (mg/dl)	87,8 ± 11,3	76,2 ± 11,3	525,1 ± 11,3†	520,1 ± 11,9†
GS final (mg/dl)	88,3 ± 32,1	86,8 ± 45,5	475,8 ± 32,1†	483,7 ± 32†
PV (mg)	1.590,00 ± 0,08*	1.930,00 ± 0,11*	1.120,00 ± 0,08	1.330,00 ± 0,08
PV/PC final (mg/g)	3,59 ± 0,4	4,72 ± 0,6‡	5,98 ± 0,4 †	7,97 ± 0,4†§

*Dados em média ± EPM. n - número de animais; CS - controles sedentários; CE - controles exercitados; DS - diabéticos sedentários; DE - diabéticos exercitados; GS - glicose sanguínea; PC - peso corporal; PV - peso dos ventrículos; *- diferente de DS e DE; †- diferente de CS e CE; ‡- diferente de CS; §- diferente de DS (p < 0, 05).*

De forma independente, o diabete reduziu o comprimento dos cardiomiócitos nos animais sedentários (DS *vs* CS) e treinados (DE *vs* CE; Tabela 2). Todavia, o programa de natação não alterou o comprimento dos cardiomiócitos nos animais diabéticos (DE *vs* DS) e nos não diabéticos (CS *vs* CE). O diabete reduziu a largura dos miócitos nos animais sedentários (DS *vs* CS) e treinados (DE *vs* CE). Todavia, o programa de natação aumentou a largura dos cardiomiócitos nos animais diabéticos (DE *vs* DS). Isso não ocorreu nos animais controles (CE *vs* CS). Houve redução do volume celular no grupo DS comparado ao grupo CS. O programa de natação aumentou o volume celular nos animais diabéticos (DE *vs* DS), mas não nos animais controles (CE *vs* CS). Observa-se que a razão comprimento/largura dos cardiomiócitos não foi afetada pelo diabete ou pelo programa de natação.

A análise da função contrátil dos cardiomiócitos mostrou que a amplitude de contração celular foi reduzida pelo diabete (CS, 11,0 ± 0,2% *vs* DS, 10,2 ± 0,2%, $p < 0,001$) (Figura 1 A). O programa de natação aumentou a amplitude de contração dos cardiomiócitos em tais animais (DS, 10,2 ± 0,2% *vs* DE, 11,6 ± 0,2%, $p < 0,001$). Entre os animais controles, o programa de natação aumentou a amplitude de contração (CS, 11,0 ± 0,2% *vs* CE, 12,4 ± 0,2%, $p < 0,001$).

Os cardiomiócitos dos animais do grupo DS apresentaram tempo para o pico de contração mais longo do que os do grupo CS (361 ± 5,7 ms *vs* 319,0 ± 5,8 ms, respectivamente, $p < 0,001$) (Figura 1 B). O programa de natação reduziu o tempo para o pico de contração nos animais diabéticos (DS, 361 ± 5,7 ms *vs* DE, 333,0 ± 4,8 ms, $p < 0,001$). O mesmo foi efeito observado nos cardiomiócitos dos animais controles (CE, 289,0 ± 6,8 ms *vs* CS, 319,0 ± 5,8 ms, $p < 0,001$).

Para 50% do relaxamento, o tempo foi maior nos cardiomiócitos dos animais diabéticos sedentários do que nos controles sedentários (DS, 756 ± 22,1 ms *vs* CS, 619,0 ± 22,2 ms, $p < 0,001$) (Figura 1 C). O programa de natação reduziu o tempo para 50% do relaxamento nos cardiomiócitos desses animais (DS, 756 ± 22,1 ms *vs* DE, 698 ± 18,6 ms, $p = 0,044$). O mesmo ocorreu nos cardiomiócitos dos animais controles (CE, 516,0 ± 26,1 ms *vs* CS, 619,0 ± 22,2 ms, $p = 0,003$).

Discussão

Nossos dados demonstram que a disfunção contrátil dos cardiomiócitos, provocada pelo diabete, foi atenuada pelo programa de treino em natação com duração de 90 minutos. Além disso, houve aumento da largura e do volume dos cardiomiócitos, sem alterar o comprimento celular, em resposta ao exercício crônico.

A redução na amplitude de contração observada aqui reflete alterações importantes no miocárdio de ratos diabéticos *in vivo*, tais como redução na fração de encurtamento, no diâmetro diastólico final, no diâmetro sistólico final do ventrículo esquerdo e no débito cardíaco[7,11]. Apesar de não termos testado os mecanismos, sabe-se que a redução da sensibilidade dos miofilamentos contráteis ao Ca^{2+} e a redução da concentração intracelular de Ca^{2+} estão envolvidos[21]. Entretanto, cardiomiócitos de ratos Goto-Kakizaki apresentaram aumento da amplitude de contração associada à redução do transiente de Ca^{2+}. Isto sugere que a sensibilidade dos miofilamentos ao Ca^{2+} estava aumentada, o que poderia ser um mecanismo compensatório para preservar a função mecânica do coração no diabete[22]. Há evidências de que a concentração intracelular de Ca^{2+} apresenta-se reduzida em cardiomiócitos de animais com diabete experimental[23]. Isto ocorre em função do aumento da atividade do trocador de sódio e cálcio (NCX) e da diminuição da recaptação de Ca^{2+} pelo retículo sarcoplasmático (RS), via cálcio ATPase do RS (SERCA2)[15] e da redução da liberação de Ca^{2+} do RS, via receptores de rianodina (RyR2)[24]. Além disso, é possível que a redução da densidade de túbulos transversos dos cardiomiócitos de animais diabéticos possa alterar o espaço entre os canais de cálcio tipo L e os RyR2, o que reduz a eficiência do acoplamento excitação-contração[15].

Em contrapartida, o exercício crônico empregado aumentou a amplitude de contração nos animais diabéticos e controles. Para os animais diabéticos, tal fato indica que o exercício promoveu adaptações positivas nos cardiomiócitos que contribuem para atenuar algumas anormalidades mecânicas do miocárdio diabético observadas *in vivo*[7,11,12]. Alguns mecanismos têm sido propostos como responsáveis pelo aumento da amplitude de contração dos cardiomiócitos de ratos diabéticos em resposta ao exercício crônico: há evidências que o exercício físico crônico pode normalizar o funcionamento do NCX e do cálcio calmodulina quinase II (CaMKII), reduzir o vazamento de Ca^{2+} do RS e aumentar o conteúdo de Ca^{2+} do RS[7,15].

O diabete experimental prolongou o tempo necessário para o pico de contração celular. Isso indica que cardiomiócitos de animais diabéticos contraiam mais lentamente do que os de seus controles. Essa alteração tem implicações negativas na função cardíaca desses animais. A velocidade de contração dos cardiomiócitos é controlada pelas proteínas reguladoras da movimentação de Ca^{2+} intracelular e pela taxa de hidrólise de ATP que, por sua vez, regula a taxa de formação de pontes

Tabela 2 - Dimensões dos cardiomiócitos dos ratos controles e diabéticos

	CS (n = 190)	CE (n = 149)	DS (n = 256)	DE (n = 253)
Comprimento (µm)	157,32 ± 1,60*	159,77 ± 1,80†	150,49 ± 1,50	151,29 ± 1,50
Largura (µm)	22,38 ± 0,41*	22,97 ± 0,44*†	19,48 ± 0,4	20,74 ± 0,4*
Volume (pL)	26,73 ± 0,55*	27,65 ± 0,65*†	22,19 ± 0,5	24,00 ± 0,5*
Comprimento/largura	7,48 ± 0,19	7,25 ± 0,19	7,51 ± 0,15	7,91 ± 0,15

*Valores em média ± EPM. n - número de cardiomiócitos; CS - controles sedentários; CE - controles exercitados; DS - diabéticos sedentários; DE - diabéticos exercitados; * - diferente de DS; † - diferente de DS e DE (p < 0,05).*

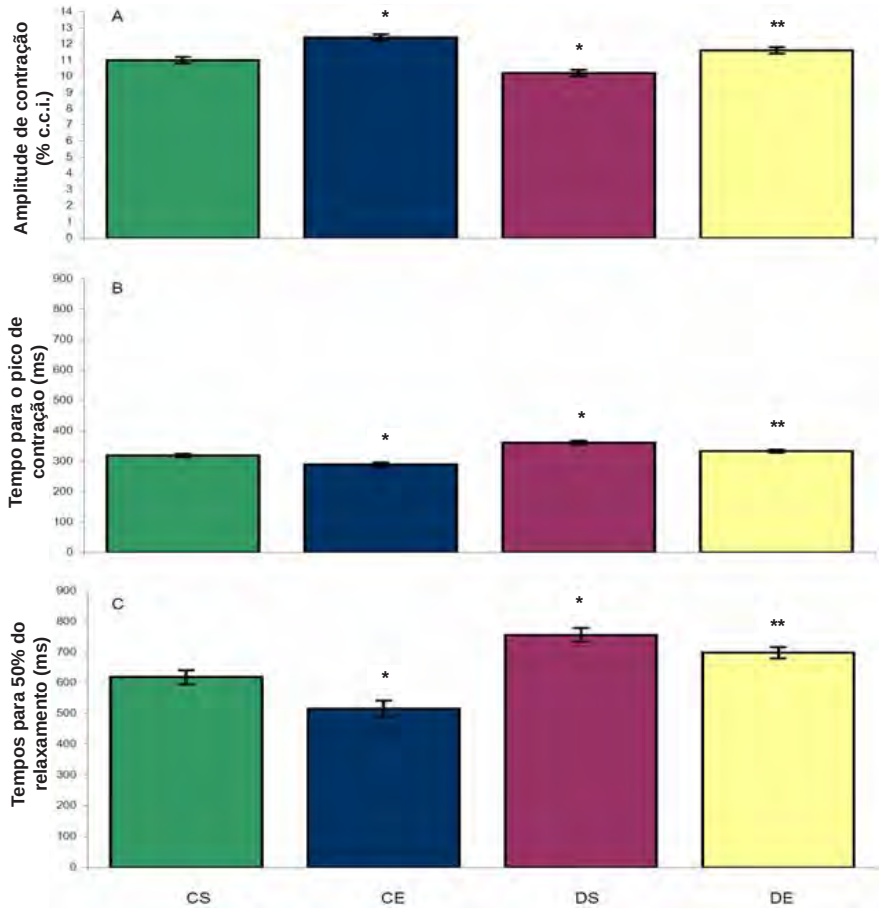

Fig. 1 - Função contrátil de cardiomiócitos de ratos controle e diabéticos. A - amplitude de contração; B - tempo para o pico de contração; C - tempo para 50% de relaxamento; CS - controles sedentários (106 células); CE - controles exercitados (78 células); DS - diabéticos sedentários (109 células); DE - diabéticos exercitados (153 células). Os dados são média ± EPM, diferente de CS**, diferente de DS (p < 0,05).*

cruzadas[21]. Cardiomiócitos de animais diabéticos apresentam redução na expressão de proteínas regulatórias, tais como CaMKII, NCX, RyR2, SERCA2 e fosfolambana (PLB)[5,7,15,24-26], o que pode retardar a disponibilidade de Ca^{2+} para a contração celular.

Entretanto, o programa de natação reduziu o tempo para o pico de contração nos animais diabéticos. As adaptações ao exercício regular, que aceleram a disponibilidade de Ca^{2+} no citosol e aumentam a taxa de hidrólise de ATP, contribuem para tal redução. A velocidade de disponibilidade de Ca^{2+} no citosol é regulada principalmente pela velocidade de saída de Ca^{2+} do RS, via RyR2[21]. Há evidências de que o exercício físico regular aumenta a expressão e/ou a atividade dos RyR2 e a sensibilidade dos RyR2 e dos miofilamentos contráteis ao Ca^{2+} em animais diabéticos[7]. Além disso, o exercício físico é capaz de aumentar a densidade e a responsividade dos receptores betadrenérgicos em ratos diabéticos[12], o que pode afetar a velocidade de contração celular.

Demonstramos também que o diabete experimental prolongou o tempo de relaxamento celular. O relaxamento dos cardiomiócitos depende da remoção do Ca^{2+} do citosol para o RS (via SERCA2, PLB), para o meio extracelular (via NCX, Ca^{2+} ATPase do sarcolema) e para a mitocôndria (via transporte de Ca^{2+} mitocondrial)[21]. A expressão e a função dessas estruturas celulares estão diminuídas nos cardiomiócitos de animais diabéticos[12,25-28]. Tal fato diminui a velocidade com que o Ca^{2+} é removido do citosol. Essas alterações estão associadas ainda à depressão da proteína quinase A (PKA) e CaMKII, proteínas estas responsáveis pela fosforilação da PLB. Além disso, a não fosforilação de PLB por CaMKII diminui a afinidade de SERCA2 por Ca^{2+} e inibe a recaptação de Ca^{2+} pelo RS, o que contribui para tornar mais lento o relaxamento celular[26]. Tais achados em nível celular são compatíveis com as disfunções diastólicas observadas em corações diabéticos *in vivo*[7,11].

O programa de natação aplicado, por sua vez, reduziu o tempo de relaxamento dos cardiomiócitos dos animais diabéticos. Esse efeito tem sido atribuído à capacidade do exercício regular de aumentar a velocidade de remoção de Ca^{2+} do citosol via aumento da expressão de SERCA2 e PLB[7,15], normalização da expressão e função dos NCX, redução na fosforilação de CaMKII e restauração da densidade de túbulos transversos[15].

O programa de natação aplicado não alterou a glicemia de jejum dos animais controles e diabéticos em repouso. Nos animais diabéticos, a STZ induz a apoptose das células β-pancreáticas[29], o que inibe a secreção de insulina. É possível também que tenha havido um aumento na secreção de glucagon em tais animais[30] e sua ação contrarregulatória tenha auxiliado na manutenção da hiperglicemia. Nossos resultados são coerentes com os de outros estudos[7,11-14,31], apesar destes terem utilizado protocolos de exercício diferentes (i.e., esteira rolante). Por outro lado, alguns estudos demonstraram que o exercício foi capaz de melhorar o metabolismo de glicose em ratos diabéticos[32,33]. Provavelmente, a falta de consenso entre os resultados desses estudos é devida ao uso de diferentes procedimentos metodológicos.

Os animais diabéticos apresentaram poliúria e polidipsia características do diabete, mas, apesar de alimentarem-se normalmente, sem restrição alimentar [ex., consumo semanal de ração (diabéticos: 199,47 ± 3,55 g *vs* controles: 194,36 ± 4,4 g)], movimentarem-se livremente dentro da caixa de alojamento (grupo DS) e exercitarem-se (grupo DE), não ganharam tanto peso quanto os controles não diabéticos. Os menores pesos corporais e ventriculares dos animais diabéticos indicam que eles tiveram o crescimento prejudicado. Em ratos com diabete induzida por STZ, além da secreção de insulina, a secreção de hormônios, tais como o hormônio de crescimento, o glucagon, o polipeptídeo pancreático e, por consequência, o fator de crescimento similar à insulina, são alteradas e afetam o crescimento[34-36]. Sabe-se também que o diabete induz o aumento da utilização de ácidos graxos e acelera o catabolismo proteico[37].

Ainda assim, o programa de natação aplicado não foi capaz de alterar significativamente o peso corporal dos animais diabéticos ou não diabéticos, mas aumentou o peso absoluto dos ventrículos nos animais não diabéticos. Entretanto, mais importante, tanto o diabete quanto o programa de natação aumentaram o peso relativo dos ventrículos nos animais diabéticos e o programa de natação aumentou este parâmetro nos animais controles não diabéticos, o que denota hipertrofia ventricular. Hipertrofia cardíaca induzida por diabete experimental (patológica) e por exercício crônico (fisiológica) já foram documentadas em estudos prévios[7,14,17,31].

A redução nas dimensões dos cardiomiócitos nos animais diabéticos em relação aos controles, observada no presente estudo, é coerente com o menor peso ventricular apresentado pelos animais diabéticos. Todavia, o programa de natação utilizado aumentou o volume dos cardiomiócitos dos ratos diabéticos. Tal fato sugere que a inibição do crescimento celular provocada pelo diabete foi afetada pelo exercício físico aplicado e denota hipertrofia celular. De fato, o aumento do peso relativo do ventrículo nos animais do grupo DE foi mais pronunciado que nos animais CE (33,3% *vs* 31,5%, respectivamente).

Conclusão

Concluímos que o programa de treinamento em natação aplicado atenuou a disfunção contrátil dos cardiomiócitos do VE de ratos com diabete experimental. Esses achados são relevantes para o conhecimento, em nível celular, dos benefícios do exercício físico na função contrátil do músculo cardíaco de indivíduos com diabete tipo I.

Potencial Conflito de Interesses

Declaro não haver conflito de interesses pertinentes.

Fontes de Financiamento

O presente estudo foi financiado pela FAPEMIG.

Vinculação Acadêmica

Este artigo é parte de dissertação de Mestrado de Márcia Ferreira da Silva pela Universidade Federal de Viçosa.

Referências

1. Fang ZY, Prins JB, Marwick TH. Diabetic cardiomyopathy: evidence, mechanisms, and therapeutic implications. Endocr Rev. 2004;25(4):543-67.
2. Jweied EE, McKinney RD, Walker LA, Brodsky I, Geha AS, Massad MG, et al. Depressed cardiac myofilament function in human diabetes mellitus. Am J Physiol Heart Circ Physiol. 2005;289(6):H2478-83.
3. Lacombe VA, Viatchenko-Karpinski S, Terentyev D, Sridhar A, Emani S, Bonagura JD, et al. Mechanisms of impaired calcium handling underlying subclinical diastolic dysfunction in diabetes. Am J Physiol Regul Integr Comp Physiol. 2007;293(5):R1787-97.
4. Reuter H, Gronke S, Adam C, Ribati M, Brabender J, Zobel C, et al. Sarcoplasmic Ca2+ release is prolonged in nonfailing myocardium of diabetic patients. Mol Cell Biochem. 2008;308(1-2):141-9.
5. Kim HW, Ch YS, Lee HR, Park SY, Kim YH. Diabetic alterations in cardiac sarcoplasmic reticulum Ca2+-ATPase and phospholamban protein expression. Life Sci. 2001;70(4):367-79.
6. Bracken N, Howarth FC, Singh J. Effects of streptozotocin-induced diabetes on contraction and calcium transport in rat ventricular cardiomyocytes. Ann N Y Acad Sci. 2006;1084:208-22.
7. Shao CH, Wehrens XH, Wyatt TA, Parbhu S, Rozanski GJ, Patel KP, et al. Exercise training during diabetes attenuates cardiac ryanodine receptor dysregulation. J Appl Physiol. 2009;106(4):1280-92.
8. Lehmann R, Kaplan V, Bingisser R, Bloch KE, Spinas GA. Impact of physical activity on cardiovascular risk factors in IDDM. Diabetes Care. 1997;20(10):1603-11.
9. Searls YM, Smirnova IV, Fegley BR, Stehno-Bittel L. Exercise attenuates diabetes-induced ultrastructural changes in rat cardiac tissue. Med Sci Sports Exerc. 2004;36(11):1863-70.
10. Monteiro P, Gonçalves L, Providencia LA. Diabetes and cardiovascular disease: the road to cardioprotection. Heart. 2005;91(12):1621-5.
11. Loganathan R, Bilgen M, Al-Hafez B, Zhero SV, Alenezy MD, Smirnova IV. Exercise training improves cardiac performance in diabetes: in vivo demonstration with quantitative cine-MRI analyses. J Appl Physiol. 2007;102(2):665-72.
12. Bidasee KR, Zheng H, Shao CH, Parbhu SK, Rozanski GJ, Patel KP. Exercise training initiated after the onset of diabetes preserves myocardial function: effects on expression of beta-adrenoceptors. J Appl Physiol. 2008;105(3):907-14.

13. Howarth FC, Almugaddum FA, Qureshi MA, Ljubisavijevic M. Effects of varying intensity exercise on shortening and intracellular calcium in ventricular myocytes from streptozotocin (STZ)-induced diabetic rats. Mol Cell Biochem. 2008;317(1-2):161-7.

14. Howarth FC, Almugaddum FA, Qureshi MA, Ljubisavijevic M. The effects of heavy long-term exercise on ventricular myocyte shortening and intracellular Ca2+ in streptozotocin-induced diabetic rat. J Diabetes Complications. 2009;24(4):278-85.

15. Stolen TO, Hoydal MA, Kemi OJ, Catalucci D, Ceci M, Aasum E, et al. Interval training normalizes cardiomyocyte function, diastolic Ca2+ control, and SR Ca2+ release synchronicity in a mouse model of diabetic cardiomyopathy. Circ Res. 2009;105(6):527-36.

16. Medeiros A, Gianolla RM, Kalil LMP, Bacurau RFP, Rosa LFBC, Negrão CE, et al. Efeito do treinamento físico com natação sobre o sistema cardiovascular de ratos normotensos. Rev paul Educ Fís. 2000;14(1):7-15.

17. Natali AJ, Wilson LA, Peckham M, Turner DL, Harrison SM, White E. Different regional effects of voluntary exercise on the mechanical and electrical properties of rat ventricular myocytes. J Physiol. 2002;541(Pt 3):863-75.

18. Prímola-Gomes TN, Campos LA, Lauton-Santos S, Balthazar CH, Guatimosim S, Capettini LS, et al. Exercise capacity is related to calcium transients in ventricular cardiomyocytes. J Appl Physiol. 2009;107(2):593-8.

19. Roman-Campos D, Duarte HL, Sales PA, Natali AJ, Ropert C, Gazzinelli RT, et al. Changes in cellular contractility and cytokines profile during Trypanosoma cruzi infection in mice. Basic Res Cardiol. 2009;104(3):238-46.

20. Satoh H, Delbridge LM, Blatter LA, Bers DM. Surface:volume relationship in cardiac myocytes studied with confocal microscopy and membrane capacitance measurements: species-dependence and developmental effects. Biophys J. 1996;70(3):1494-504.

21. Bers DM. Calcium cycling and signaling in cardiac myocytes. Annu Rev Physiol. 2008;70:23-49.

22. Howarth FC, Qureshi MA. Myofilament sensitivity to Ca2+ in ventricular myocytes from the Goto-Kakizaki diabetic rat. Mol Cell Biochem. 2008;315(1-2):69-74.

23. Ren J, Bode AM. Altered cardiac excitation-contraction coupling in ventricular myocytes from spontaneously diabetic BB rats. Am J Physiol Heart Circ Physiol. 2000;279(1):H238-44.

24. Bidasee KR, Nallani K, Yu Y, Cocklin RR, Zhang Y, Wang M, et al. Chronic diabetes increases advanced glycation end products on cardiac ryanodine receptors/calcium-release channels. Diabetes. 2003;52(7):1825-36.

25. Bidasee KR, Zhang Y, Shao CH, Wang M, Patel KP, Dincer UD, et al. Diabetes increases formation of advanced glycation end products on Sarco(endo) plasmic reticulum Ca2+-ATPase. Diabetes. 2004;53(2):463-73.

26. Choi KM, Zhong Y, Hoit BD, Grupp IL, Hahn H, Dilly KW, et al. Defective intracellular Ca2+ signaling contributes to cardiomyopathy in Type 1 diabetic rats. Am J Physiol Heart Circ Physiol. 2002;283(4):H1398-408.

27. Hattori Y, Matsuda N, Kimura J, Ishitani T, Tamada A, Gando S, et al. Diminished function and expression of the cardiac Na+-Ca2+ exchanger in diabetic rats: implication in Ca2+ overload. J Physiol. 2000;527(Pt 1):85-94.

28. Vasanji Z, Cantor EJ, Juric D, Moyen M, Netticadan T. Alterations in cardiac contractile performance and sarcoplasmic reticulum function in sucrose-fed rats is associated with insulin resistance. Am J Physiol Cell Physiol. 2008;291(4):C772-80.

29. Konrad RJ, Mikolaenko I, Tolar JF, Liu K, Kudlow JE. The potential mechanism of the diabetogenic action of streptozotocin: inhibition of pancreatic beta-cell O-GlcNAc-selective N-acetyl-beta-D-glucosaminidase. Biochem J. 2001;356(1):31-41.

30. Ponery AS, Adeghate E. Distribution of NPY and SP and their effects on glucagon secretion from the in vitro normal and diabetic pancreatic tissues. Peptides. 2000;21(10):1503-9.

31. Howarth FC, Marzouqi FM, Al Saeedi AM, Hameed RS, Adeghate E. The effect of a heavy exercise program on the distribution of pancreatic hormones in the streptozotocin-induced diabetic rat. JOP. 2009;10(5):485-91.

32. Broderick TL, Poirier P, Gillis M. Exercise training restores abnormal myocardial glucose utilization and cardiac function in diabetes. Diabetes Metab Res Rev. 2005;21(1):44-50.

33. Hall JL, Sexton WL, Stanley WC. Exercise training attenuates the reduction in myocardial GLUT-4 in diabetic rats. J Appl Physiol. 1995;78(1):76-81.

34. Gomes RJ, Leme JA, de Moura LP, de Araújo MB, Rogatto GP, de Moura RF, et al. Growth factors and glucose homeostasis in diabetic rats: effects of exercise training. Cell Biochem Funct. 2009;27(4):199-204.

35. de Almeida Leme JA, de Araújo MB, de Moura LP, Gomes, RJ, de Moura RF, Rogatto GP, et al. Effects of physical training on serum and pituitary growth hormone contents in diabetic rats. Pituitary. 2009;12(4):304-8.

36. Menon RK, Stephan DA, Rao RH, Shen-Orr Z, Downs LS, Roberts CT, et al. Tissue-specific regulation of the growth hormone receptor gene in streptozocin-induced diabetes in the rat. J Endocrinol. 1994;142(3):453-62.

37. Howarth FC, Chandler NJ, Kharche S, Tellez JO, Greener ID, Yamanushi TT, et al. Effects of streptozotocin-induced diabetes on connexin43 mRNA and protein expression in ventricular muscle. Mol Cell Biochem. 2008;319(1-2):105-14.